REPUBLIC OF CAMEROON

REPUBLIQUE DU CAMEROUN

MINISTRY OF HIGHER EDUCATION

MINISTERE DE L'ENSEIGNEMENT SUPERIEUR

Ecole Nationale Supérieure des Travaux Publics

UNIVERSITÀ DEGLI STUDI DI PADOVA

DEPARTMENT OF CIVIL ENGINEERING

DEPARTEMENT DE GENIE CIVIL

DEPARTMENT OF CIVIL, ARCHITECTURAL AND ENVIRONMENTAL ENGINEERING

SEISMIC BEHAVIOUR OF TALL REINFORCED CONCRETE BUILDINGS DESIGNED WITH DIFFERENT LEVELS OF DUCTILITY: CASE STUDY OF A RESIDENTIAL BUILDING AT TOUTOULI IN YAOUNDE, CAMEROON

A thesis submitted in partial fulfilment of the requirements for the degree

Of Master of Engineering (MEng) in Civil Engineering

Curriculum: **Structural Engineering**

Presented by:

FOGWOUNG TAFADJI Didier Rostand

Student number: **16TP21105**

Supervised by:

Prof. Carmelo MAIORANA **Eng. Giuseppe CARDILLO** **Dr. Eng. Guillaume Hervé POH'SIE**

Defended on 12 September 2022 in front of the jury composed of:

President:	Pr. George ELAMBO NKENG
Vice-president:	Pr. Carmelo MAIORANA
Examiner:	Pr. Michel MBESSA
Rapporteur:	Dr. Eng. Guillaume Hervé POH'SIE

Academic year: 2020/2021

DEDICATION

To my dear and tender grandmother, Mrs. Lucienne DJOUFACK, for always watching over me, believing in me and loving me.

ACKNOWLEDGEMENTS

This thesis is the fruit of the combined efforts of several individuals who contributed either directly or indirectly to its elaboration. I wish to express my sincere thanks and gratitude to:

- The Presidents of the jury**,** Professors **George NKENG** and **Carmelo MAIORANA** who makes us the great honour of chairing this jury;
- The Examiner, Prof. **Michel MBESSA**, for accepting to bring his observations to ameliorate this work;
- My supervisors Prof. **Carmelo MAIORANA**, Eng. **Giuseppe CARDILLO** and Dr Eng. **Guillaume Hervé POH'SIE** for all the guidance and advice they provided me with, during this thesis work;
- Professors **George NKENG** and **Carmelo MAIORANA** for all their academic and administrative support during these five years spent at the National Advanced School of Public Works (NASPW) in the MEng program in partnership with University of Padua in Italy;
- The Vice-director of ENSTP, Dr. **BWEMBA Charles** for his help and advice during our time spent at the NASPW;
- Prof. **MBESSA Michel**, the Head of Department of Civil Engineering for his guidance and valuable advice;
- All the **teaching staff** of NASPW and University of Padua for their good teaching qualities and all the motivation;
- My family and more specially my father **FOGWOUNG Jean-Claude** and my mother Mrs **FOGWOUNG Evrone**, for the love, the education, the trust they place in me and the financial support during all these years;
- Eng. **TOKA** and all his team at MATECH for allowing me to perform my study on their project and for all the help they gave me;
- Eng. **DONGMO Beaudin** for his advice which helped me during this work;
- Eng. **TATCHA Loïc**, who personally mentored me in the achievement of this degree;
- My siblings, **Joël**, **Cecile**, **Sarah**, **Junior**, **Boriana**, **Roxanne** and **Zita**. Their presence, encouragement and love have been indispensable to this work;
- My friends and more specially **Jordan**, **Laurian, Aminatou**, **Mathias**, **Santini**, **Romeo, Djunis, Christian, Evrad** and **Karelle** for their encouragement and support;
- All my **classmate**s and **friends** who were a source of motivation to me;

LIST OF ABREVIATIONS

3D	Three Dimensions
CCSZ	Central Cameroon Shear Zone
CM	Centre of Mass
CP	Collaspe Prevention
CQC	Complete Quadratic Combination
CR	Centre of Rigidity
CTBUH	Council on Tall Building and Urban Habitat
CVL	Cameroon Volcanic Line
DCH	Ductility Class High
DCL	Ductility Class Low
DCM	Ductility Class Medium,
EC	Eurocode
EMS	European Macroseismic Scale
EN	European Norm
FEMA	Federal Emergency Managament Agency
IO	Immediate Occupancy
LS	Life Safety
MDOF	Multiple degrees of freedom
M_L	Local (or Richter) Magnitude
MSK	Medvedev-Sponhueur Karnik scale
RC	Reinforced Concrete
SAP	Structural Analysis Program
SEAOC	Structural Engineers Association of California
SDOF	Single Degree of Freedom
SLS	Serviceability Limit State
SSI	Soil-Structure-Interaction
SRSS	Square Root of Sum of Square
SSR	Seismic Source Region
SSZ	Sanaga Shear Zone
ULS	Ultimate Limit State
USA	United States of America

LIST OF SYMBOLS

A	Area of the cross section
A_c	Area of the concrete cross section
A_s	Area of the lower longitudinal reinforcement of a cross-section
A'_s	Area of the upper longitudinal reinforcement of a cross-section
$A_{s,min}$	Minimum cross-sectional area of reinforcement
$A_{s,max}$	Maximum cross-sectional area of reinforcement
A_{sw}	Cross sectional area of the shear reinforcement
C	Modulus of subgrade reaction of the soil
c	Concrete cover
C_{min}	Minimum concrete cover
$C_{min,b}$	Minimum cover due to bond requirement
$C_{min,dur}$	Minimum cover due to environmental conditions
d_r	Design inter-storey drift
ex	Eccentricity along x axis
ey	Eccentricity along y axis
fcd	Design resisting strength of the concrete
f_{ctm}	Tensile strength of the concrete
f_y	Design yielding strength of the steel
f_{yd}	Design yielding strength of the steel
f_{yk}	Characteristic yield strength
f_{ywd}	Design yield strength of the shear reinforcement
F_b	Base shear force
F_i	Lateral force on the i level of one frame
G_{1k}	Structural permanent load
G_{2k}	Non-structural permanent load
h	Total height of the building
I_{xx}	Moment of inertia of the section along x axis
I_{yy}	Moment of inertia of the section along y axis
K_j	Static stiffness
ki	Spring stiffness of the foundation
M_{Ed}	Design bending moment
M_{Rd}	Resisting moment

m_i	Mass of the building at storey i
m_t	Total mass of the building
N_{Ed}	Design axial compression force
N_{Rd}	Resisting axial force
q	Behaviour factor
q	Allowable bearing capacity
q_0	Basic value of the behaviour factor
S	Soil factor
s	Spacing of the transverse reinforcement
T	Period of the structure
T_B	Lower limit of the period of the constant spectral acceleration branch
T_C	Upper limit of the period of the constant spectral acceleration branch
T_D	Value defining the beginning the constant displacement response range of the spectrum
μ	Ductility coefficient
V_{Ed}	Design shear force
$V_{Rd,C}$	Design shear resistance of the member without shear reinforcement
V_{Rd}	Design shear resistance of the member with shear reinforcement
W	Weight of the structure
θ	Interstorey-drift sensitivity coefficient

LIST OF FIGURES

LIST OF TABLES

ABSTRACT

The main objective of this work was to analyse the seismic behaviour of a tall building when the ductility level increases and to evaluate the correlation between its predicted behaviour and the obtained one. To better understand the subject, a review of the literature on reinforced concrete, tall buildings, seismic, ductility and different seismic analysis methods was first presented. The methodology used consisted first in presenting the building considered for this study then linear static analysis was applied to determine the concrete and reinforcement sections required to resist the vertical and wind actions at the ultimate and serviceability limit states. Subsequently, two levels of ductility were defined by choosing two behaviour factors, q=2.5 and q=3.9. On the basis of these behaviour factors, the elastic response spectrum of the seismic action was reduced to a design spectrum and the resulting loads were used to design the building for each level of ductility considering the soil-structure interaction. The main results obtained by the modal response spectrum analysis method revealed a decrease in the base shear force resulting in a decrease in the internal stresses in the structural elements and a decrease in their cross-sections. An increase in the behaviour coefficient of 56% produced a reduction in the base shear force of 35.9%. This analysis also revealed an increase in the inter-storey displacements when the ductility level increases. The pushover analysis was then performed on the models obtained with each level of ductility to evaluate their actual performance. The results obtained showed an increase in the ductility coefficient as the ductility level increases, which reflects a better capacity of the structure to support large displacements when the level of ductility increases. However, it was also shown that there is a decrease between the ductility level chosen by the behaviour factor according to Eurocode 8 and the effective ductility level of the building obtained by the pushover method. An increase in the effective ductility of 19.31% along x and 2.41% along y was obtained for q=2.5 and a decrease of 5.98% along x and 16.69% along y for q=3.9. This led to the conclusion that reinforced concrete buildings behave better when subjected to seismic actions when designed with a high ductility level, but a reduction between the predicted and the achieved ductility level can be observed. This represents a limitation of Eurocode 8 regarding ductility design.

Keywords: Tall reinforced concrete building, Behaviour factor, Ductility, Seismic behaviour, Eurocode 8

RESUME

L'objectif principal de ce travail était d'analyser le comportement sismique d'un immeuble à grande hauteur lorsque le niveau de ductilité augmente et d'évaluer la corrélation entre son comportement prévu et celui obtenu. Afin de mieux cerner le sujet, une revue de la littérature sur les notions liées au béton armé, aux bâtiments à grande hauteur, au séisme, à la ductilité et aux différentes méthodes d'analyse sismiques a d'abord été présentée. La méthodologie utilisée a consisté à présenter dans un premier temps le bâtiment considéré pour cette étude. Une analyse statique linéaire a été appliquée afin de déterminer les sections de béton et d'aciers nécessaires pour résister aux actions verticales et celle du vent aux états limites ultime et de service. Par la suite, deux niveaux de ductilités ont été définis par le choix de deux coefficients de comportement, q=2.5 et q=3.9. Sur la base de ces coefficients de comportement, le spectre de réponse élastique de l'action sismique a été réduit en spectre de calcul et les sollicitations obtenues ont permis de dimensionner le bâtiment pour chaque niveau de ductilité en prenant en compte l'interaction sol-structure. Les principaux résultats obtenus par la méthode d'analyse par spectre de réponse modale ont révélé une diminution de l'effort tranchant à la base entrainant une diminution des sollicitations internes dans les éléments structuraux et une diminution de leurs sections, et une augmentation des déplacements inter-étages lorsque le niveau de ductilité augmente. Une augmentation du coefficient de comportement de 56% a produit une réduction de l'effort tranchant de 35.9%. L'analyse pushover a ensuite été effectuée sur les modèles obtenus pour chaque niveau de ductilité afin d'évaluer leurs comportements réels. Les résultats obtenus montrent une augmentation du coefficient de ductilité lorsque le niveau de ductilité augmente, ce qui traduit une meilleure capacité de la structure à supporter des larges déplacements. Cependant, une diminution entre le niveau de ductilité choisi par le coefficient de comportement, suivant l'Eurocode 8, et le niveau de ductilité effectif du bâtiment évalué par la méthode pushover a été observé. Une augmentation du niveau de ductilité de 19.31% suivant x et 2.41% suivant y a été obtenu pour q=2.5 et une diminution de 5.98% suivant x et 16.69% suivant y pour q=3.9. Ceci a donc conduit à conclure que les bâtiments à grande hauteur en béton armé présentent un meilleur comportement sismique lorsqu'ils sont dimensionnés pour des niveaux de ductilité élevés mais une réduction est à noter entre le niveau de ductilité obtenu et celui prévu. Ceci représente une limite de l'Eurocode 8 en ce qui concerne le dimensionnement en ductilité.

Mots clés : Immeuble en béton armé à grande hauteur, Coefficient de comportement, Ductilité, Comportement sismique ; Eurocode 8.

TABLE OF CONTENTS

GENERAL INTRODUCTION

Earthquakes are amongst the most devastating natural disasters. It is well known that most of the human damage and economic losses due to moderate or severe ground movements are caused by the failure of civil engineering facilities, especially tall reinforced concrete buildings, many of which were supposed to have been designed and constructed to provide protection against natural hazards (Fajfar & Krawinkler, 1992). This has been confirmed with the recent earthquakes around the world such as, the Nepal earthquake in 2015 which killed 8,000 people, the Japan earthquake in 2011 which killed 19,000 people and the deadliest earthquake since 2000, the Haiti earthquake in 2010 which killed 230,000 people.

Although Cameroon is rated as low in seismic hazard, seismic shocks preceding Mt Cameroon eruptions have damaged houses in the past. Later eruptions may be more damaging considering the increasing population density and infrastructural development in the urban areas within the vicinity of the volcano (Bang, 2022). Therefore, it is important to realise that Cameroon is not excluded from the seismic hazard, and it would be important to ensure seismic resistance to buildings, particularly high-rise buildings, in their designing.

To protect buildings against earthquake disasters, seismic codes have been developed. The first seismic codes were published in the early 1920s in Japan and in the 1930s in California. At that time, the main points of discussion concerned the fraction of the structure's weight to be taken into account in the evaluation of seismic forces using the concept of lateral forces. Experience has shown that the design of elastic structures generates substantially high costs and makes this design principle inapplicable and economically unacceptable (Gieu S., 2012). Therefore, it becomes necessary to improves codes in such a way that they could both ensure a good behaviour of buildings against earthquakes and remain economically acceptable.

The biggest revolution appearing in seismic codes concerns ductility. Ductility can be seen as a means of dissipating input seismic energy through inelastic mechanisms of structural behaviour. These mechanisms are activated by allowing the structure to yield in a controlled manner (i.e., without leading to overall instability or collapse) and, therefore, allowing structural damage to occur under the designated seismic action (Avramidis et al., 2016).

In seismic active zones, experience shows that ductile design of buildings would have great effects; be it cost wise or the structural stability of the building. If there is more confidence in the design with ductility, limitations in the understanding of the behaviour of the building when designed with different levels of ductility still exist. These limitations are mainly related to the

choice of the behaviour factor, defining a particular level of ductility according to Eurocode 8, and assumed to be equal to the ductility coefficient. But due to the complexity of the seismic phenomena, the prediction of the behaviour of the structure may raise some doubts.

The objective of this work is to analyse the behaviour of a tall reinforced concrete building when the ductility level increases and to evaluate the correlation between the predicted behaviour and the obtained one. To this end, the present work is divided into three chapters. The first chapter, entitled literature review, presents the concepts related to reinforced concrete, tall buildings, earthquake, ductility, as well as the different methods of seismic analysis. The second chapter is the methodology presenting the path followed to meet the expectations of this research. This chapter highlights the different seismic analysis methods used to obtain the results of this study. Finally, the third chapter is a summary of the results obtained and their interpretations.

CHAPTER 1. LITERATURE REVIEW

Introduction

Concrete is arguably the most important building material, playing a part in all building structures, both single-storey and multiple-storey. It is very durable and has a very good resistance to seismic action when specification and construction procedures are correct. This chapter aims to present the state of the art in the fields of seismic analysis and ductility of tall reinforced concrete buildings. To this end, the chapter starts with reinforced concrete, its main properties and generalities of tall reinforced concrete buildings. Then, a brief description of the seismic source regions in Cameroon is given, followed by a presentation of the seismic analysis methods present in the current standard. Finally, a special emphasis is made on the ductility of reinforced concrete buildings.

1.1. Reinforced concrete

1.1.1. Definition and properties of reinforced concrete

Reinforced concrete is a strong durable building material that can be formed into many varied shapes and sizes ranging from a simple rectangular column to a slender curve dome or shell. Its utility is achieved by combining the best features of concrete and steel (Mosley et al., 2012).

1.1.1.1. Definition of reinforced concrete

Concrete has relatively high compressive strengths (commonly in the range of 20-35 MPa), but its tensile strength is low (in the order of a tenth of the compressive strength) and random (in the most common sense of the term). Concrete is therefore a fragile material. To overcome the disadvantages of this brittleness, steel reinforcement is added to concrete; the resulting material is known as reinforced concrete. At times, steel bars are also used in compression zone to gain extra strength with a leaner concrete size as in reinforced concrete columns and doubly reinforced beams.

Because of its monolithic nature and the deformability of certain elements, reinforced concrete has enabled various constructions to resist, without excessive or irremediable damage, to various types of stresses and even those of an accidental nature.

The advantages of reinforced concrete are many: relatively low cost, good weather resistance, good fire resistance, and excellent formability of concrete, which makes it usable in various structures, including buildings, bridges, culverts, dams, reservoirs, silos, tanks, and many others.

1.1.1.2. Properties of concrete

a. Mechanical properties

Concrete is a type of artificial stone made by mixing dry aggregates (sand and gravel) and cement, then adding water. This makes a soft mix that can be moulded easily or transported in a rotating concrete mixer which harden with time. Concrete is a material that works well in compression, and knowledge of its mechanical properties is essential for the design of structures.

i. Compressive strength

Many concrete professionals consider that the most important characteristic of the concrete is its mechanical strength in compression at a given age of 28 days. The compression strength of concrete is denoted by concrete strength classes which relate to the characteristic (5%) cylinder strength f_{ck}, or the cube strength $f_{ck,\ cube}$ in accordance with EN 206-1. The compressive strength classes are expressed by the letter C followed by two numbers. The first number represents f_{ck} and the second one represents $f_{ck,\ cube}$. In Cameroon, compressive stress has traditionally been measured and expressed in terms of 150 mm diameter cylinders with 300 mm long, crushing strength at an age of 28 days. Some countries use 150 mm cube.

A typical curve for concrete in compression known as stress-strains diagrams is shown in figure 1.1. As the load is applied, the ratio between the stresses and the strains is approximately linear at the beginning and the concrete behaves as an elastic material with virtually full recovery of displacement if the load is removed. Eventually, the curve is no longer linear, and concrete does not behave elastically over a major range. The concrete behaves more and more as a plastic material. If the load were removed during the plastic range, the recovery would no longer be complete and a permanent deformation would remain (Mosley et al., 2012).

ii. Tensile strength

Another important property of the concrete is the tensile strength. Although concrete is not normally designed to resist direct tension, the knowledge of tensile strength is of interest to

estimate the load under which cracking will develop. The absence of cracking is of considerable importance in maintaining the continuity of a concrete structure and in many cases, in the prevention of corrosion of reinforcement.

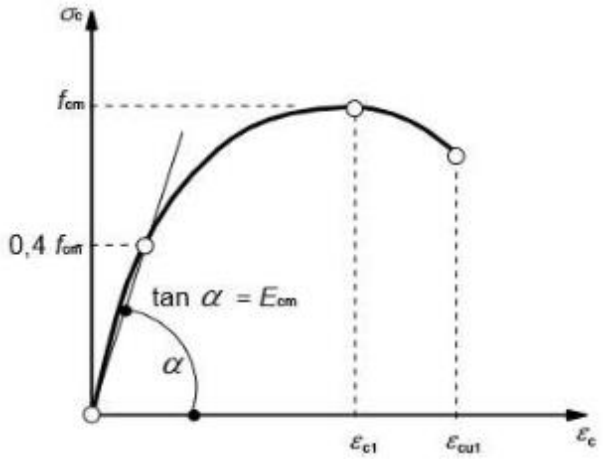

Figure 1.1. Stress-strain curve for concrete under compression (EN 1992-1-1:2004)

b. Creep and shrinkage in concrete

There are two types of deformations:

- short-term deformation, which refers to the immediate deflection after casting and application of partial or full-service loads.
- long-term deformation, which occurs over a long period of time, and it is largely due to creep and shrinkage of the material. The long-term deflection is almost two or three times bigger than the short-term deflection.

Shrinkage and creep are time-dependent properties of concrete. Their effects should be considered for the verification of serviceability limit states (SLS) and generally ignored in the ultimate limit state (ULS), except when their effects are significant, as for example in the ULS verification of stability where second order effects are of importance (EC2-1-1-2.3.2.2).

Creep in concrete is the phenomenon whereby deformation of concrete subjected to a constant load continues to increase with time. For most structural purposes, creep is assumed to be proportional to stress. In construction, creep has three major effects. Creep causes deflection in structures under continuous loading. It also causes stress relief that reduces cracking. Finally, creep causes loss of prestress in construction due to creep of both the concrete and the prestressing steel.

As concrete hardens there is a reduction in volume. The change in the volume of drying concrete is not equal to the volume of water removed. The evaporation of free water causes little or no shrinkage. As concrete continues to dry, water evaporates and the volume of the

restrained cement paste changes, causing concrete to shrink. Shrinkage is a reduction on the volume of non-loaded concrete that starts during its hardening and continues until its definite maturing. For the calculations of stresses, the effect of shrinkages no longer intervenes in the general case where loads other than shrinkage are applied and conversely, the effect of shrinkage and delayed shrinkage is a cause of cracking and merits a special study.

1.1.1.3. Properties of reinforcing steel

a. Yield strength and elastic modulus

Reinforcement for concrete generally consists of round, deformed steel rebars or steel mesh fabric. Steel rebars are used for longitudinal reinforcement (i.e., flexure) and transverse internal reinforcement (i.e., shear) in beams, columns, and walls. They are ribbed to increase bond with the concrete. Adequate bond may be assumed by compliance with the specification of projected rib area. Steel mesh also known by welded wire mesh reinforcement are used for longitudinal reinforcements in slabs and thin walls.

The most useful properties of reinforcing steel are the yield strength f_{yk} and the modulus of elasticity Es. The yield strength is the characteristic value of the yield load divided by the nominal cross-sectional area. The modulus of elasticity is the measure of stiffness of an elastic material. It is used to describe the elastic properties of an elastic material when it is stretched or compressed. For all particle purposes, modulus of elasticity of all tool steels in all conditions is about 200 GPa at room temperature. Figure 1.2 presents the stress-strain diagrams for both hot rolled steel and cold worked steel.

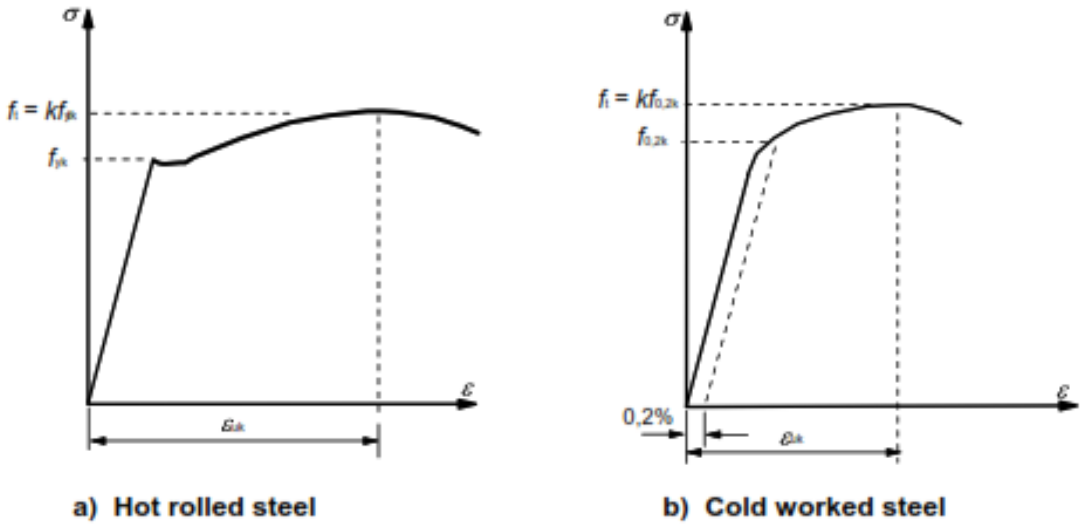

Figure 1.2. Stress-strain diagrams of typical reinforcing steel (EN 1992.1.1:2004)

The application rules for design in Eurocode 2 are valid for a specified yield strength range, f_{yk}= 400 to 600 MPa. The design should be based on the nominal cross-section area of the reinforcement and the design values derived from the characteristic values. Figure 1.3 presents the idealized and design stress-strain diagrams for reinforcing steel (for tension and compression).

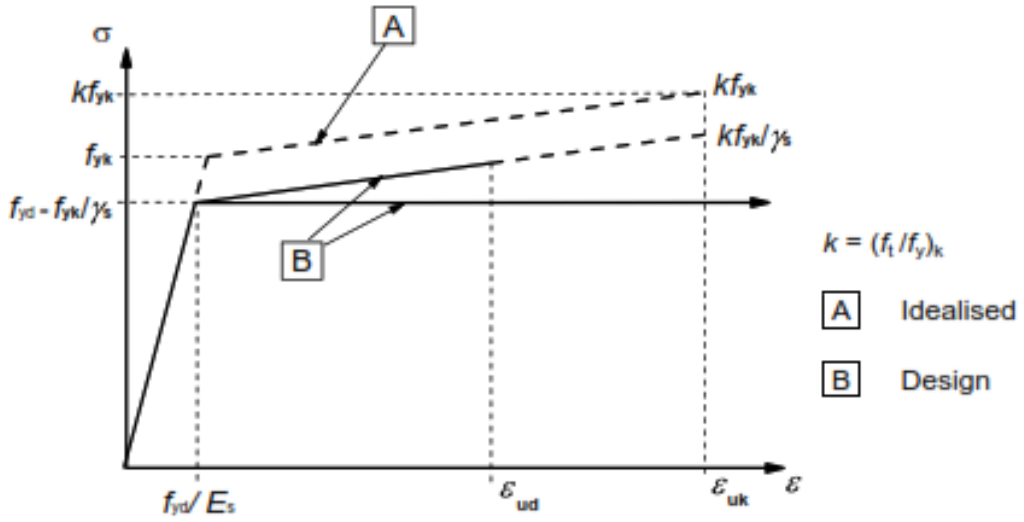

Figure 1.3. Idealised and design stress-strain diagrams for reinforcing steel (EN 1992.1.1:2004)

b. Ductility

Other properties can help to have a good behaviour of the reinforcing steel. Those properties can be the maximum actual yield ($f_{y,\,max}$), the tensile strength f_{tk}, the bendability, the bond characteristics (f_R), the section sizes and tolerances, the fatigue strength, the weldability, and the ductility. Talking about the last one, the reinforcement shall have adequate ductility. It is defined by the ratio of tensile strength to yield stress (f_t/f_{yk}) and elongation (ε_{uk}) at maximum force. With reference to the ultimate strain of the material and the design purposes, three ductility classes are distinguished:

- Class A (Low ductility) with $\varepsilon_{uk} \geq 2.5\%$ and $f_t/f_{yk} \geq 1.05$. It is normally associated with small diameter (≤12 mm) cold-worked bars used in mesh and fabric. This is the lowest ductility category and will include limits on moment redistribution which can be applied and higher quantities for fire resistance.
- Class B (Normal ductility) with $\varepsilon_{uk} \geq 5.0\%$ and $f_t/f_{yk} \geq 1.08$. It is the most commonly used for reinforcing bars.

- Class C (High ductility) with $\varepsilon_{uk} \geq 7.5\%$ and $f_t/f_{yk} \geq 1.15$. It may be used in earthquake design or similar situations.

1.1.2. Tall reinforced concrete building

Today's modern urban landscape is mostly built with reinforced concrete, a concrete reinforced with steel bars and stronger than either material alone. Reinforced concrete was invented in the second half of the 19th century. "The development in concrete technology over the twentieth century covering materials, structural systems, analysis and construction techniques, made it possible to build concrete tall buildings such as Petronas towers (452m high and 85 floors), Jin Mao (421m high and 88 floors) and Burj Dubai (800m+ and 160 floors)." (Rizk, 2010).

1.1.2.1. Evolution and feasibility of tall reinforced concrete building

In the early days, the construction industry establishment was sceptical about this strange association of concrete and steel, and theoretical approaches started only in 1886 with the works of Koenen. They were followed by those of E. Coignet, Tedesco, Considère, Mörsch and others. It is in the early years of the 20th Century that a theory shared by most scientists and practitioners started to appear, along with the first codes (Moussard et al., 2017).

Although the first true reinforced concrete civil engineering work was the bridge built in Wiggen, Switzerland, by Hennebique's company in 1892, the most iconic work of those early days is probably the sixteen stories' Ingalls Building (see figure 1.4), the first reinforced concrete tall buildings (16-story, 64 m) in Cincinnati. Until then, high rise buildings were built in brick masonry (van Damme, 2018).

Figure 1.4. Ingalls Building (Photo by Rick Dikeman)

When considering skyscrapers, until recently, the observer was drawn to great cities such as New York and Chicago. Today, after a century during which New York and Chicago went unchallenged as home to the world's tallest modern buildings, the crown has been snatched first by Kuala Lumpur's twin Petronas Towers in Malaysia (see figure 1.5), then by Taipei's 101 Tower in Taiwan (see figure 1.6), and in May 2008 by the Burj Khalifa in Dubai (see figure 1.7). More recently, Jeddah Tower is a skyscraper under construction in Jeddah, Arabia, which will reached 1000m in height. The tower is to reach an unprecedented height, becoming the tallest building in the world, in addition to be the first structure to exceed the kilometre.

Figure 1.5. Kuala Lumpur's twin Petronas Towers in Malaysia **(**Source: www.tripadvisor.fr)

Figure 1.6. Taipei's 101 Tower in Taiwan (Photo by Ronnie Chua)

Figure 1.7. Burj Khalifa in Dubai (Source: www.dubai-prestige.com)

The feasibility of tall buildings has always depended upon the available materials and the development of the vertical transportation necessary for moving people up and down the buildings. The ensuing growth that has occurred from time to time may be traced back to two major technical innovations that occurred in the middle to the end of the 19th century: the development of wrought iron and subsequently steel, and the incorporation of the elevator in high-rise buildings. The introduction of elevators made the upper floors as attractive to lease as the lower ones and, as a result, made the taller buildings financially successful (Taranath, 2009).

1.1.2.2. Definition of tall reinforced concrete building

While the world is full of interesting structures, large and small, old and modern, the most eye-catching and the ones that instil the greatest sense of wonder in the onlooker are the modern tall buildings.

According to the public, a tall building is a building consisting of many floors. The tallness of a building is relative and cannot be defined in specific terms related to height or number of floors. There is not an international consensus on what constitutes a tall building or at what height, number of stories or proportion a building can be call tall. According to the Council on Tall Buildings and Urban Habitat (CTBUH) in the report entitled "Height Criteria for Measuring and Defining Tall Buildings", there is no absolute definition of what constitutes a "tall building"; it is a building that exhibits some element of "tallness" in one or more of the following categories:

a. Height relative to context

It is not just about the height but the context in which it exists. Thus, whereas as 8-storey building may not be considered a tall building in a high-rise city such as Chicago or Hong Kong, in an African city like Yaoundé in Cameroon, this may be distinctly taller than the urban norm as illustrated in figure 1.8.

Figure 1.8. Illustration of height relative to context (CTBUH, 2017)

b. Proportion relative to context

Again, a tall building is not just about height but also about proportion. There are numerous buildings which are not particularly high but are slender enough to give the appearance of a tall building, especially against low urban backgrounds. Conversely, there are numerous big/large footprint buildings which are quite tall but their size/floor area rules them out as being classed as a tall building. This rule can be illustrated by the figure 1.9.

Figure 1.9. Illustration of proportion condition (CTBUH, 2017)

c. Tall building technologies

If a building contains technologies which may be attributed as being a product of "tall" (e.g., specific vertical transport technologies, structural wind bracing as a product of height, etc.), then this building can be classified as a tall building. Figure 1.10 illustrates well this rule.

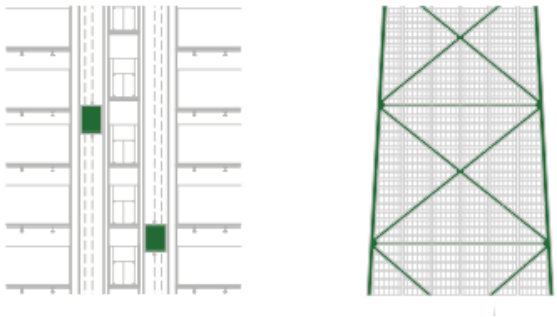

Figure 1.10. Illustration of tall building technologies condition (CTBUH, 2017)

Moreover, according to Taranath (2009), perhaps the dividing line for tall building should be drawn where the design of the structure moves from the field of statics into the field of structural dynamics. From the structural design point of view, it is simpler to consider a building as tall when its structure analyses and design are in some way affected by the lateral loads, particularly the sway caused by such loads like seismic force for example. This can be justified by the fact that in contrast to vertical loads that may be assumed to increase linearly with height, lateral loads are quite variable and increase rapidly with height.

1.2. Earthquake

Most vibrations in structures are undesirable because of the increased stresses and the input energy that accompany them. They should therefore be eliminated or reduced as much as possible by appropriate design. Of the various sources of vibration, earthquakes are undoubtedly the most energetic. Many scientists and engineers such as Anil k. Chopra, Rakesh Goel, Victor Davidovici, Joseph Penzien, Luigi Di Sarno and others have revolutionised structural engineering by studying not only the static but also the dynamic behaviour of structures in both the elastic and inelastic domains.

1.2.1. Definition and causes of earthquake

Earthquakes are one of the most devastating natural hazards that cause great loss of life and livelihood. An earthquake is manifested as ground shaking caused by the sudden release of energy in the Earth's crust accumulated in the adjacent layers by the effect of global tectonic processes. This energy may originate from different sources, such as dislocations of the crust, volcanic eruptions or even by man-made explosions or the collapse of underground cavities, such as mines or karsts. Richter (1958) has provided a list of major causes of earthquake recorded by seismograph as shown in figure 1.11.

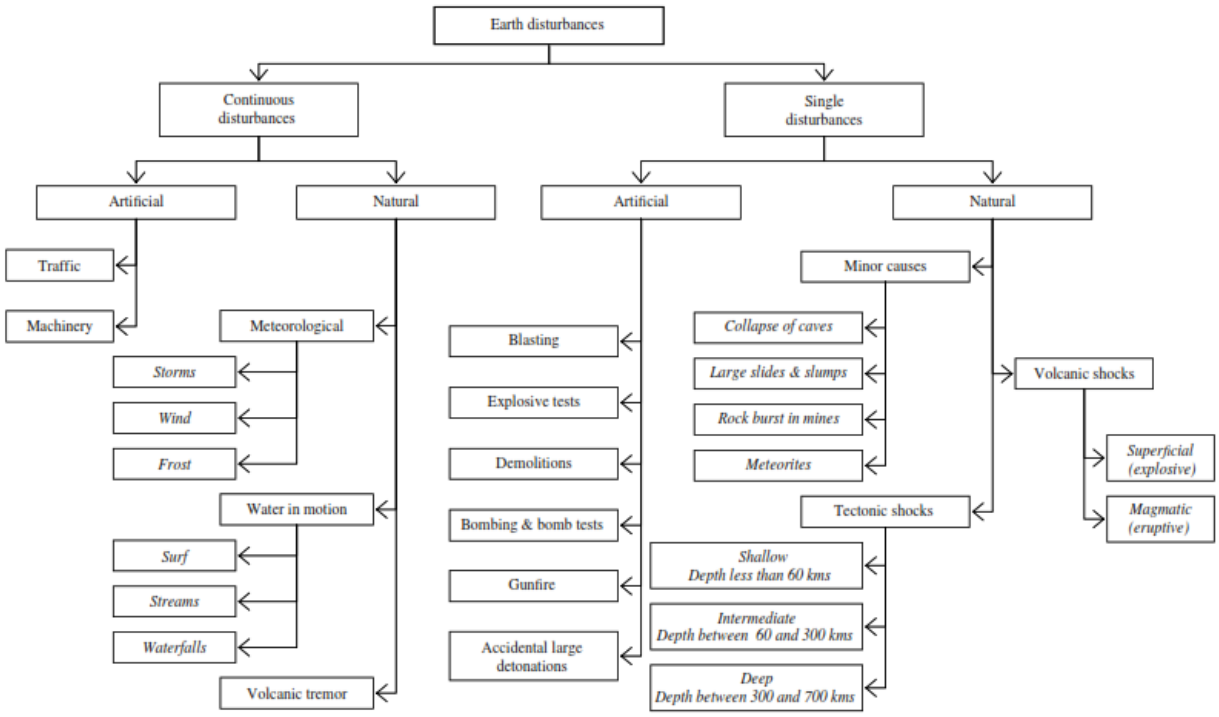

Figure 1.11. Earth disturbances recorded by seismographs (Elnashai & di Sarno, 2015)

When the tensile, compressive and shear stresses exceed the mechanical strength of the layers, fracturing occurs, and seismic waves are generated. These waves propagate through the ground and are transmitted to buildings and structures, subjecting them to dynamic horizontal, vertical and torsional forces. The characteristics of these vibrations do not depend exclusively on the earthquake that caused them. The local geology, the state of the surface layers, the type of construction, etc… influence the actual damage caused by an earthquake.

1.2.2. Measuring of earthquake

Earthquakes effects is expressed is several ways. Qualitative or non-instrumental and quantitative or instrumental measurements exits, the latter can be either based on regional calibrations or applicable worldwide. For earthquakes that have been instrumentally recorded, qualitative scales are complementary to the instrumental data (Elnashai & di Sarno, 2015).

Descriptive methods related to the qualitative and quantitative measure can be used to establish the earthquake-induced damage and its spatial distribution. In so doing, magnitude and intensity are the two principals descriptive methods used.

1.2.2.1. Intensity

Intensity is a non-instrumental perceptibility measure of damage to structures, ground surface effects and human reactions to earthquake shaking. It is a descriptive method which has been traditionally used to establish earthquake size especially for pre-instrumental events. It is a subjective damage evaluation metric because of its qualitative nature, related to population density, familiarity with earthquake and type of constructions, and is dependent on peak acceleration, velocity and duration on the earthquake.

Discrete scales are used to quantify seismic intensity; the levels are represented by roman numerals and each degree of intensity provides a qualitative description of earthquake effects. A presentation of the most common intensity scales is given the Appendix A. Intensity scales may include description of construction quality for structures in the exposed region. The Medvedev-Sponhueur-Karnik (MSK) scale, which has been widely used since 1964, is increasingly being replaced by the EMS scale, which is destined to become a standard in Europe but also in other continents. The table 1.1 presents a brief description of the European Macroseismic Scale.

Table 1.1. European Macroseismic Scale (EMS) description (Source: www.uib.no)

EMS intensity	Definition	Description of typical observed effects (abstracted)
I	Not felt	Not felt.
II	Scarcely felt	Felt only by very few individual people at rest in houses.
III	Weak	Felt indoors by a few people. People at rest feel a swaying or light trembling.
IV	Largely observed	Felt indoors by many people, outdoors by very few. A few people are awakened. Windows, doors and dishes rattle.
V	Strong	Felt indoors by most, outdoors by few. Many sleeping people awake. A few are frightened. Buildings tremble throughout. Hanging objects swing considerably. Small objects are shifted. Doors and windows swing open or shut.
VI	Slightly damaging	Many people are frightened and run outdoors. Some objects fall. Many houses suffer slight non-structural damage like hair-line cracks and fall of small pieces of plaster.
VII	Damaging	Most people are frightened and run outdoors. Furniture is shifted and objects fall from shelves in large numbers. Many well built ordinary buildings suffer moderate damage: small cracks in walls, fall of plaster, parts of chimneys fall down; older buildings may show large cracks in walls and failure of fill-in walls.
VIII	Heavily damaging	Many people find it difficult to stand. Many houses have large cracks in walls. A few well built ordinary buildings show serious failure of walls, while weak older structures may collapse.
IX	Destructive	General panic. Many weak constructions collapse. Even well built ordinary buildings show very heavy damage: serious failure of walls and partial structural failure.
X	Very destructive	Many ordinary well built buildings collapse.
XI	Devastating	Most ordinary well built buildings collapse, even some with good earthquake resistant design are destroyed.
XII	Completely devastating	Almost all buildings are destroyed.

However, intensity scales do not account for local soil conditions which may significantly affect the earthquake-induced damage and its distribution. It has been observed repeatedly that structures in the immediate vicinity of earthquake sources experience very high ground accelerations but sustain little or no damage (e.g., Elnashai et al. 1998). On the other hand, intensity is a measure of the perceptibility of the earthquake and its actual consequential damage. Therefore, relating intensity to peak ground acceleration is, in principle, illogical.

1.2.2.2. Magnitude

In 1931, a Japanese seismologist named Kiyioo Wadati constructed a diagram reproducing the ground motion generated by earthquakes as a function of distance. He found that the resulting curves, regardless of the earthquake, formed straight lines parallel to each other. The fact that earthquakes of different sizes produce parallel lines thus suggests that it is possible to characterise the size of an earthquake by a simple number. In 1935, based on this idea, the American Charles Francis Richter classified the size of earthquakes on a scale characterising the amount of ground motion produced. Using data from the Californian network at the time, he found a repetitive relationship of ground motion attenuation as a function of distance. He

then defined a quantitative method of measuring earthquake size faults dimensions, called magnitude, and proposed the first magnitude scale, the Richter scale.

Thus, the relationship established in 1935 by Richter cannot be extrapolated stricto-sensus to other regions of the world, to other data, without taking into account the earthquake mechanisms used, the recording instruments and the attenuation of waves with distance in the earth's crust. It is also only valid for data collected at short distances collected at short distances and, therefore, this magnitude has since been called the local magnitude M_L. Several scales exist and the most common magnitude scales are described in Appendix A.

The local (or Richter) magnitude (M_L) measures the maximum seismic wave amplitude. Earthquake with M_L greater than 5.5 causes significant damage, while an earthquake of M_L=2 is the smallest event normally felt by people.

The accepted relationship between energy released, E, and Richter magnitude, M_L, is given by equation **(1.1)**:

$$\log_{10} E = 11.4 + 1.5\, M_L \qquad (1.1)$$

1.2.3. Earthquake in Cameroun

Cameroon has been the subject of several structural studies (de Plaen et al., 2014; Reusch et al., 2010; Tokam et al., 2010). According to these studies, the available geotechnical data, combined with historical and recent seismic data, have allowed and improvement of the knowledge of the seismo-tectonics in the study area. Although seismic activities are scattered all over the country, spatial distribution of seismic events have been used to delineate Cameroon into four main seismic source regions (SSRs) (Bang, 2022).

1.2.3.1. Seismic source regions in Cameroun

A seismic source region is a zone where a given seismo-tectonic structure is active (Noel et al., 2014). It is determined based on detailed geological studies of the zone, as well as consistent and comprehensive historical and instrumental data on seismic events to supports the results. Several types of seismic region model have identified. Each source region model is adopted and assumed to have homogeneous seismicity, because the seismic activities are scattered over a large area with no well identified point or specific fault location to justify a point or plane seismic source. Here, the tectonic characteristics of each area and density of spatial distribution of seismic events are used to delineate Cameroon into four main seismic source regions, illustrated in figure 1.12 and figure 1.13.

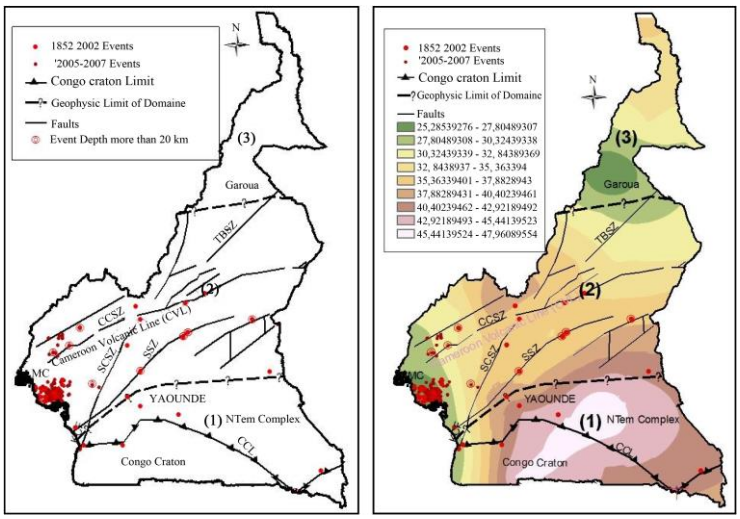

Figure 1.12. Seismicity map of Cameroon (Noel et al., 2014)

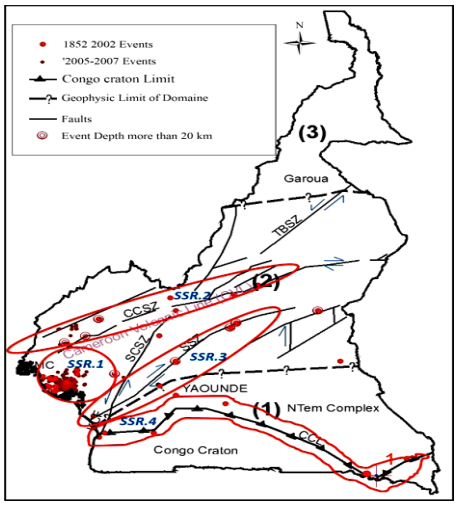

Figure 1.13. Seismic Source Regions (SSR) in Cameroon (Noel et al., 2014)

a. Seismic source region I

It corresponds to the area of "Mount Cameroon" volcano, in South-West Cameroon. From data recorded by temporary seismic network, 93.4% of seismic events are in this region. Mostly events are shallow with depth inferior to 25 km. Geotechnic data shows that most of the seismicity is concentrated around the Mt Cameroon region and the strongest felt earthquake (4.4Mb magnitude) was associated to the 1999 Mt Cameroon eruption. Indeed, seismicity in this region is generally low and probably associated with magmatic mantle convection (Koch et al., 2012).

b. Seismic Source Region II

It is found in the north-est of Mt Cameroon region and characterised by diffuse, weak, irregular to moderate seismicity. The maximum magnitude recorded is 5.1 Mb. This region is

characterised by Tombel and Kumba grabens on southern segments faults of the "Central Cameroon Shear Zone" (CCSZ) (Noel et al., 2014).

c. Seismic Source Region III

It occurs in the central part of the country along the Western Cameroon Highlands. Prominent in this region are Eocene to Pliocene volcanic eruptions, the "Sanaga Shear Zone" (SSZ) and crater lakes. Seismicity here is diffuse and seismic events have occurred at average depths of 33 km. The maximum magnitude recorded earthquakes in this source region was 5.8 Mb. Although this might suggest a moderate seismicity, the parameter of SSZ with average depth of 33 km and length of 900 km, convinced us that it is an important seismogenic area (Noel et al., 2014).

d. Seismic source region IV

It is in the northern boundary of the Congo Craton with the characteristic magnitude of 6 Mb and 33 km depth. Despite its relatively shallow and weak magnitude earthquakes, arguably, this source region has the potential to generate large earthquakes (Bang, 2022).

1.2.3.2. Recent earthquakes in Cameroon

Although Cameroon is rated as low in seismic hazards, seismic shocks preceding Mt Cameroon eruptions have damaged houses in the past. Later eruptions may be more damaging considering the increasing population densities and infrastructural development in the urban areas within the vicinity of the volcano like Buea and Limbe for example. Table 1.2 illustrates some previous earthquakes recorded according to Cameroon's 2011 National contingency plan.

Table 1.2. Past seismic events in Cameroon (National Contingency Plan Cameroon, 2011)

Date	Locality concerned	Fault involved	Magnitude (Richter scale)	Damage-observations
1911	Lolodorf	Mbalmayo	6	High potential risk
1945	Ouesso	Centre region	5.6	High potential risk
1969	Yoko	Centre region	4.6	High potential risk
1983	Maga	Centre region	4.1	Building's destruction
1987	Kribi	Eseka-Kribi	4	High potential risk
2002	Kribi	Eseka-Kribi	-	Damaged recorded
2005	Monatélé	Sanaga	4.4	High potential risk

Moreover, the Institute of Geological and Mining Research (IRGM) had confirmed the occurrence on 19 December 2019 of an earthquake felt by the inhabitants of several localities in South Cameroon. According to the analyses, this earthquake had its epicentre located in the Atlantic Ocean off Sao Tome and Principe. It had a magnitude of 5.7. Indeed, an earthquake of such magnitude would have caused significant material damage if it was in the continental part of the territory. No loss of life had been recorded, still less damage to property and infrastructure.

1.3. Seismic analysis methods

The main objectives of seismic design codes are the protection of human lives, the limitation of structural damage and the ensuring of the functional efficiency of buildings and structure that are of relevance to public safety. Most seismic design codes, including Eurocode 8, have adopted the performance-based design approach and include four analysis methods that can be classified into two groups, linear and non-linear analysis methods. Linear analysis approaches include equivalent static analysis, and the modal response spectrum analysis. Non-linear methods comprise non-linear static (pushover) analysis and non-linear dynamic (time-history) analysis.

1.3.1. Performance-based seismic design

Allowing for structural damage to occur for a certain level of "design seismic action", lies at the core of all modern seismic design codes of practice for ordinary structures, in accordance with the performance-based seismic design philosophy.

Performance-based seismic design is the seismic design methodology of the future. In addition to meeting the basic safety objective of avoiding loss of life, performance-based seismic design can be a cost-effective way to reduce financial losses due to structural and non-structural damage and to ensure minimal structural and non-structural damage during a moderate seismic event.

The practical implementation of this seismic design philosophy can be qualitatively framed via the three fundamental structural design objectives for earthquake resistance, as prescribed in early seismic codes (see e.g., the commentary of the Structural Engineers Association of California Blue Book (SEAOC, 1967) which introduced the general philosophy of the earthquake resistant design of buildings that is still conceptually valid today) (Avramidis et al., 2016). Eurocode 8 (EC8) prescribes two requirements that are assumed to cover all the design objectives.

1.3.1.1. No-collapse requirement

The structure shall be designed and constructed to withstand the design seismic action without local or global collapse, thus retaining its structural integrity and a residual load bearing capacity after the seismic event.

This requirement is related to the protection of life under a rare event, through the prevention of the global or local collapse of the structure that, after the event, should retain its integrity and a sufficient residual load bearing capacity. After the event, the structure may present substantial damages, including permanent drifts, to the point that it may be economically unrecoverable, but it should be able to protect human life in the evacuation process or during aftershocks. In the framework of the Eurocodes, that uses the concept of Limit States, this performance requirement is associated with the Ultimate Limit State (ULS) since it deals with the safety of people or the whole structure (Athanasopoulou et al., 2012).

1.3.1.2. Damage limitation requirement

The structure shall be designed and constructed to withstand a seismic action having a larger probability of occurrence than the design seismic action, without the occurrence of damage and the associated limitations of use, the costs of which would be disproportionately high in comparison with the costs of the structure itself.

This second requirement is related to the reduction of economic losses in frequent earthquakes, both in what concerns structural and non-structural damages. Under such kind of events, the structure should not have permanent deformations and its elements should retain its original strength and stiffness and hence should not need structural repair. In view of the minimization of non-structural damage the structure should have adequate stiffness to limit, under such frequent events, its deformation to levels that do not cause important damage on such elements. Some damage to non-structural elements is acceptable but they should not impose significant limitations of use and should be repairable economically (Athanasopoulou et al., 2012).

Considering again the framework of the Eurocodes, this performance requirement is associated with the Serviceability Limit State (SLS) since it deals with the use of the building, comfort of the occupants and economic losses.

1.3.2. Linear methods

The choice of analytical method is subjected to limitations based on building characteristics. The linear procedures maintain the traditional use of a linear stress strain relationship but incorporate adjustments to overall building deformations and material acceptance criteria to permit better consideration of the probable non-linear characteristics of seismic response.

1.3.2.1. Equivalent static analysis

The equivalent static analysis also referred as lateral force method is the simplest procedure used to assess the seismic response of structures. This analysis is based on the linear-elastic behaviour of the structure and may be applied to buildings whose response is not significantly affected by the contributions from modes of vibrations higher than the fundamental mode in each principal direction. Here the system is accurately modelled by a single degree of freedom system and the equivalent static forces are computed as shown in figure 1.14. In the figure, m_i represent the storey masses, s_i correspond to the displacements of masses in the fundamental mode, z_i are the height of each storey from the base and Fi are the equivalent horizontal forces applied at the height of each floor. According to EC8, they are related by the equation **(1.2)** ($\boldsymbol{s_i}$ and $\boldsymbol{s_j}$ can be replaced by $\boldsymbol{z_i}$ and $\boldsymbol{z_j}$ respectively).

$$\boldsymbol{F_i = F_b \cdot \frac{s_i \cdot m_j}{\sum s_j \cdot m_j}} \qquad \textbf{(1.2)}$$

A classical static analysis can be performed under action of these equivalent static forces. This method is an approximative method, which is adequate for certain types of structures (regular buildings) and ground motions (having natural periods close to the fundamental period of vibration of the structure). Contrary, the results of this procedure can be very inaccurate when applied to a building with a highly irregular structure system, unless the building is capable of response to seismic loads in a nearly elastic manner. When the contribution of higher modes of vibration is significant, this method is not conservative. In these cases, a complete dynamic response spectrum analysis is advisable.

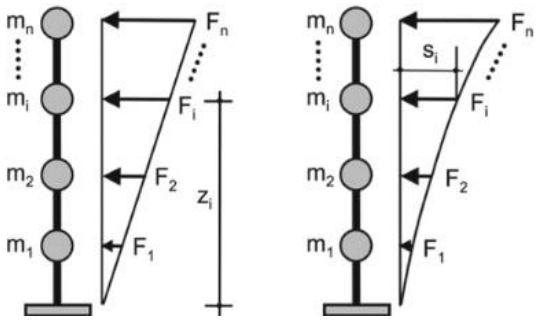

Figure 1.14. Distribution of the total earthquake force Fb over the building height **(Giresini & Butenweg, 2019)**

1.3.2.2. Modal response spectrum analysis

The modal response spectrum analysis is the standard procedure of the modern seismic design codes, and it is applicable for all type of buildings. The modal response spectrum approach considers the dynamic response of the building but is not computationally as expensive as a non-linear analysis. It aims to directly give the maximum effects of earthquake in various elements of the structure. The general method, called also the multi-modal method, consists on computing the various modes of vibration of the structure and the maximum response of each mode with reference to a response spectrum by determining the lateral distribution of seismic forces for each mode and the corresponding internal forces.

The response of all modes of vibration significantly contributing to the global response has to be taken into account. This means that only modes with effective modal masses greater than 5% of the total mass must be considered. The sum of the effective modal masses for the modes taken into account must amount to at least 90% of the total mass of the structure.

The structure response can be defined as a combination of significant modes (i = 1,2…N). A rule is then used to combine the responses E_{Ei} of these different modes. For this reason, the method is also known as the superposition modal response method. For the combination of these modal responses, two methods are generally used:

- The square root of the sum of the squares (SRSS) of forces and displacements. This modal combination rule provides excellent response estimates for structures with well-separated natural frequencies. The SRSS rule is applied using equation **(1.3)**.

$$E_E \cong \sqrt{\sum E_{Ei}^2} \qquad \textbf{(1.3)}$$

- The complete quadratic combination (CQC) of modal responses. It is an accurate method which is based on random vibration theories in order to minimize the introduction of avoidable errors. The CQC rule is applied using equation **(1.4)**.

$$E_E \cong \sqrt{\sum_i \sum_j \rho_{ij} \cdot E_{Ei} \cdot E_{Ej}} \qquad (1.4)$$

where E_{Ei} and E_{Ej} are the seismic effects of the modes i and j and ρ_{ij} is the correlation coefficient between the modes i and j**.**

There are computational advantages in using the response spectrum method of seismic analysis for the prediction of member forces and displacements in structural systems. But the use of the response spectrum method has some limitations, being only an approximate method. The first approximation refers to the use of spectra given for a single degree of freedom system, valuable only for the first vibration mode, to determine the structural response for the superior vibration modes. The second one is that it is restricted to linear elastic analysis, in which the damping properties can only be estimated with low degree of confidence. The third one refers to the procedure of superposition of different response modes, in which, due to the sum of square values, the sign of the values disappears (Gioncu & Mazzolani, 2010).

1.3.3. Non-linear methods

1.3.3.1. Non-linear static (pushover) analysis

A non-linear static analysis allows a more accurate estimation of the inelastic structure response than linear methods using behaviour factors, since the deformation of the plastic effects and the redistribution of forces are considered. We distinguish two different approaches in pushover analysis: traditional and modal (adaptative) pushover analysis. Here, the modal pushover method proposed by Chopra and Goel (2001) based on the structural dynamics is used.

The pushover analysis estimates the overall building load-carrying capacity by means of a non-linear load-displacement curve determined under monotonously increasing horizontal loads while the vertical loads are kept constant. Such an investigation is commonly called "pushover analysis". The resulting non-linear load-displacement curve is shortly denoted as pushover curve. Figure 1.15 depicts the pushover curve of a three-storey frame representing the total base shear F_b as a function of the roof displacement Δ_{top}. Eurocode 8-1 (2004) and numerous international standards and guidelines propose the pushover analysis as one of the standard non-linear calculation methods.

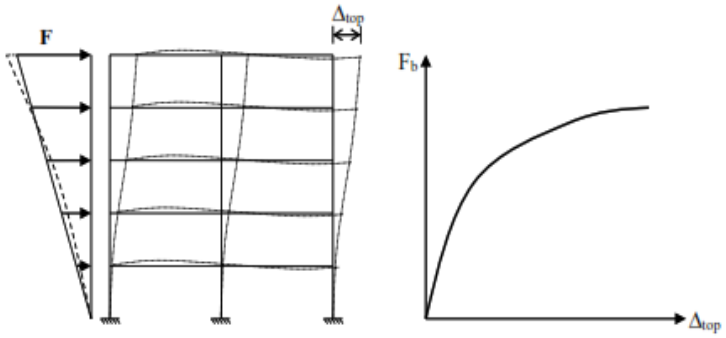

Figure 1.15. Non-linear pushover curve (Giresini & Butenweg, 2019)

The pushover curve approximates the way the structure behaves after exceeding the elastic limit and shows that the structure has 4 levels of damage (see figure 1.16):

- Immediate Occupancy: elastic behaviour (no damage);
- Life Safety: minor damage is likely to develop;
- Collapse Prevention: advanced state of damage with no resisting capacity;
- Collapse: Collapse of the structure.

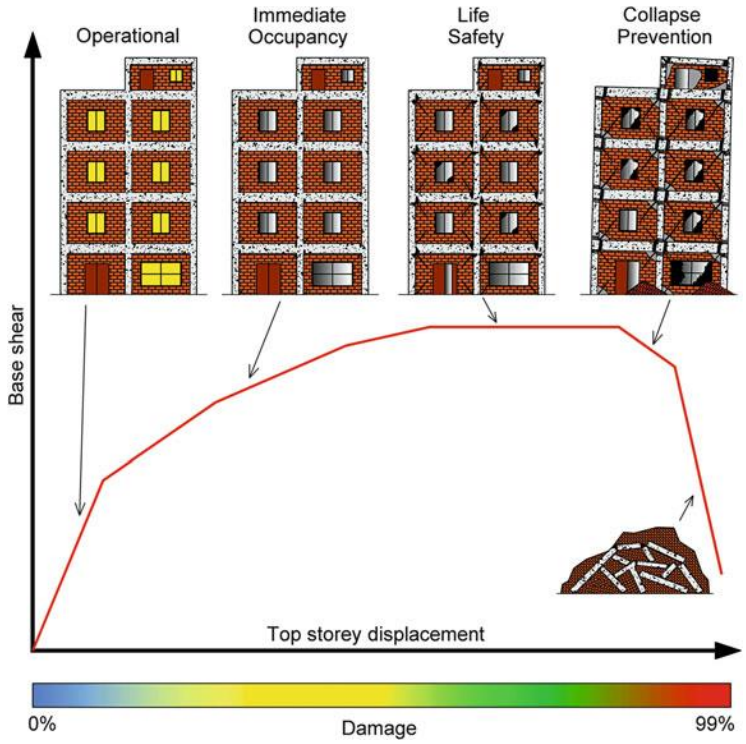

Figure 1.16. Levels of damage described by pushover curve (Avramidis et al., 2016)

In addition, pushover analysis is expected to provide information on many response characteristics, which cannot be obtained from an elastic static and dynamic analysis (Krawinkler & Seneviratna, 1998); some of them are:

- identification of the critical regions where the deformation demands are expected to be higher and which must become the focus of thorough detailing;

- estimation of inter-story drifts which account for strength or stiffness discontinuities;
- estimation of the ductility demands for elements which have to deform inelastically in order to dissipate the induced seismic energy.
- estimation of the expected plastic mechanism and the distribution of damage.

The pushover analysis procedure is generally considered more realistic in gauging the seismic vulnerability of structures than the existing code procedures which are "force-based". Although the procedure is "displacement-based" and threats non-linearity in a more explicit manner, the proposed procedure suffers from several fundamental deficiencies. One of them is that the pushover analysis procedure implies that there is a separation between the structural capacity and earthquake demand. There are numerous research findings which establish that the structural capacity and earthquake demand are interrelated. It is incorrect to assume that there is a unique, intrinsic structural capacity irrespective of the earthquake demand. Non-linear structural behaviour is load path dependent, and it is not possible to separate the loading input from the structural responses (Bertero, 1991).

1.3.3.2. Non-linear dynamic (time-history) analysis

Non-linear dynamic analyses of MDOF oscillators are procedures for evaluating the dynamic response of structures over time. Such analyses are the most accurate calculation methods in that they simulate the transient behaviour of structures considering their non-linear material behaviour. Indeed, the practical application of non-linear dynamic analyses is limited as they are computationally expensive, and the huge amount of the produced time-dependent results is not easy to use for the subsequent dimensioning of the structural elements. However, in some cases a detailed non-linear time-history analysis can be reasonable. The structural response can be obtained through a direct numerical integration of the differential equations of motion. The number of accelerograms to be used as inputs must be at least three and Eurocode 8-1 (2004) proposes in section 3.2.3.1.2 the following three types:

- Artificial accelerograms: generated to match the elastic site specific response spectra for 5% viscous damping. The minimum duration should be 10 s.
- Recorded accelerograms: real seismic records recorded by stations can be used provided that they are adequately qualified with respect to the seismogenetic features of the sources and to the soil conditions appropriate to the site. The records must be scaled to the value of a_gS for the earthquake zone under consideration.

- Simulated accelerograms: accelerograms generated by site-specific hazard analysis considering parameters such as seismic sources, rupture types, site characteristics and the travel path mechanism (Plevris et al. 2017).

The use of the artificial time-history representation seems to be very promising for structural design time-history analysis. The method is based on the direct numerical integration of the motion differential equations. In this aim, different algorithms can be adopted, where the elasto-plastic deformation of the structure must be considered.

1.4. Ductility of reinforced concrete buildings

The biggest "revolution" in seismic codes probably concerns ductility design. Experience had shown that the design of elastic structures was substantially costly and made this design principle unworkable and economically unacceptable. Ductility design then became widely used and accepted by the community.

1.4.1. Generalities on ductility

1.4.1.1. Definition of ductility

Ductility is defined as the ability of a material, component, connection or structure to undergo inelastic deformations with acceptable stiffness and strength reduction, as well as the capacity to dissipate earthquake energy through hysteric loops. Ductility is a desirable property in reinforced concrete as it induces redistribution of stresses and can give a warning of impeding failure.

Figure 1.17 compares the structural response of brittle and ductile systems. In the figure, curves A and B express force–displacement relationships for systems with the same stiffness and strength but distinct post-peak (inelastic) behaviour. Brittle systems fail after reaching their strength limit at very low inelastic deformations in a manner similar to curve A. The collapse of brittle systems occurs suddenly beyond the maximum resistance, denoted as Vmax, because of lack of ductility. Conversely, curve B corresponds to large inelastic deformations which are typical of ductile systems. Whereas the two response curves are identical up to the maximum resistance Vmax, they should be treated differently under seismic loads. The ultimate deformations δu corresponding to load level Vu are higher in the curve B with respect to curve A, that is $\delta_{u,B} \gg \delta_{u,A}$ (Gioncu & Mazzolani, 2010).

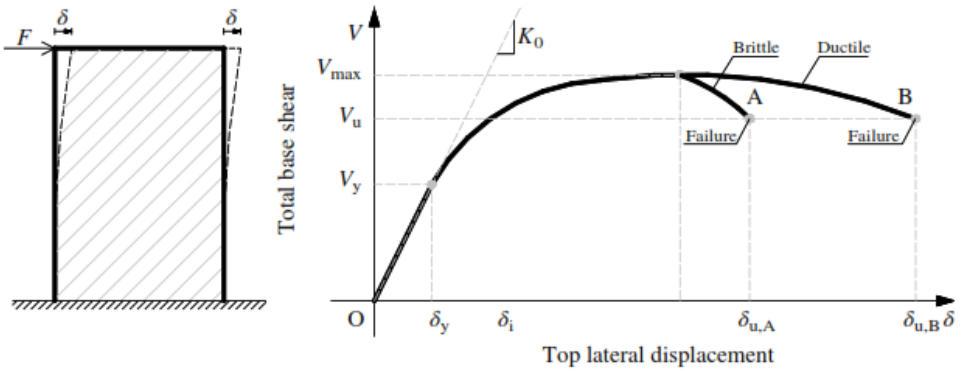

Figure 1.17. Definition of structural ductility **(Gioncu & Mazzolani, 2010)**

Figure 1.18 shows examples of brittle and ductile failures in reinforced concrete structural members. On the left is a brittle failure of a column caused using inappropriate reinforcement. On the right is a ductile failure of a viaduct pier. The arrangement of the longitudinal and transverse reinforcement very close together and of moderate cross-section allows good plasticity or ductility of the reinforced concrete.

Figure 1.18. Examples of brittle and ductile failures in reinforced concrete (Balandier, 2004)

Most structures are designed to behave inelastically under strong earthquakes for reasons of economy. The response amplitudes of earthquake-induced vibrations are dependent on the level of energy dissipation of structures, which is a function of their ability to absorb and dissipate energy by ductile deformations.

The general analytical definition of displacement ductility is given in equation **(1.5)**.

$$\mu = \frac{\Delta_u}{\Delta_y} \qquad \textbf{(1.5)}$$

where Δ_u and Δ_y are displacements at ultimate and yield points, respectively. The displacements Δ may be replaced by curvatures, rotations, or any deformational quantity. The ratio μ in equation **(1.5)** is referred as the "ductility coefficient".

In seismic design, high available level of ductility is essential to ensure plastic redistribution of actions among components of lateral resisting systems and to allow for large absorption and dissipation of earthquake input energy.

Ductile systems may withstand extensive structural damage without collapsing or endangering life safety; this corresponds to the 'collapse prevention' limit state. Structural collapse is caused by earthquakes which may impose ductility demand μ_{dem} that may exceed the available ductility μ_{cap} of the structural system. Imminent collapse occurs when $\mu_{dem}>\mu_{cap}$.

1.4.1.2. Ductility demand and ductility capacity

Allowing for a structure to sustain damage under the "design seismic action" implies that, under this action, the structure exhibits significant inelastic deformations beyond its yielding deformation without collapsing (ductile behaviour). This highlights two important concepts related to ductility: ductility demand μ_{dem} and ductility capacity μ_{cap}.

a. Ductility demand

The ductility demand is the peak ductility that a yielding building will exhibit under a specific earthquake induced strong ground motion without any partial or global collapse. In other words, this is the ductility "demanded" by the particular strong ground motion (seismic action) to avoid failure. It depends not only on the properties of the building, but also on the characteristics of the considered strong ground motion (e.g., peak ground acceleration, duration, frequency content, etc.). According to Avramidis et al. (2016), the ductility demand coincides with the reduction factor between the design seismic load and the load that the structure would have to be designed to remain elastic, the behaviour factor q.

b. Ductility capacity

In case a building exhibits inelastic behaviour without failing under a specific earthquake ground motion, it can be stated that the ductility demand μ_{dem} posed by this particular ground motion to the structure is smaller than the ductility capacity μ_{cap} of the structure.

1.4.1.3. Factors influencing ductility

Several factors may influence the ductile response of a building. Gioncu and Mazzolani, (2010) present the most common factors which are the material properties, the section properties, the member property and the system properties.

a. Material properties

The ductility of structural systems significantly depends on the material response. Inelastic deformations at the global level require that the material possesses high ductility. Concrete and masonry are brittle materials. They exhibit sharp reductions of strength and stiffness after reaching the maximum resistance in compression. Both materials possess low tensile resistance which is followed by abrupt loss of strength and stiffness. The material ductility μ_ε can be expressed as shown is equation **(1.6)**.

$$\mu_\varepsilon = \frac{\varepsilon_u}{\varepsilon_y}. \qquad \textbf{(1.6)}$$

Where:

ε_u the ultimate strain;

ε_y the strain at yield.

Consequently, the ductility μ_ε of concrete and masonry in tension is equal to unity, while μ_ε is about 1.5–2.0 in compression. For concrete, the higher the grade the lower is the inelastic deformation capacity. To enhance the ductility of concrete structure, confinement provided by transverse steel reinforcement can be used.

b. Section properties

The ductile response of cross-sections of structural members subjected to bending moment is generally measured by the curvature ductility μ_χ, which is defined in equation **(1.7)**.

$$\mu_\chi = \frac{\chi_u}{\chi_y} \qquad \textbf{(1.7)}$$

Where:

χ_u the ultimate curvatures;

χ_y the yield curvatures.

In reinforced concrete (RC) buildings, the curvature ductility significantly depends on the ultimate concrete compressive strain ε_{cu}, the compressive concrete strength f_{ck}, the yield strength of the steel reinforcement bars f_{yk}, the stress ratio f_u/f_{yk} of reinforcement steel, the ratio of compression-to tension steel A'_s/A_s and the level of axial load $\nu = N/A_c f_c$.

The variation of μ_χ with the aforementioned design parameters, for practical values of RC cross-section dimensions and steel reinforcement layouts, is summarized in table 1.3.

Table 1.3 Variation of curvature ductility in RC members (Gioncu and Mazzolani, 2010)

Parameters	Curvature ductility	
	Increment	Decrement
Ultimate concrete compressive strain (ε_{cu})	↑	↓
Compressive concrete strength (f_c)	↑	↓
Reinforcement steel yield strength (f_y)	↓	↑
Overstrength of steel reinforcement (f_u/f_y)	↑	↓
Percentage of steel in compression (A'_s/A_s)	↑	↓
Level of axial load ($\nu = N/A_c f_c$)	↓	↑

↑ = increase and ↓ = decrease.

c. Member properties

An adequate metric for ductile behaviour of structural members is the rotation ductility factor μ_θ computed using equation **(1.8)**.

$$\mu_\theta = \theta_u/\theta_y \quad \textbf{(1.8)}$$

Where:

θ_u and θ_y are the ultimate and yield rotations, respectively.

Inelasticity is concentrated in flexural plastic hinges at the ends of beams and columns. It is often assumed that curvatures within plastic hinges are constant thus allowing plastic rotations θ_p to be expressed using equation **(1.9)**.

$$\theta_p = \chi_p L_p \quad \textbf{(1.9)}$$

Where:

χ_p is the plastic curvature and L_p the length of the plastic hinge.

The ductility of a frame member depends on the spreading of inelasticity which takes place in the region corresponding to the plastic hinge of length Lp.

To ensure adequate rotational ductility (e.g., $\mu_\theta \geq 10–15$) in flexural plastic hinges, it is necessary to carefully detail critical regions (plastic hinges). For example, in RC members, it is essential to provide closely spaced stirrups which effectively confine the concrete and use sufficient lap splices and anchorage lengths.

d. System properties

The most convenient parameter to quantify the global ductility of structural systems under earthquake loads is the displacement or translation ductility μ_δ which is defined as given in equation **(1.5)**.

1.4.2. Capacity design method

As highlighted in this section, in seismic design of buildings, ductility is of major importance, since the performance of the building under seismic action relies on its capacity to deform beyond the elastic range. Thus, to take full advantage of the favourable effect of the plasticity of the structure, a particular dimensioning method aimed at ensuring the adequate ductile behaviour of the building has been developed, the capacity design method.

1.4.2.1. Presentation of the capacity design method

This method was developed in the 1970s by Professors T. Paulay and R. Park of Christchurch University in New Zealand and is adopted in many seismic design standards such as Eurocode 8. It defines a hierarchical designation of the types of failure mechanism and their location within the lateral load-resisting structural system to maximize seismic input energy dissipation through ductile behaviour. In other words, the method can be stated as follows: The engineer dictates to the structure where it "'must" plasticize and where it "must not". The engineer chooses the areas where the plastic deformations should be concentrated (plastic hinges) in the case of an earthquake. These areas are designed to accommodate these deformations, thereby dissipating energy, but without threatening the structure's ability to carry vertical loads. The rest of the structure is reinforced to ensure that it remains in an elastic state even as the plastic hinges develop their effective strength (Lestuzzi et al., 2008).

The capacity design method can be readily visualized by means of plain, statically determined chain structure comprising links of different strength shown in figure 1.19. The strength capacity of this chain (i.e., the peak static external force that the chain can resist) is equal to the strength F of its weakest link. If this specific link is brittle, the chain fails in a brittle manner, that is, suddenly, without exhibiting any significant inelastic deformation first. However, if the weakest chain link is ductile, then the chain yields under an externally applied force F prior to breaking, exhibiting (large) plastic deformation. In the case of seismic/cyclic dynamic applied loads, such a failure entails (large) dissipation of seismic energy (Avramidis et al., 2016).

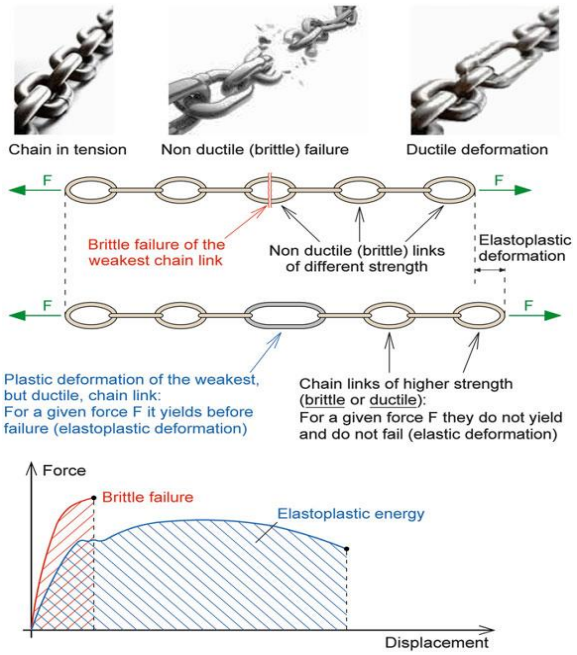

Figure 1.19. Fundamental concept of the capacity design (Avramidis et al., 2016)

1.4.2.2. Capacity design rules for ductile global collapse mechanism

In case a large value of behaviour factor, which implies a high level of ductility, is adopted in design, several structural members must yield and deform far into the inelastic range under the design seismic action for the structure to withstand the input seismic forces.

In the case of pure moment resisting frame structural systems, three collapse mechanism can occur. The "desirable" plastic mechanism commonly referred to as the "beam-sway mechanism" is the one targeted via capacity design rules and requirements in code-compliant seismic design. The "storey-sway mechanism" due to a soft and/or weak storey and "column-sway mechanism" which seismic codes of practice aim to avoid by relying on both capacity design and conceptual design rules.

a. Beam-sway mechanism

The desirable beam-sway plastic mechanism develops upon plastic hinge formation at the ends of all beams and at the base of the columns of the ground storey. As shown in figure 1.20, the required rotation θ_1 at each one of the several plastic hinges of the beam-sway mechanism is much smaller than the required rotation θ_2 at the few plastic hinges of the storey-sway mechanism for the same top-storey peak displacement u_{tot}. Clearly, local ductility demands of the beam-sway mechanism are significantly smaller. Furthermore, it is easier to accommodate ductility demands of a beam-sway mechanism, since beams of typical building structures carry negligible axial force compared to columns due to the diaphragmatic action of floors. The low

axial load level positively influences the local ductility capacity of beams compared to that achieved by columns.

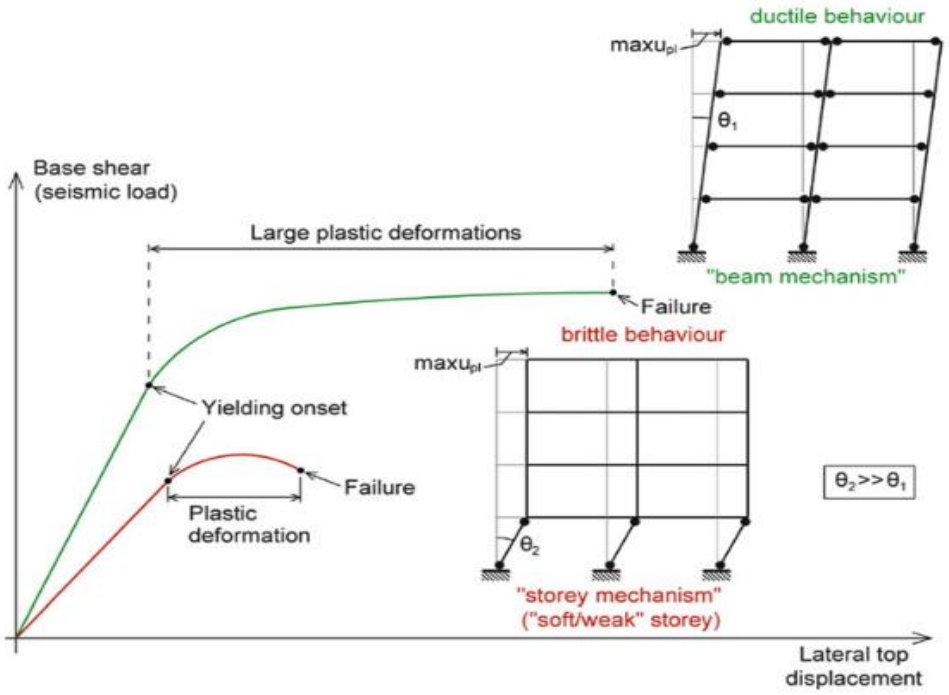

Figure 1.20. Moment frames: Unfavourable ‘‘storey mechanism’’ to be avoided (*red*) and favourable ‘‘beam mechanism’’ (*green*) (Avramidis et al., 2016)

Nevertheless, it is pointed out that, in a beam-sway mechanism, the base of the columns at the ground floor will eventually yield due to unavoidable high values of locally developed moments. Therefore, it is recommended to increase the flexural strength of the columns at the ground floor (beyond the strength required to accommodate calculated moments from the structural analysis step) to “delay” the formation of plastic hinges. Ideally, plastic hinges at the base of columns should form last, upon yielding of all the beams.

b. Storey-sway mechanism

The storey-sway mechanism is avoided by application of the well-established capacity design rule of “weak beams-strong columns” which needs to be verified/checked quantitatively (section 4.4.2.3 of EC8-1). In particular, at every joint, the column longitudinal reinforcement ratios should be computed such that the sum of the flexural strength capacity (peak bending moments calculated based on the longitudinal reinforcement) of columns is higher than the flexural strength capacity of beams accounting for the potential overstrength factors. This rule is verified using equation **(1.10).**

$$\sum M_{Rc} \geq 1.3 \sum M_{Rb} \qquad \textbf{(1.10)}$$

Where:

$\sum M_{Rc}$ is the sum of the design values of the moments of resistance of the columns framing joint;

$\sum M_{Rc}$ is the sum of the design values of the moments of resistance of the beams framing joint.

As a final note, it is emphasized that the development of a storey-sway mechanism must be avoided not only for the ground storey as shown in figure 1.20 for the sake of exemplification, but also for each storey of the building.

c. Column sway mechanism

The column sway mechanism involves plastic hinge formation at the ends of columns at all stories (see figure 1.21). Ensuring the reliable development of such a mechanism is very challenging at design, if not unfeasible. This is because the (time-varying during an actual earthquake) axial load carried by each column and, consequently, the flexural strength of each column changes significantly at each storey. In practice, the column-sway mechanism will most probably degenerate into a "storey-sway mechanism" at the weakest storey. Further, designing for a column sway mechanism is not practical, since repairing plastic hinges at columns is considered to be harder and more expensive than repairing plastic hinges at beams. For these reasons, capacity design to achieve column-sway mechanism should be avoided.

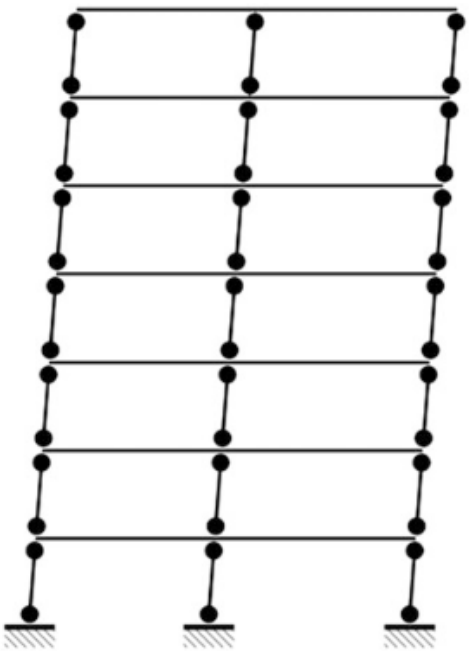

Figure 1.21. Unfavourable ''column-sway mechanism'' (Avramidis et al., 2016)

1.4.3. Ductility levels in seismic design standards

1.4.3.1. Behaviour factor

Currently, all seismic design codes are based on the forced-based design methodology using elastic analysis. The effect of inelastic energy dissipation is considered by reducing the design seismic force by a response reduction factor called behaviour factor. It has an important role in the estimation of the design force of a structure. Its value depends on the parameters that directly affect the energy dissipation capacity of the structure: the ductility, added viscous damping and strength reserves coming from its redundancy and the overstrength individual members.

Values of the behaviour factor provided different levels ductility to the buildings. Main codes used nowadays provide constant behaviour factors for a particular construction type. Eurocode 8, which will be used in this work, classifies the building ductility as Low (DCL), Medium (DCM), and High (DCH) according to the values of the behaviour factor. (Khose et al., 2012)

1.4.3.2. Ductility Class Low (DCL)

In this case, RC buildings are designed for low energy dissipation according to Eurocode 8 and they are designed according to Eurocode 2 without any additional requirement for seismic design/detailing except for the use of reinforcing steel of class B or C as defined in. table C.1 of EN1992-1-1:2004 (section 5.3.2 of EC8-1). Design of DCL reinforced concrete buildings is recommended only in geographic regions of low seismicity (sections 5.3.1 and 3.2.1(4) of EC8-1), and the maximum allowable behaviour factor q is 1.5 for all structural systems.

1.4.3.3. Ductility Class Medium and High (DCM and DCH)

The concepts discussed in sections 1.4.1.1 and 1.4.2 for achieving ductile RC structures are relevant in the case of EC8-compliant DCM and DCH buildings. Specifically, adequate (either "medium" or "high") ductility capacity, and, thus, capacity for seismic energy dissipation through inelastic behaviour, is aimed for by ensuring that local ductile failure modes (dominantly flexural) precede brittle failure modes (dominantly shear) with sufficient reliability and that ductility demands are uniformly distributed in plan and elevation across designated "critical" zones of structural members detailed for enhanced ductility capacity.

The design of DCM RC building structures involves satisfying the requirements and provisions included in clause 5.4 of EC8-1, while for DCH RC buildings, the additional (more stringent) requirements included in clause 5.5 of EC8-1 must be satisfied. The different levels

of ductility capacity achieved by DCM and DCH structures reflect the different maximum allowable behaviour factors q prescribed for each class in clause 5.2.2.2 of EC8. For DCM, the maximum allowable behaviour factor is 3.9 and for DCH the maximum allowable behaviour factor is 5.85.

Conclusion

The main objectives of this chapter were to introduce some notions of seismology both globally and locally (in Cameroon) and to present the different methods of analysis that can be performed on a tall reinforced concrete building subjected to an earthquake, considering its ductility. It was found that the seismic event can be measured by its intensity or magnitude and that Cameroon has 4 seismic regions namely the central, southern, coastal, and western parts of the country. To protect human lives and to limit structural damage to buildings, engineers have set up very advanced analysis methods taking into account the seismic action and the ductile behaviour of the building. In the following chapter, the modal response spectrum analysis and the pushover analysis will be applied to a tall building designed in two medium class ductility levels given the moderate seismic hazard in Cameroon.

CHAPTER 2. METHODOLOGY

Introduction

First, it is important to point out that it is not earthquakes that kill, but buildings that collapse on their occupants. This is because most buildings have been constructed without consideration of seismic aspects or, at best, with inappropriate methods. Today's building standards consider recent advances in earthquake engineering and include modern design methods that ensure favourable seismic behaviour of structures. This chapter will be structured around three analyses, the linear static analysis, the linear dynamic analysis through modal analysis using the response spectrum, and the non-linear static analysis through the pushover analysis for each level of ductility. These analyses will be presented in detail in this chapter along with the case study, the standards used, the types of materials, the acting loads, and the design parameters.

2.1. General site recognition

The general recognition of the site involves a site visit and documentary research to discover the general physical parameters of the site, such as its location, climate, relief, geology and hydrology.

2.2. Data collection

In this work, the project data collected will be classified into three types, architectural data, structural data, and geotechnical data.

2.2.1. Architectural data

The data collected here is intended to provide information on the geometry, configuration, extent, layout, specific use, and classification of the building. This data will be much more easily obtained through the various architectural plans available.

2.2.2. Structural data

The structural data collected informs us about the structural type of the building, the configuration of the structural elements and their cross-sections, the materials used and their properties.

2.2.3. Geotechnical data

Geotechnical data will be collected based on laboratory tests and site observations. These geotechnical data will be used mainly to determine the bearing capacity of the foundation soil to be considered in the calculations, to give recommendations concerning the foundations of the structure and finally to give the ground type.

2.3. Codes and standards

Many codes exist and are used around the world. The use of a code depends on the continent, country, or region where the project is located. For this study, the European Norm, also known as Eurocode, will be used. Depending on specific parameters such as the type of material, the type of design and others, there are different Eurocodes and each one consists of several parts.

The Eurocodes that will be used in this study are the following:

- Eurocode 0 or EN 1990: Basis of the structural design
- Eurocode 1 or EN 1991 : Actions on structures
- Eurocode 2 or EN 1992: Design of concrete structures
- Eurocode 7 or EN 1997: Geotechnical design
- Eurocode 8 or EN 1998: Design of structures for earthquake resistance

2.4. Evaluation procedure of actions

The classification of the action is defined in EN 1990. In this study we are interested by the seismic behaviour of the structure so three different types of loads are considered: the permanent loads, the variable-live loads, the wind actions, and the seismic action.

2.4.1. Permanent loads

These loads acting during the whole nominal life of the building with negligible variation of their intensity and constant in time. They are generally presented by the letter G and is constituted by:

- Permanent structural loads represented by G_{1k}, that are self-weight of structural elements
- Permanent non-structural loads represented by G_{2k}, that are self-weight of non-structural elements given by Eurocode 1.

2.4.2. Imposed loads

Imposed loads are those arising from occupancy. It includes normal use by people, the furniture and moveable objects and others. EN 1991 classifies building into different use categories and each category has a correspond imposed load represented by the letter Q. Table B. 1 of appendix B shows the classification of the use categories and table B.2 shows imposed loads for each category.

2.4.3. Wind actions

An important issue is to bring out an analytical expression for the wind action on a given surface. The wind actions on a structure are functions the building's dimensions and intrinsic properties of the wind. The former includes length, width, and height of the buildings while latter include wind's speed, terrain orography and topography. The wind pressure on our structure is calculated using the equations provided in EN 1991-1-4.

First, the basic wind velocity, v_b**,** shall be calculated using equation **(2.1).** Secondly, from the basic wind velocity, the peak and basic velocities pressures shall be determined using equations **(2.2)** and **(2.3)** respectively. Finally, the wind pressures on external surfaces and internal surfaces shall be determined using equations **(2.4)** and **(2.5)** respectively.

$$v_b = c_{dir} \times c_{season} \times v_{b,0} \quad \textbf{(2.1)}$$

$$q_b = \frac{1}{2} \times \rho_{air} \times v_b^2 \quad \textbf{(2.2)}$$

$$q_p(z) = c_e(z) \times q_b \quad \textbf{(2.3)}$$

$$w_e = q_p(z_e) \times c_{pe} \quad \textbf{(2.4)}$$

$$w_i = q_p(z_i) \times c_{pi} \quad \textbf{(2.5)}$$

Where:

c_{dir} and c_{season} are respectively the directional and season factors. EN 1991-1-4 recommends these values to be taken as 1.0;

$v_{b,0}$ is the fundamental wind velocity, given by Syros (1994) as $22.0 m/s$;

$\rho_{air} = 1.25 kg/m^3$ air density;

$c_e(z)$ is the exposure factor, function of height above terrain and the terrain category (table B.4 of Appendix B);

z_e is the reference height for the external pressure;

c_{pe} is the pressure coefficient for the external pressure;

z_i is the reference height for the internal pressure;

c_{pi} is the pressure coefficient for the internal pressure.

2.4.4. Horizontal seismic actions

Within the scope of EN 1998, the earthquake motion at a given point on the surface is represented by the elastic ground acceleration response spectrum, henceforth called an "elastic response spectrum". The seismic action has three components, which are two horizontal components and one vertical component. In this work, the focus will be on the horizontal components as these are the ones that cause the most significant damage in majority of cases.

The horizontal seismic action is described by two orthogonal components assumed as being independent and represented by the same response spectrum. For the horizontal components of the seismic action, the elastic response spectrum $S_e(T)$ is defined by the following expressions:

$$0 \le T \le T_B: \quad S_e(T) = a_g \cdot S \cdot \left[1 + \frac{T}{T_B} \cdot (\eta \cdot 2.5 - 1)\right] \tag{2.6}$$

$$T_B \le T \le T_C: \quad S_e(T) = a_g \cdot S \cdot \eta \cdot 2.5 \tag{2.7}$$

$$T_C \le T \le T_D: \quad S_e(T) = a_g \cdot S \cdot \eta \cdot 2.5 \left[\frac{T_C}{T}\right] \tag{2.8}$$

$$T_D \le T \le 4s: \quad S_e(T) = a_g \cdot S \cdot \eta \cdot 2.5 \left[\frac{T_C T_D}{T^2}\right] \tag{2.9}$$

Where:

$S_e(T)$ is the horizontal elastic response spectrum;

T is the vibration period of linear single-degree-of-freedom system (SDOF);

a_g is the design ground acceleration on type A ground ($a_g = \gamma_1 \cdot a_{gR}$);

T_B is the lower limit of the period of the constant spectral acceleration branch;

T_C is the upper limit of the period of the constant spectral acceleration branch;

T_D is the value defining the beginning of the constant displacement response range of the spectrum;

S is the soil factor

η is the damping correction factor with a reference value of $\eta = 1$ for 5% viscous damping; $\eta = \sqrt{10/(5+\xi)} \ge 0$

ξ is the viscous damping ratio

The values of the periods T_B, T_C and T_D and the soil factor S describing the shape of the elastic response spectrum depend upon the ground type (see table B.7 and table B.8 of Appendix B).

2.4.5. Loads combination

EN 1990 gives the following combinations of loads depending on whether the verification is for the ultimate limit state (ULS) or the serviceability limit state (SLS). The ULS are divided into the following categories:

- EQU Loss of equilibrium of the structure;
- STR Internal failure or excessive deformation of the structure or structural member;
- GEO Failure due to excessive deformation of the ground;
- FAT Fatigue failure of the structure or structural members.

For the purposes of this study, only the STR and GEO ultimate limit state will be considered.

2.4.5.1. Combination for ULS design

The combination of actions for persistent or transient design situations (fundamental combinations) at ULS is given by:

$$\sum_{j\geq 1} \gamma_{G,j}\, G_{k,j} + \sum_{j\geq 1} \gamma_{Q,1}\, Q_{k,1} + \sum_{i>1} \gamma_{Q,i}\, \psi_{0,i} Q_{k,i} \qquad \textbf{(2.10)}$$

Where:

$G_{k;j}$ is the characteristic value of the permanent action j;

$Q_{k;1}$ is the characteristic value of the leading variable action 1;

$Q_{k;i}$ is the characteristic value of the accompanying variable action;

ψ is the combination factors that is function of the use category of the building (see Table B. 3 of Appendix B).

The coefficients $\gamma_{G,j}$ and $\gamma_{Q,i}$ are partials factors which minimize the action which tends to reduce the solicitations and maximize the one which tends to increase it. The recommended values preconized by the EN 1990 for structural (STR) and geotechnical (GEO) verifications are:

- $\gamma_{G,j,sup} = 1.35$ and $\gamma_{G,j,inf} = 1$
- $\gamma_{Q,1} = 1.5$ for unfavourable conditions and 0 for favourable
- $\gamma_{Q,i} = 1.5$ for unfavourable conditions and 0 for favourable

2.4.5.2. Combination for SLS verification

The combinations of actions for serviceability limit states are defined symbolically by the following expressions:

- **Characteristic or rare combination**, normally used for irreversible limit states:

$$\sum_{j\geq 1} G_{k,j} + Q_{k,1} + \sum_{i>1} \psi_{0,i} Q_{k,i} \qquad \textbf{(2.11)}$$

- **Frequent combination**, normally used for reversible limit states:

$$\sum_{j\geq 1} G_{k,j} + \psi_{1,1} Q_{k,1} + \sum_{i>1} \psi_{1,i} Q_{k,i} \qquad \textbf{(2.12)}$$

- **Quasi-permanent combination**, normally used for long-term effects and the appearance of the structure:

$$\sum_{j\geq 1} G_{k,j} + \psi_{2,1} Q_{k,1} + \sum_{i>1} \psi_{2,i} Q_{k,i} \qquad \textbf{(2.13)}$$

Where $\psi_{0,i}$, $\psi_{1,i}$ and $\psi_{2,i}$ are combination coefficient given in EN 1990.

2.4.5.3. Seismic combination

Lateral seismic forces imposed on a structure due to strong ground motion are mass proportional. Therefore, apart from the intensity of the ground motion (expressed in terms of the design spectrum), nominal (design) mass/inertial structural properties need to be specified as well to determine the seismic effects according to equation **(2.14)**.

$$\sum_{j\geq 1} G_{k,j} + \sum_{i\geq 1} \psi_{E,i} Q_{k,i} \qquad \textbf{(2.14)}$$

With $\psi_{E,i}$ is the combination coefficient for variable action given as $\psi_{E,i} = \varphi \cdot \psi_{2,i}$.

The design value E of the effects of actions in the seismic design situations shall be determined in accordance with EN 1990. It is classified as an ‘accidental’’ action and the total design action combination, which includes permanent and variable actions together with the seismic action, is defined in equation **(2.15).**

$$\sum_{j\geq 1} G_{k,j} + E + \sum_{i\geq 1} \psi_{E,i} Q_{k,i} \qquad \textbf{(2.15)}$$

Let Ex and Ey be the seismic forces in the x and y directions respectively. The different combinations of loading of the seismic action are presented in equation **(2.16)**.

$$\begin{aligned} &\mathbf{1.00 \cdot E_x" + " 0.30 \cdot E_y} \\ &\mathbf{0.30 \cdot E_x" + " \ 1.00 \cdot E_y} \end{aligned} \qquad \textbf{(2.16)}$$

where " + " implies “to be combined with”.

2.5. Durability and concrete cover

The material used is the reinforced concrete made of concrete and steel (rebar and stirrups). EN 1992 states that the durability of a structure shall meet the requirements of serviceability, strength and stability throughout its design working life, without significant loss of utility or excessive unforeseen maintenance. The required protection of the structure shall be established by considering its intended use, working life, maintenance program and actions.

The possible significance of direct and indirect actions, environmental conditions and consequential effects shall be considered. In particular, corrosion protection of steel reinforcements depends on thickness of concrete cover. The necessary cover depends on the grade of concrete, the exposure conditions and the required fire resistance. EN 1992 defines it as being the distance between the surface of the reinforcement closest to the nearest concrete surface (including links and stirrups and surface reinforcement where relevant) and the nearest concrete surface as we can see in figure 2.1.

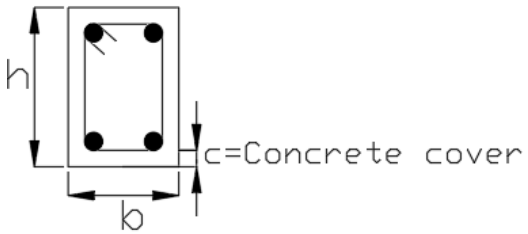

Figure 2.1. Illustration of the concrete cover

The nominal value of the concrete cover is defined as a minimum cover C_{min} plus an allowance in the design for deviation ΔC_{dev} with a recommended value of 10 mm, as shown in equation **(2.17)**.

$$C_{nom} = C_{min} + \Delta C_{dev} \qquad \textbf{(2.17)}$$

The minimum concrete cover C_{min} is defined in equation **(2.18)**.

$$C_{min} = \max\left(C_{min,b}; C_{min,dur} + \Delta C_{dur,\gamma} - \Delta C_{dur,st} - \Delta C_{dur,add}; 10mm\right) \qquad \textbf{(2.18)}$$

With:

$C_{min,b}$: the minimum cover due to bond requirement, equal to the diameter of the bars or the equivalent diameter in the case of bundled bars (see table B.9Table B. 9 of Appendix B);

$C_{min,dur}$: minimum cover due to environmental conditions which depends on the exposure and the structural class of the building (see table B.10 of Appendix B);

$\Delta C_{dur,\gamma}$: the additive safety element with a recommended value of 0;

$\Delta C_{dur,st}$: reduction of minimum cover for use of stainless steel, without specifications, the recommended value is 0;

$\Delta C_{dur,add}$: reduction of minimum cover for use of additional protection, without specification, the recommended value is 0;

2.6. Linear static analysis and design methodology

The linear static analysis studies the behaviour of the structural elements under static loads only; but because – to some extent – reinforced concrete is a plastic material, a limited redistribution of the elastic moments is sometimes allowed. In this section, the procedures to analyse, design and verify beams and column line elements according to Eurocodes 2 and footings according to Eurocode 7 are presented.

2.6.1. Analysis and design of beams

Beams are horizontal structural elements. They support the loads from slab, walls, other beams and sometimes columns. They transfer the loads to the columns supporting them. Beams can be simply supported, continuous, or cantilevered.

Reinforced concrete beam design consists primarily of producing member details which will adequately resist the ultimate bending moments and shear forces. At the same time serviceability requirements must be considered to ensure that the member will behave satisfactory under working loads. It is difficult to separate these two criteria, hence the design procedure consists of a series of interrelated steps and checks. These steps are condensed into three basic stages (Mosley et al., 2012).

2.6.1.1. Preliminary analysis and determination of solicitations

The strength of a beam is affected considerably more by its depth than its width. The span-depth ratios usually vary between 14 and 30 but for large spans the ratios can be greater. The beam

should not be too narrow; if it is less than 20 cm wide, there may be difficulty in providing adequate side cover and space for the reinforcing bars.

Suitable dimensions for width (b) and depth (h) can be determined with the help of equations **(2.19)** to **(2.21)** for specific cases:

- For simply supported beams

$$h \geq \frac{L}{14} \; and \; b \cong 0.5\, h \qquad \textbf{(2.19)}$$

- For cantilevered beams

$$h \geq \frac{L}{18} \; and \; b \cong 0.5\, h \qquad \textbf{(2.20)}$$

- For embedded beams

$$h \geq \frac{L}{20} \; and \; b \cong 0.5\, h \qquad \textbf{(2.21)}$$

Where L, is the longest span of the beam.

After determining the size of the element, the solicitations due to loads acting on the beam (bending moment and shear force) are determined. Several load arrangements will be used and they will give different solicitations diagrams, which will allow to represent the envelope curve.

2.6.1.2. Detailed analysis and design of reinforcement

This step consists of determining the cross-sections and the longitudinal and transverse steel sections and arrangements to be used in the selected beam so that it can resist the maximum loads presented on the envelope curve at any point.

a. Design for bending moment

i. The design diagrams

Bending moment acting on the beam is mainly resisted by the longitudinal reinforcement. Hence, the amount of longitudinal reinforcements needed is obtained through the envelope curve of the bending moment. For continuous beams, the value of the reduction is function of the connection between the beam and the support as shown in figure 2.2.

Where a beam is monolithic with its supports, the critical design moment at the support should be taken as that at the face of the support as presented in point 1 of the figure 2.2. Where a beam is continuous over a support as shown in point 2 in figure 2.2, the analysis is done considering that the support does not provide a rotational restraint. The amount of this reduction is defined in equation **(2.22)**, whereby $F_{ED,sup}$ is the design support reaction and t is the breadth of the support.

$$\Delta M_{ED} = F_{ED,sup} \cdot t/8 \qquad \textbf{(2.22)}$$

The final diagram obtained after this transformation is called the design diagram.

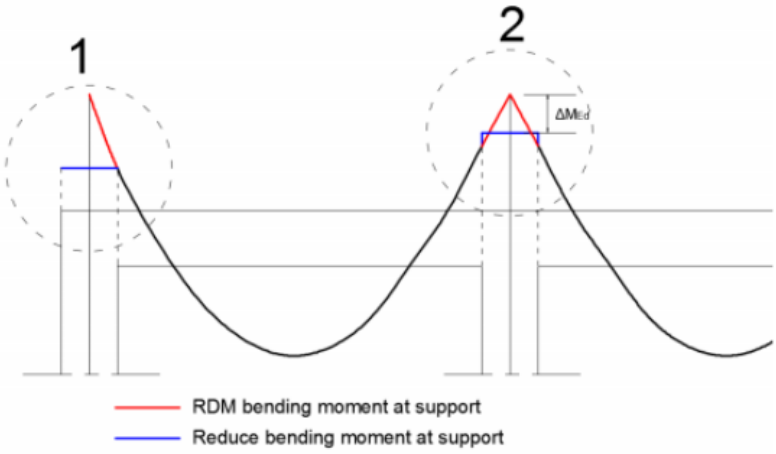

Figure 2.2. Reduction of the bending moment at support (Djeukoua,2019)

ii. The longitudinal steel reinforcement

Under bending moment, the lower fibre is in tension at the span and the upper fibre at the supports. Due to the low tensile strength of concrete, it is necessary to adequately reinforce these areas, especially with longitudinal reinforcement. The quantity of steel reinforcement is computed for a rectangular cross-section with height h, width b and effective depth d as shown in figure 2.3.

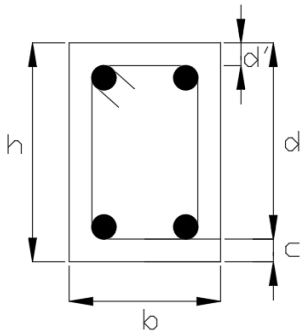

Figure 2.3. Cross-section of the beam

The procedure to determine the amount of steel reinforcement is given below step by step:

(1). Determination of X_{lim}

The neutral axis is the boundary between the tension and compression zones of the beam section as shown in figure 2.4. It depends on the material properties of the section.

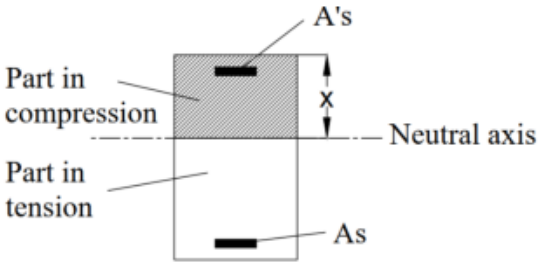

Figure 2.4. Neutral axis position

X_{lim} is the neutral axis limit, is when the concrete has reached its compressive strength and the steel has reached its yield strength. It is obtained using equation **(2.23)**.

$$X_{lim} = \frac{\varepsilon_{cu}}{\varepsilon_{cu} + \varepsilon_{yd}} \cdot d \qquad \textbf{(2.23)}$$

With:

ε_{cu} the ultimate strain of concrete;

ε_{yd} the yield strain of steel;

d the effective depth;

(2). Determination of the limit bending moment ($M_{Rd,lim}$) of the section

The limit resisting bending moment $M_{Rd,lim}$ with tensioned reinforcement only is calculated using equation **(2.24)**, whereby Fc is the resultant of compression stresses and Z_{lim} is the inner lever arm (distance between the resultant of compression stress and the tension stress in the section) as shown in figure 2.5.

$$M_{Rd,lim} = Fc \cdot Z_{lim} \qquad \textbf{(2.24)}$$

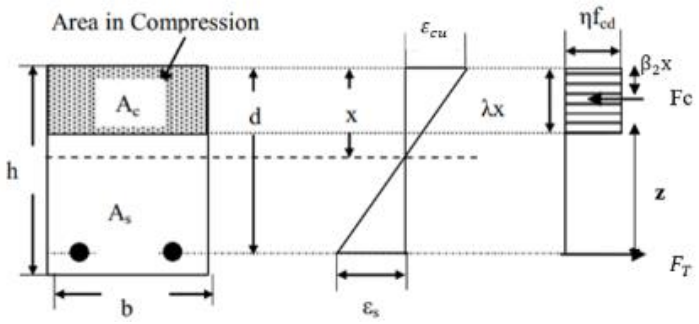

Figure 2.5. Simplify rectangular stress and strain distribution

Fc and $\boldsymbol{Z_{lim}}$ are defined in equations **(2.25)** and **(2.26)** respectively.

$$F_C = f_{cd} \cdot \beta_1 \cdot X_{lim} \cdot b \qquad \textbf{(2.25)}$$

$$Z_{lim} = d - \beta_2 \cdot X_{lim} \qquad \textbf{(2.26)}$$

With:

f_{cd} the design compressive strength of the concrete

β_1 the ratio between the area of the parabola-rectangle diagram at certain deformation and the area of rectangle at the same deformation, $\beta_1 = \lambda \cdot \eta = 0.8$;

β_2 the position factor, $\beta_2 = \lambda/2 = 0.4$.

(3). Determination of the section of longitudinal reinforcement

- If $\mathbf{M_{Rd,lim}} > \mathbf{M_{Ed}}$,

The reinforcement is need only on the lower fibre of the section (As). The neutral axis of the section undergoing the bending moment M_{Ed} is determined using equation **(2.27)** and the reinforcement steel As is obtained using equation **(2.28)**

$$x = \frac{d}{2\beta_2} - \sqrt{\left(\frac{d}{2\beta_2}\right)^2 - \frac{M_{Ed}}{\beta_1 \cdot \beta_2 \cdot b \cdot f_{cd}}} \quad \textbf{(2.27)}$$

$$A_s = \frac{M_{Ed}}{f_{yd} \cdot z} \quad \textbf{(2.28)}$$

With $z = (d - \beta_2 \cdot x)$;

- If $\mathbf{M_{Rd,lim}} \leq \mathbf{M_{Ed}}$,

The reinforcement is need both in the lower (As) and upper fibre (As') of the section. To determine As and As', we start by determine ΔM_{Ed} by equation **(2.29)**, after we determine As' by equation **(2.30)** and finally, we determine As by equation **(2.31)**.

$$\Delta M_{Ed} = M_{Ed} - M_{Rd,lim} \quad \textbf{(2.29)}$$

$$A'_s = \frac{\Delta M_{Ed}}{f_{yd} \cdot (d - d')} \quad \textbf{(2.30)}$$

$$A_s = \frac{M_{Rd,lim}}{f_{yd} \cdot z_{lim}} + A'_s \quad \textbf{(2.31)}$$

Here an alternative procedure will be to increase the depth of the concrete section in such a way that there is no need of reinforcement in the upper fibre.

(4). Basic verifications

After determining the longitudinal reinforcement that resits to the bending moment, some basic verifications should be done. Those verification concerns the minimum and maximum reinforcement areas and the spacing of the bars.

The area of longitudinal tension reinforcement should not be taken as less than $A_{s,min}$ and the cross-sectional area of the tension or compression reinforcement should not exceed $A_{s,max}$. The recommended values of $A_{s,min}$ and $A_{s,max}$ for beams are given in equations **(2.32)** and **(2.33)** respectively.

$$A_{s,min} = 0.26\frac{f_{ctm}}{f_{yk}} b_t d \quad \text{but not less than } 0.0013 b_t d \quad \textbf{(2.32)}$$

$$A_{s,max} = 0.04A_c \quad \textbf{(2.33)}$$

Where:

b_t denotes the mean width of the tension zone;

f_{ctm} mean tensile strength of the concrete;

A_c cross-sectional area of the concrete.

The spacing of bars shall be such that the concrete can be placed and compacted satisfactorily for the development of adequate bond. The maximum clear distance Cs_{max} (horizontal and vertical) between individual parallel bars or horizontal layers of parallel bars is define by the formula in equation **(2.34)**, whereby k1 and k2 are respectively equal to 1 and 5 mm, and dg is the maximum size of aggregate.

$$Cs_{max} = \max\{k_1 \cdot d_g\ , (d_g + k_2)\ , 20\}\ mm \quad \textbf{(2.34)}$$

b. Design for shear

In elements such as slabs, footing and thin walls, it is often very inconvenient to provide shear reinforcement. In beams and columns, due to the various shear failure models, some shear reinforcement (stirrups) will always be provided. EN 1992 presents two methods of analysis and design for shear, the standard and the variable inclination method of stirrups. Here we will use the standard method whose procedure is the following:

(1). Determination of the shear capacity of concrete without reinforcement

The shear capacity of the concrete can be estimated as follows:

$$V_{Rdc} = \left[C_{Rd,c}k(100\rho_1 f_{ck})^{1/3} + k_1\sigma_{cp}\right]b_w d \ \geq \ \left[\nu_{min} + k_1\sigma_{cp}\right]b_w d \quad \textbf{(2.35)}$$

Where:

f_{ck} is the characteristic compressive strength of concrete in MPa

$C_{Rd,c}$ = $0.18/\gamma_c$ with γ_c the partial safety factor of concrete (assumed =1.5)

k = $1 + \sqrt{\frac{200}{d}} \leq 2.0$ with d in mm

ρ_1 = $\frac{A_{sl}}{b_w d} \leq 0.02$ reinforcement ratio corresponding to longitudinal steel area A_{sl}

k_1 = 0.15

σ_{cp} = N_{sd} / A_c, the average stress in the concrete due to the axial compressive force N_{sd}, with A_c the concrete area;

ν_{min} =$0.035k^{3/2}f_{ck}^{1/2}$

(2). Comparison between shear force on the section and shear capacity of the concrete without stirrups

The first step for shear verification consists of determining if the shear capacity of the concrete V_{Rdc} can be enough to resist shear force V_{Ed}.

- If $\boldsymbol{V_{Ed} \leq V_{Rdc}}$

Specific shear reinforcement is not required, and the minimum quantity must be adopted. The minimum shear reinforcement and maximum spacing is given respectively by equations **(2.36)** and **(2.37)**.

$$\frac{A_{s,min}}{s} = \frac{0.8 \cdot f_{ck}^{0.5} \cdot b_w}{f_{yk}} \quad \textbf{(2.36)}$$

$$S_{max} = \min\left(0.8 \cdot d\,;3\ stirrups/m\right) \quad \textbf{(2.37)}$$

- If $\boldsymbol{V_{Ed} > V_{Rdc}}$

Shear reinforcement should be provided and the area of the shear reinforcement and their spacing are determined using equation **(2.38)**

$$\frac{A_{sw}}{s} = \frac{V_{Ed}}{0.9 \cdot d \cdot f_{ywd}} \quad \textbf{(2.38)}$$

Where:

f_{ywd} is the design yielding strength of the shear reinforcement;

A_{sw} is the cross-sectional area of the shear reinforcement;

s is the spacing of the stirrups;

2.6.1.3. Serviceability Limit State (SLS) verification

The serviceability limit states (SLS) are the states beyond which requirements for the correct exercise and use of the structure are not satisfied. The common SLS for verification of reinforced concrete section, according to EN 1992-1, are stress limitation, cracking control and deflection control. SLS verifications are performed in the most critical section.

a. Stress limitation

High compression stresses in the concrete can lead to microcracking and durability problems. High stresses in the reinforcement can imply high crack widths and durability problems. According to EN 1992, the compressive stress in concrete shall be determined in order to avoid longitudinal cracks, micro-cracks or high level of creep, where they result in unacceptable effects on the

function of the structure, the characteristic combination and the quasi-permanent combination of loads are used for this verification; quasi-permanent is usually use for long term effects. The stress value is function of the modular ratio in short terms and long terms expressed in equation **(2.39)** and **(2.40)** respectively.

$$n_0 = \frac{E_s}{E_c} \tag{2.39}$$

$$n_\infty = n_0(1 + \varphi_L \cdot \varphi_\infty) \tag{2.40}$$

Where φ_L= 0.55 for shrinkage of concrete and parameter $\varphi_\infty = 2 \div 2.5$

The procedure for the stress limitation verification is as follows

(1). Determination of the position of the neutral axis of the uncracked concrete section

The position of the neutral axis is given by equation **(2.41).**

$$x = \frac{n(A_s + A'_s)}{b} \cdot \left[-1 + \sqrt{\frac{2b(A_s \cdot d + A'_s \cdot d')}{n(A_s + A'_s)^2}}\right] \tag{2.41}$$

Where A_s and A'_s are respectively the upper and lower steel reinforcement in the section; and b, d, and d' are the geometrical characteristics of the section presented in figure 2.3.

(2). Determination of the moment of inertia of the uncracked section

The moment of inertia is given by equation **(2.42).**

$$I = \frac{bx^3}{3} + nA'_s(x - d')^2 + nA_s(d - x)^2 \tag{2.42}$$

(3). Determination of the stress in concrete and steel

The stress in concrete and steel are given by equations **(2.43)**, **(2.44)** and **(2.45)**.

$$\sigma_c = \frac{M}{I} \cdot x \tag{2.43}$$

$$\sigma_s = n \cdot \frac{M}{I} \cdot (d - x) \tag{2.44}$$

$$\sigma'_s = n \cdot \frac{M}{I} \cdot (x - d') \tag{2.45}$$

(4). Verifications

The last step of the procedure consists to verify that the stress in concrete and limit for the different combinations are beyond the limits using equations **(2.46)**, **(2.47)** and **(2.48)**.

For characteristic combination of loads: $\sigma_c \leq 0.6 f_{cm}$ **(2.46)**

For quasi permanent combination of loads: $\sigma_c \leq 0.45 f_{cm}$ **(2.47)**

For characteristic combination of loads: $\sigma_s \leq 0.8 f_{yk}$ **(2.48)**

b. Deflection control

Deformation of a member or a structure shall not be such that it adversely affects its proper functioning or appearance. High displacements, deformations can produce damage in non-structural element and affect the comfort of the occupants. Appropriate limiting values of deflecting considering the nature of the structure, of the finishes, partitions and fixings and upon the function of the structure should be established.

According to EC2, limit state of deformation may be checked by either limiting the span/depth ratio or by comparing a calculated deflection with a limit value. In this work, the first method will be use.

(1). Determine the limiting span/depth ratio

The limiting span/depth ratio may be estimated using equations **(2.49)** or **(2.50)** and multiplying this by correction factors to allow for the type of reinforcement used and other variables.

$$(l/d)_{lim} = K\left[11 + 1.5 \cdot \sqrt{f_{ck}}\frac{\rho_0}{\rho} + 3.2 \cdot \sqrt{f_{ck}}\left(\frac{\rho_0}{\rho} - 1\right)^{3/2}\right] \; if\ \rho \leq \rho_0 \qquad \textbf{(2.49)}$$

$$(l/d)_{lim} = K\left[11 + 1.5 \cdot \sqrt{f_{ck}}\frac{\rho_0}{\rho - \rho'} + \frac{1}{12} \cdot \sqrt{f_{ck}}\sqrt{\frac{\rho'}{\rho_0}}\right] \quad if\ \rho > \rho_0 \qquad \textbf{(2.50)}$$

Where:

$(l/d)_{lim}$ is the limit span/depth;

K is the factor to consider the different structural systems (see table B. 12 of Appendix B);

ρ_0 is the reference reinforcement ratio = $\sqrt{f_{ck}}10^{-3}$;

ρ and ρ' is the required tension and compression reinforcement ratio at mid-span to resist the moment due to the design loads (or at supports for cantilevers);

(2). Determine the correction factor for the limit span/depth

The equations **(2.49)** and **(2.50)** have been derived on the assumption that the steel stress, under appropriate design load at SLS at a cracked section at mid-span of a beam or slab or at the support of cantilever, is 310 MPa (corresponding roughly to f_{yk}= 500MPa). Where other stress levels are used, the values obtained using those equations should be multiplied by $310/\sigma_s$ which is calculated using equation **(2.51)**.

$$310/\sigma_s = 500/(f_{yk}A_{s,req}/A_{s,prv}) \quad \textbf{(2.51)}$$

Where:

σ_s is the tensile steel stress at mid-span (at support for cantilevers) under the design load at SLS quasi-permanent combination;

$A_{s,prv}$ is the area of steel provided at this section;

$A_{s,req}$ is the area of steel required at this section for ultimate limit state;

(3). Comparison between the actual span/depth ratio with the limit value

The deflection is tolerable if the equation **(2.52)** is verified.

$$\frac{l}{d} \leq ((l/d)_{lim} \cdot 310/\sigma_s) \quad \textbf{(2.52)}$$

c. Crack control

Cracks with widths can compromise the use of the structure. Cracking shall be limited to an extent that will not impair the proper functioning or durability or cause its appearance to be unacceptable. It is possible to conduct the verification with two methods: direct and indirect calculation. In this work, the direct calculation method will be used.

A limiting calculated crack width, w_{max}, considering the proposed function and nature of the structure and the costs of limiting cracking, should be established. The recommended values for relevant exposure classes are given in table B. 13 of Appendix B.

(1). Determine the maximum bar diameter of the longitudinal bars to be used to avoid limit cracking

To do this, table B. 14 of appendix B which presents the maximum diameter $\emptyset_s^*$ of the longitudinal reinforcements as a function of the stress acting on these bars and the maximum crack width, is used.

Once determined, it is sufficient to calculate the adjusted maximum bar diameter using equation **(2.53).**

$$\emptyset_s = \emptyset_s^* \left(\frac{f_{ct,eff}}{2.9} \cdot \frac{k_c h_{cr}}{2(h-d)} \right) \quad \textbf{(2.53)}$$

This value must be greater than the diameters of the longitudinal reinforcement we used in the design of the beam.

(2). Determine the maximum spacing between the longitudinal bars

Here the table B. 15 of Appendix B is used. It shows the maximum spacing between the longitudinal reinforcements according to their stresses and the maximum crack width.

2.6.2. Analysis and design of columns

The column in a structure carry load from the beams and slabs down the foundations, and therefore they are primarily compression members, although they must also have to resist bending forces due to the continuity of the structure (Mosley et al., 2012). Design of columns is governed by the ultimate limit state; deflection and cracking during service are not usually a problem, but nevertheless, correct detailing of reinforcement, adequate cover and slenderness verifications are important.

2.6.2.1. Preliminary analysis and determination of the solicitations

The preliminary static analysis consists first in the design of the column which consists in determining the dimensions of its section. According to EC8, in seismic area the value of the normalised axial force shall not exceed 0.65. Using this condition, the minimum section of the column can be estimated using equation **(2.54)** and after, the column dimensions can be defined.

$$\frac{N_{Ed}}{A_c f_{cd}} \leq 0.65 \qquad \textbf{(2.54)}$$

Where A_c is the area of the column section and N_{Ed} is the axial load computed using the influence area of the column;

Having the section of the column, the second part on the analysis consist in determining the solicitations on the columns. For this purpose, a 3D modelling of the building is necessary and it will be done with software SAP2000 v22. Different load arrangements are considered to obtain the envelope curve for each solicitation. The envelope curve will give the design loads which are:

- N_{Ed} the design axial load obtained by the envelope curve of axial solicitations;
- M_{top} and M_{bottom} are the design moments at the top and bottom of the column.

But before obtaining the maximum solicitations, a modal analysis (see section **2.8.2.1**) will be done on the building to validate the sections of the columns.

2.6.2.2. Slenderness verification

After determining the correct section of the column, the slenderness must be checked in order to know if second order effects have to be considered or not. It consists in verifying if the slenderness of the element is below a limit value, defined by EC2 in equation **(2.55)**.

$$\lambda_{lim} = 20 \cdot A \cdot B \cdot C / \sqrt{n} \qquad \textbf{(2.55)}$$

Where:

$A = \dfrac{1}{1 + 0.2 \cdot \varphi_{ef}}$ (A=0.7 if the effective creep ratio φ_{ef} is not known) **(2.56)**

$B = \sqrt{1 + 2\omega}$ ($\omega = \dfrac{A_s f_{yd}}{A_c f_{cd}}$, is the mechanical reinforcement ratio; B=1.1 may be used if ω is not known) **(2.57)**

$C = 1.7 - r_m$ ($r_m = \dfrac{M_{01}}{M_{02}}$, is the moment ratio of the first moments order at the end of the column) **(2.58)**

$n = N_{Ed}/(A_c f_{cd})$ is the relative normal force **(2.59)**

The slenderness of an element is evaluated by the formula given in equation **(2.60)**.

$$\lambda = \frac{l_o}{i} = \frac{l_o}{\sqrt{I/A_c}} \quad \textbf{(2.60)}$$

Where:

l_o is the effective height of the column;

i is the gyration radius about the axis considered;

I is the second moment area of the section about the axis;

2.6.2.3. Longitudinal reinforcement

For columns, there are several methods for determining the amount of the longitudinal reinforcements depending on whether the column is slender or not. The simplest method is the Design Charts Methods, that considers a symmetric distribution of longitudinal reinforcements.

If the column is not slender, that means $\lambda \leq \lambda_{lim}$, $M_{Ed} = M_{02}$ and we use the appropriate design chart to find the value of As required for N_{Ed} and M_{Ed}. The design will consist of determining the longitudinal reinforcement due to (Mx, N_{Ed}) and (My, N_{Ed}), with Mx and My the design bending moments around x-x and y-y axis of the section respectively (see figure 2.6).

The procedure for designing a rectangular section as shown in figure 2.7 using the design charts method, carried out in the same way in the x-x and y-y planes, is as follows:

(1). Determination of the appropriate design charts

The design chart is a diagram that express $\dfrac{A_s f_{yd}}{b h^2 f_{cd}}$ as function of $\dfrac{N}{b h f_{cd}}$ and $\dfrac{M}{b h^2 f_{cd}}$.

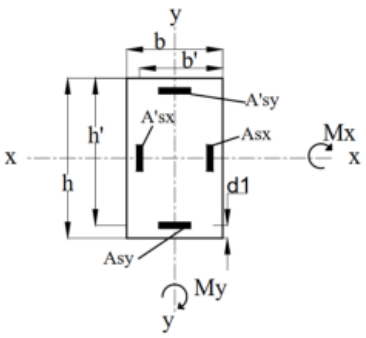

Figure 2.6. Section with biaxial bending (Tatcha, 2020)

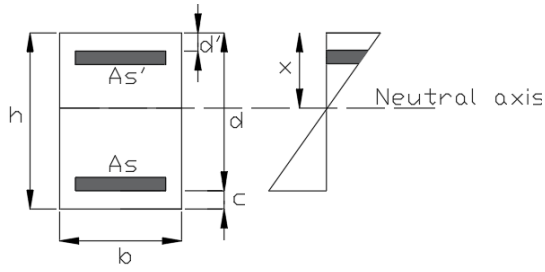

Figure 2.7. Column section

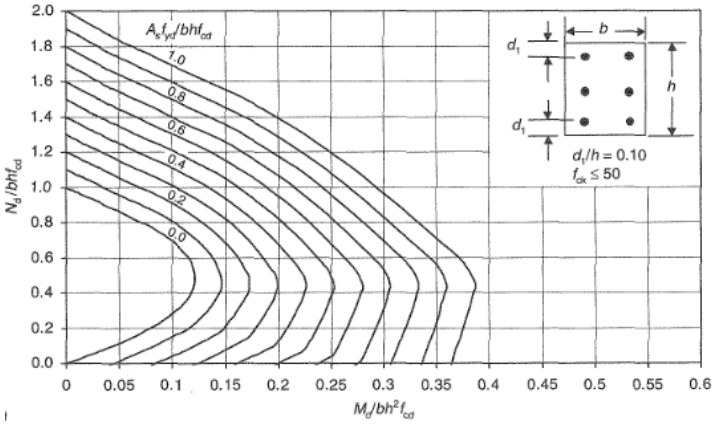

Figure 2.8. Example of rectangular design chart (Beeby & Narayanan, 2005)

It is possible to draw a design chart using equations **(2.61)** and **(2.62)** or to use the diagrams that have already been defined.

$$\frac{N}{bhf_{cd}} = \frac{0.56 \cdot s}{h} + \frac{f_{sc} \cdot A_s}{f_{ck} \cdot b \cdot h} + \frac{f_s \cdot A_s}{f_{ck} \cdot b \cdot h} \quad \textbf{(2.61)}$$

$$\frac{M}{bh^2 f_{cd}} = \frac{0.56 \cdot s}{h}\left(0.5 - \frac{s}{2h}\right) + \frac{f_{sc} \cdot A_s}{f_{ck} \cdot b \cdot h}\left(\frac{d}{h} - 0.5\right) - \frac{f_s \cdot A_s}{f_{ck} \cdot b \cdot h}\left(\frac{d}{h} - 0.5\right) \quad \textbf{(2.62)}$$

Where f_{sc} and f_s are the steel stress for steel in compression and in tension respectively. They are determined using equations **(2.63)** and **(2.64)** .

- If $\varepsilon_s < \varepsilon_{yd}$, then $f_s = E_s \cdot \varepsilon_s$ **(2.63)**
- If $\varepsilon_s \geq \varepsilon_{yd}$, then $f_s = f_{yd}$ **(2.64)**

The equations are not suitable for direct solution and the design with symmetrical reinforcement in each face is best carried out using predefined design charts as illustrated in figure 2.8. They depend on the properties of the cross-section, materials and reinforcement arrangements. The cross-section property is function of the shape of the section (circular or rectangular) and the ratio d_1/h for the rectangular section The material property is reduced to the concrete class.

(2). Determination of the corresponding point

The corresponding point has coordinates given in equation **(2.65)**.

$$\left(\frac{N_{Ed}}{bhf_{cd}};\frac{M}{bh^2f_{cd}}\right) \quad \textbf{(2.65)}$$

(3). Determination of the ratio $\frac{A_s f_{yd}}{bh^2 f_{cd}}$ using the chart

The point determined in **(2)** is represented in the design chart and allows the value of the ratio $\frac{A_s f_{yd}}{bh^2 f_{cd}}$ to be determined by interpolation with its curves.

(4). Determination of As

From the ratio obtained in step 3, we can easily come out the value of As.

This procedure is carried out in the x and y direction with the moments Mx and My respectively. It must also be considered that the depth (h) and effective depth of the section changes depending on whether the x or y axis is considered.

The recommended value for the minimum and maximum longitudinal area of reinforcement following EN 1992-1 is given by equations **(2.66)** and **(2.67)** respectively.

$$A_{s,min} = \max\left(\frac{0.1N_{Ed}}{f_{yd}}; 0.002 \cdot A_c\right) \quad \textbf{(2.66)}$$

$$A_{s,max} = 0.4 \cdot A_c \quad \textbf{(2.67)}$$

The design chart method is an approximate method to determine the amount of longitudinal reinforcement in a column section. To ensure its effectiveness, it is necessary to check the section design by the M-N interaction diagram.

2.6.2.4. The M-N interaction diagram

The M-N interaction diagram is a diagram that shows all the limit situation that can determine the failure of the section. The points which are lying onto the diagram represent the limit configuration: beyond them, failure occurs. This diagram is computed by determining 6 significant points, and each point is formed by a couple (N_{Rd}; M_{Rd}), where N_{Rd} and M_{Rd} are the resisting axial force and the resisting moment of the cross-section respectively. The procedure is presented below considering a rectangular section presented in figure 2.7.

a. First point

The section is assumed to be completely in tension; the concrete does not react. $\varepsilon_s = \varepsilon_{su}, \varepsilon'_s > \varepsilon_{yd}$ and coordinates of the first point are obtain using equations **(2.68)** and **(2.69)**.

$$N_{Rd} = -A_s \cdot f_{yd} - A'_s \cdot f_{yd} \quad \textbf{(2.68)}$$

$$M_{Rd} = A_s \cdot f_{yd} \cdot \left(d - \frac{h}{2}\right) - A'_s \cdot f_{yd} \cdot \left(d' - \frac{h}{2}\right) \quad \textbf{(2.69)}$$

b. Second point

The section is completely subjected to traction. $\varepsilon_s = \varepsilon_{ud}$, $\varepsilon_c = 0$ and ε'_s and N_{Rd} are calculated using equations **(2.70)** and **(2.71)** respectively.

$$\varepsilon'_s = \varepsilon_{ud} \cdot {}^{d'}/_{d} \quad \textbf{(2.70)}$$

$$N_{Rd} = -A_s \cdot f_{yd} - A'_s \cdot f'_s \quad \textbf{(2.71)}$$

f'_s is defined according to equation **(2.63)** and **(2.64)** and M_{Rd} is calculated using equation **(2.69)**.

c. Third point

The failure is imposed to be due to concrete and the lower reinforcements is yielded. $\varepsilon_s > \varepsilon_{yd}$, $\varepsilon_c = \varepsilon_{cu2}$ and the position of the neutral axis x and ε'_s are determined using equations **(2.72)** and **(2.73)** respectively. The coordinates of this point are determined using equations **(2.74)** and **(2.75)**.

$$x = d \cdot \varepsilon_c / (\varepsilon_c + \varepsilon_s) \quad \textbf{(2.72)}$$

$$\varepsilon'_s = \varepsilon_c \cdot (x - d')/x \quad \textbf{(2.73)}$$

$$N_{Rd} = bs \cdot f_{cd} + A'_s \cdot f_{sc} - A_s \cdot f_{yd} \quad \textbf{(2.74)}$$

$$M_{Rd} = A_s \cdot f_{yd} \cdot \left(d - \frac{h}{2}\right) + A'_s \cdot f_{yd} \cdot \left(d' - \frac{h}{2}\right) + bs \cdot f_{cd} \left(d' - \frac{h}{2}\right) \quad \textbf{(2.75)}$$

f_{sc} is defined according to equation **(2.63)** and **(2.64)**.

d. Fourth point

The failure is imposed to be due to concrete and the lower reinforcement reaches exactly the value $\varepsilon_s = \varepsilon_{yd}$. The neutral axis x and ε'_s are determine using equations **(2.72)** and **(2.73)** respectively. The resisting axial force and the resisting moment is determine using equations **(2.74)** and **(2.75)**.

e. Fifth point

The failure is imposed to be due to concrete and no strain in As ($\varepsilon_s = 0$). The neutral axis position will be equal to the effective depth of the section and ε'_s is determined using equation **(2.70)**. The coordinates of this point is determined using equations **(2.76)** and **(2.77)**.

$$N_{Rd} = bs \cdot f_{cd} + A'_s \cdot f_{sc} \quad \textbf{(2.76)}$$

$$M_{Rd} = A'_s \cdot f_{sc}\left(d' - \frac{h}{2}\right) + bs \cdot f_{cd}\left(\frac{h}{2} - \frac{s}{2}\right) \quad \textbf{(2.77)}$$

f. Sixth point

The section uniformly compressed and $\varepsilon_s = \varepsilon'_s = \varepsilon_c = \varepsilon_{c2}$. The resisting axial force is determined using equation **(2.78)**.

$$N_{Rd} = bh \cdot f_{cd} + A'_s \cdot f_{yd} - A_s \cdot f_{yd} \quad \textbf{(2.78)}$$

M_{Rd} is calculate using equation **(2.69)**.

2.6.2.5. Shear verification

Just like the beam, the procedure goes same. Provisions given by the Eurocode 2 requires a minimum diameter of 6 mm or one quarter of the maximum diameter of the longitudinal bars. The maximum spacing of the transverse reinforcement is given by the equation **(2.79)**.

$$S_{cl,max} = \min\left(20\emptyset_{l,min}; b; 400mm\right) \quad \textbf{(2.79)}$$

Where:

$\emptyset_{l,min}$ is the minimum diameter of the longitudinal bars;

b is the lesser dimension of the column.

This maximum spacing must be reduced by a factor 0.6 in sections within a distance equal to the larger dimension of the column cross-section above or below the beam (Mosley et al., 2012).

2.6.3. Design of footings

A building is generally composed of a superstructure above the ground and a substructure which forms the foundation below ground. Foundations transfer and spread the load from a structure's column and walls into the ground. Foundations are generally of two types: shallow and deep foundations. In this work we will use shallow foundations, also designated as footings. Figure 2.9 presents an illustration of an isolated footing with details. The design of the footings will be done according to this illustration.

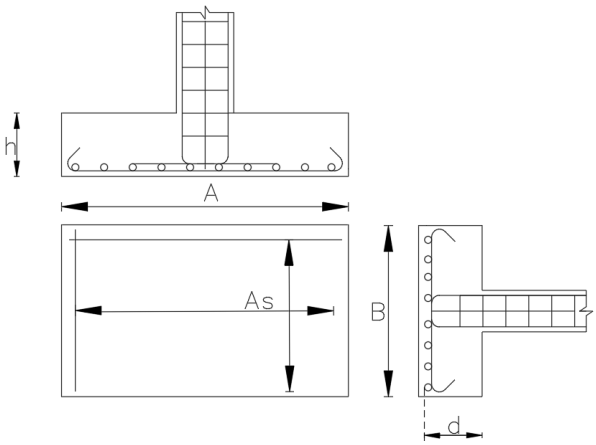

Figure 2.9 Isolated footing details

2.6.3.1. Preliminary analysis

This preliminary analysis consists first on calculate the plan size of the footing using the allowable bearing capacity and the critical load arrangement for the service ability limit state (SLS). The minimal base area is defined as shown in equation **(2.80)**.

$$A_{s,prov} \geq A_{s,req} = {}^{P_{SLS}}/_{q} \qquad \textbf{(2.80)}$$

Where:

$A_{s,prov}$ and $A_{s,req}$ base area of the footing provided and required respectively;

P_{SLS} design service load where the load is the service load added to the self-weight of the footing which from the start is taken as 10% of the service load;

q allowable bearing capacity.

Having determine the base area of the footing, the bearing pressure associated with the critical load arrangement at the ultimate limit state (ULS) is calculated using equation **(2.81)**.

$$q' = \frac{P_{ULS}}{A_{prov}} + \frac{6M}{AB^2} \qquad \textbf{(2.81)}$$

With:

P_{ULS} design ultimate vertical load;

M the acting moment;

q' ultimate pressure.

2.6.3.2. Determination of the thickness of the footing

First assume a suitable value of the thickness (h) and effective depth (d) of the footing. They are obtained using equation **(2.82)** and **(2.83)** respectively.

$$h \geq \max\left(\frac{A-a}{4}; \frac{B-b}{4}\right) \quad \textbf{(2.82)}$$

$$d = h - C_c \quad \textbf{(2.83)}$$

Where:

A and B are the footing dimensions;

a and b are the columns dimensions;

C_c is the concrete cover for the footings which is equal to 50 mm.

For the assumed value of the thickness, check that the shear force P_{ULS}, at the column face are less than a critical value defined in equation **(2.84)**.

$$P_{ULS} \leq 0.5 \cdot \nu_1 f_{cd} u d \quad \textbf{(2.84)}$$

Where:

ν_1 is the strength reduction factor, $\nu_1 = 0.6(1 - f_{ck}/250)$;

u is the perimeter of the column;

f_{cd} design compression strength of the concrete;

2.6.3.3. Determination of the reinforcements

The reinforcement should be determined according to the maximum bending at the critical section of the footing. The critical bending moment and the reinforcement are determined using equation **(2.85)** and **(2.86)** respectively.

$$M_{Ed,x} = \frac{1}{2} \cdot q' B \cdot \left(\frac{A-a}{2}\right)^2 \quad \textbf{(2.85)}$$

$$A_{sy} = \frac{M_{Ed,x}}{0.9d \cdot f_{yd}} \quad \textbf{(2.86)}$$

Where:

$M_{Ed,x}$ is the maximum bending moment at the critical section around x direction

A_{sy} is the reinforcement required parallel to y-axis.

The other parameters have been already described. The procedure should be done for $M_{Ed,y}$ also.

The minimum area of reinforcement is defined as shown is equation **(2.87)**.

$$\frac{A_{s,min}}{ad} \geq 0.26 \cdot \frac{f_{ctm}}{f_{yk}} \quad \textbf{(2.87)}$$

2.7. Design parameters for seismic analysis according to Eurocode 8

2.7.1. Centre of mass and centre of rigidity

Centre of mass and centre of rigidity are two important concepts in the analysis of a building. They enable the effects of the building configurations on the response of the structural systems to lateral forces to be better appreciated. While the centre of mass is given by the geometry of the building, the centre of rigidity is given by the pillars and the rigidity given by each pilar.

2.7.1.1. Centre of mass

The centre of a distribution of mass in space is the unique point where the weighted relative position of the distributed mass sums to zero or the point where if a force is applied causes it to move in the direction of force without rotation. The distribution of mass is balanced around the centre of mass and the average of the weighted position coordinates of the distributed mass defines its coordinates. In this case, the centre of mass is evaluated for each level according to the surfaces which are considered as shown in equation **(2.88)**.

$$\begin{Bmatrix} X_{CM} = \frac{\Sigma(A_i * x_i)}{\Sigma \mathrm{A_i}} \\ Y_{CM} = \frac{\Sigma(\mathrm{A_i} * y_i)}{\Sigma \mathrm{A_i}} \end{Bmatrix} \quad \textbf{(2.88)}$$

Where:

X_{CM} the abscissa of the centre of mass according to the origin;

Y_{CM} the ordinate of the centre of mass according to the origin;

$\mathrm{A_i}$ Area of the subdivided section i;

$\mathrm{x_i}$ the abscissa of the centre of gravity of the subdivided zone;

$\mathrm{y_i}$ the ordinate of the centre of gravity of the subdivided zone.

2.7.1.2. Centre of rigidity

The centre of rigidity of a floor is defined as the point on the floor such that the application of lateral load passing through that point does not cause any rotation of that floor, while the other floors may rotate. When the centre of rigidity is subjected to lateral loading, the floor diaphragm will experience only translational displacement. The formula to evaluate the centre of rigidity coordinates is define in equation **(2.89)**.

$$\begin{Bmatrix} X_{CR} = \frac{\Sigma(K_{yi} * x_i)}{\Sigma K_{\mathrm{yi}}} \\ Y_{CR} = \frac{\Sigma(\mathrm{K_{xi}} * y_i)}{\Sigma K_{\mathrm{xi}}} \end{Bmatrix} \quad \textbf{(2.89)}$$

Where:

X_{CR} the abscissa of the centre of rigidity according to the origin;

Y_{CR} the ordinate of the centre of rigidity according to the origin;

K_{xi} the rigidity of the frame i with respect to x axis (see equation (2.90));

K_{yi} the rigidity of the frame i with respect to y axis (see equation (2.90));

xi the abscissa of the frame i with respect to x axis;

yi the ordinate of the frame i with respect to y axis;

$$\begin{Bmatrix} K_{xi} = \sum \frac{12EI_{yy,i}}{h^3} \\ K_{yi} = \sum \frac{12EI_{xx,i}}{h^3} \end{Bmatrix} \quad \textbf{(2.90)}$$

Where:

EI is the flexural rigidity of the section;

h is the height of the frame.

2.7.1.3. Torsion and eccentricities

Torsion in buildings during earthquake shaking may be caused from a variety of reasons, the most common of which are non-symmetric distributions of mass and stiffness. Modern codes deal with torsion by placing restrictions on the design of buildings with irregular layouts and through the introduction of an accidental eccentricity that must be considered in design.

Two types of eccentricity must be distinguished for the analysis:

a. Structural eccentricity

This is the offset between the centre of mass and the centre of rigidity of the structure. In a simplified seismic analysis via 2D models, where typically the x and y directions are analysed separately, the impact of the structural eccentricity is considered by manually distributing the torsional effects on the structure. It is calculated using equation **(2.91)**.

$$\begin{cases} e_x = X_{CM} - X_{CR} \\ e_y = Y_{CM} - Y_{CR} \end{cases} \quad \textbf{(2.91)}$$

Where e_x and e_y are the values of the eccentricity according to x and y axis respectively.

b. Accidental eccentricity

The accidental eccentricity accounts for inaccuracies in the distribution of masses in the structure. Regardless of the selected method, the value of the accidental eccentricity must be specified. According to the EC8, to account for uncertainties in the location of masses and in the spatial variation of the seismic motion, the calculated centre of mass at each floor *i* shall be considered as being displaced from its nominal location in each direction by an accidental eccentricity defined in equation **(2.92)**.

$$e_{ai} = \pm 0{,}05 L_i \qquad \textbf{(2.92)}$$

Where:

e_{ai} is the accidental eccentricity of storey mass i from its nominal location, applied in the same direction at all floors;

L_i is the floor-dimension perpendicular to the direction of the seismic action.

2.7.2. Regularity of the structure

According to EC8, for the purpose of seismic design, building structures are categorised into being regular and non-regular. This distinction has implications in the structural model, the method of analysis and the value of the behaviour factor of the seismic design.

2.7.2.1. Criteria for regularity in plan

In general, the regularity in plan can be checked when the structural model is defined. The necessary criteria for regularity in plan are described in EN 1998-1 (4.2.3.2):

- with respect to the lateral stiffness and mass distribution, the building structure shall be approximately symmetrical in plan with respect to two orthogonal axes;
- at each level and for each direction of analysis x and y, the structural eccentricity e_0 and the torsional radius r shall be in accordance with the conditions given in equations **(2.93)** and **(2.94)**, which are expressed for the direction of analysis:

$$\boldsymbol{e_{0x} \leq 0.30 \cdot r_x \ and \ e_{0y} \leq 0.30 \cdot r_y} \qquad \textbf{(2.93)}$$

$$\boldsymbol{r_x \geq l_s \ and \ r_y \geq l_s} \qquad \textbf{(2.94)}$$

Where:

e_{0x} is the distance between the centre of stiffness and the centre of mass, measured along the x direction, which is normal to the direction of analysis considered;

r_x is the square root of the ratio of the torsional stiffness to the lateral stiffness in the y direction;

I_s is the radius of gyration of the floor mass in plan which is equal to the square root of the polar moment of inertia of the floor mass in plan with respect to the centre of mass of the floor to the floor mass.

- the ration between the larger and smaller sizes respectively in which the construction results also known as the slenderness of the building, shall be not higher than 4;
- the plan configuration shall be compact. If set-backs exist, the plan can be estimated as "compact" if the differential area is less than 5% of the total floor area.

2.7.2.2. Criteria of regularity in elevation

Most of the criteria concerning regularity in elevation are easy to understand and apply. The following conditions are required for a building to be classify as regular in elevation:

- All lateral load resisting vertical systems, such as cores, structural walls, or frames, shall run without interruption from the top of the building (or top of the setback) to the foundations;
- The lateral stiffness and mass of floors shall remain constant or reduce gradually (without abrupt changes) from the base to the top;
- The actual storey resistance (considering masonry infills) should not vary disproportionately between adjacent storeys.
- When setbacks are present, the following conditions given figure 2.10 shall be respected.

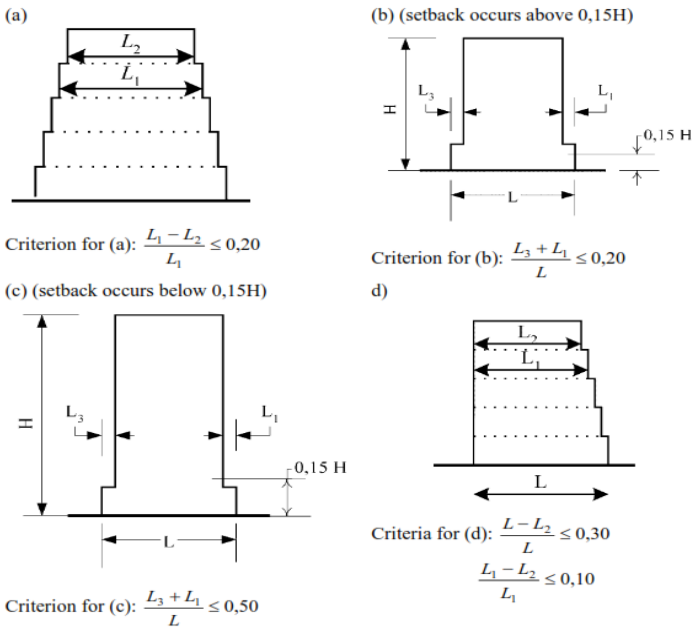

Figure 2.10. Criteria of regularity of buildings with setbacks (EN 1998-1)

2.7.3. Structural type and behaviour factor

2.7.3.1. Structural type of the building

Concrete buildings shall be classified into one of the following structural types according to their behaviour under horizontal seismic actions:

- frame system;
- dual system (frame or wall equivalent);
- ductile wall system (coupled or uncoupled)
- system of large lightly reinforced walls;
- inverted pendulum system;
- torsionally flexible system.

Except for those classified as torsionally flexible systems, concrete buildings may be classified to one type of structural system in one horizontal direction and to another in the other. The structural type of the building is related to the behaviour factor.

2.7.3.2. Behaviour factor

According to the required energy dissipation capacity, three ductility classes are considered in EC8: low (DCL), medium (DCM) and high (DCH) (see section **1.4.3**). For concrete buildings designed to provide energy dissipation capacity and overall ductile behaviour, only DCM and DCH are considered. In correspondence with the different levels of ductility available in the two ductility classes, different values of the behaviour factor q are used. The behaviour factor is a factor used for design purposes to reduces the forces obtained from a linear analysis to account for the non-linear response of the structure, associated with the material, the structural system and the design procedures. Its maximum allowable value is defined by the equation **(2.95)**.

$$q = q_0 \cdot k_w \qquad \textbf{(2.95)}$$

Where:

k_w is the factor reflecting the prevailing failure mode in structural systems with walls; $k_w = 1$ for frame and frame-equivalent systems;

q_0 is the basic value of the behaviour factor, dependent on the type of the structural system and on its regularity in elevation (see table 2.2);

Table 2.1. Basic value of the behaviour factor, $\boldsymbol{q_0}$, for systems regular in elevation (EN 1998-1:2004)

STRUCTURAL TYPE	DCM	DCH
Frame system, dual system, coupled wall system	$3.0\ \alpha_u/\alpha_1$	$4.5\ \alpha_u/\alpha_1$
Uncoupled wall system	3.0	$4.5\ \alpha_u/\alpha_1$
Torsionally flexible system	2.0	3.0
Inverted pendulum system	1.5	2.0

For buildings which are not regular in elevation, the value of q_0 should be reduced by 20%.

When the multiplicator factor α_u/α_1 has not been evaluated through an explicit calculation, for buildings which are regular in plan the following approximate values of α_u/α_1 may be used for frames or frame-equivalent dual systems:

- one-storey buildings: $\alpha_u/\alpha_1 = 1.1$;
- multi-storey, one-bay frames: $\alpha_u/\alpha_1 = 1.2$;
- multistorey, multi-bay frames or frame-equivalent dual structures: α_u/α_1=1.3

2.8. Analysis of the structure according to Eurocode 8

This section presents the steps of linear dynamic analysis and non-linear static analysis of the structural elements of the building when it is subjected to seismic action according to Eurocode 8. According to EC 8, the design of the structure is done for a specific level of ductility given by the choice of the behaviour factor. Considering the low to moderate seismic hazard in Cameroon, the choice of the behaviour factors will be made in the medium ductility class.

2.8.1. Design spectrum for elastic analysis

The capacity of structural systems to resist seismic actions in the non-linear range generally permits their design for resistance to seismic force smaller than those corresponding to a linear elastic response. To avoid explicit inelastic structural analysis in design, the capacity of the structure to dissipate energy, through mainly ductile behaviour of its elements and/or other mechanisms, is taken into account by performing an elastic analysis based on a response spectrum (see section **2.4.4**) reduced with respect to the elastic one, henceforth called a "design spectrum". This reduction is accomplished by introducing the behaviour factor q defined previously.

For the horizontal components of the seismic action, the design spectrum, $S_d(T)$, shall be defined using equations **(2.96)** to **(2.99)**.

$$0 \le T \le T_B: \quad S_d(T) = a_g \cdot S \cdot \left[\frac{2}{3} + \frac{T}{T_B} \cdot \left(\frac{2{,}5}{q} - \frac{2}{3}\right)\right] \tag{2.96}$$

$$T_B \le T \le T_C: \quad S_d(T) = a_g \cdot S \cdot \frac{2{,}5}{q} \tag{2.97}$$

$$T_C \le T \le T_D: \quad S_d(T) \begin{cases} = a_g \cdot S \cdot \frac{2{,}5}{q} \cdot \left[\frac{T_C}{T}\right] \\ \ge \beta * a_g \end{cases} \tag{2.98}$$

$$T_D \le T: \quad S_d(T) \begin{cases} = a_g \cdot S \cdot \frac{2{,}5}{q} \cdot \left[\frac{T_C T_D}{T^2}\right] \\ \ge \beta \cdot \mathrm{a_g} \end{cases} \tag{2.99}$$

Where:

a_g, S, T_B, T_C, T_D	are as defined in section **2.4.4**
$S_d(T)$	is the design spectrum;
q	is the behaviour factor which is function of the ductility class;
β	is the lower bound factor for the horizontal design spectrum; the recommended value is $\beta = 0.2$.

2.8.2. Modal response spectrum analysis

The modal response spectrum analysis is an elastic dynamic analysis method that allows to determine elastically the peak dynamic responses of all significant modes of the structure using the ordinates of the site dependent design spectrum. Generalities and principle of modal response spectrum analysis has been presented in section **1.3.2.2**. This section will focus in the application of this analysis in the case study.

2.8.2.1. Modal analysis

Modal analysis is indispensable to understand the behaviour of the structure to a dynamic action, it allows to understand how the structure vibrates by determining its modal properties, which are independent from the earthquake action. This analysis will be performed numerically using the software SAP2000 v22.

a. Modelling of the structure

The modelling of the structure, taking into account as correctly as possible the mass and stiffness of structural elements, is an essential phase for the study of the seismic response (Corvez & Davidovici, 2016).

The important elements in the modelling are those that affect the mass, strength, stiffness, and deformability of the structure. Those elements are the slab, the beams, the columns, and foundations. The beams and columns are modelled as frame elements and the weight, and the load of the slab are applied to the beams directly. The slab being considered rigid. In general, non-structural elements do not affect the stiffness and strength of a structure, but there are special elements such as stair and special infills that can significantly affect them and should not be overlooked.

Moreover, a particular emphasis is put on the modelling of foundations to simulate the real behaviour of the soil-structure interaction (SSI) during the different analyses. The SSI is defined as the process in which the response from the soil influences the motion of the structure and the response of the given structure affects the response from the soil. Thus, it is very important to consider this parameter when modelling the building. The approach used in this work to consider the SSI is based on Winkler's assumptions which assume the soil medium as a system of identical but mutually independent, closely, spaced, discrete linearly elastic springs. The stiffnesses of the springs are obtained from the modulus of subgrade reaction of the soil by equation **(2.100)**.

$$k_{zi} = 2 \cdot k_{xi} = 2 \cdot k_{yi} = C \cdot A_i \qquad \textbf{(2.100)}$$

Where:

$k_{xi}, k_{yi}\ and\ k_{zi}$ are the stiffness of the spring along x, y and z axis at the ith node;

C in kN/m^3 is the modulus of subgrade reaction given in table B.16 in Appendix B;

A_i in m² is the tributary area, the influence area of the ith node of a plate.

b. Determination of the modal properties

Once the material and cross-section of the different elements have been defined, the structure is modelled and thus the modal properties of the structure can be determined using the software. These properties include:

- The modal circular frequencies, ω, and period, T;
- The modal shape, Φ;
- The modal participation factor, Γ;
- The effective modal mass, m.

2.8.2.2. Response spectrum analysis

The modal response spectrum analysis will use the elastic and design response spectra of the earthquake to estimate the response of the structure for each of the useful vibration modes

obtained. The effective modal mass obtained by modal analysis will enabled the selection of the useful vibration modes. The response spectrum analysis consists of the following steps:

- Selection of the useful modes of vibration;
- Determination of the acceleration at the level of the ground;
- Combination of modal responses;
- Cumulation of the effects of the components of the seismic movement.

a. Selection of the useful modes

The modal analysis gives various vibration modes identifies by their eigen periods (or frequencies) and eigen forms. In practice, only a part of these modes will make a significant contribution to the response of the structure, and it is this set of modes that must be considered for the analysis. Generally, the effective modal mass is a good criterion to evaluate the importance of each of the modes and to select those for the analysis. The conditions use here is that the sum of the effective modal masses for the modes considered must be greater than or equal to 90% of the total mass of the structure.

b. Acceleration of the structure at the ground level

Due to the earthquake motion, the structure will be accelerated according to the modes of vibration it adopts. These accelerations are determined using the design response spectrum. Practically, the periods of the useful modes selected for analysis will be projected into the design response spectrum to determine the corresponding accelerations as a function of the acceleration of the gravity, and then converted to acceleration in m/s^2. for each vibration mode, an acceleration will be determined.

c. Response of the structure

The response of the structure is the sets of effects observed on the structure after the application of the seismic action. The most important effects are the base shear force, the displacements and accelerations of the nodes or storeys, the inter-storey drifts and the internal forces generated on the structural elements (shear force, axial forces, bending moment and torsion). For each selected vibration mode, the maximum effects generated in the structure will be determined and then combined to obtain the overall response of the structure.

i. Base shear force

The base shear force is an estimate of the maximum lateral force expected on the base of the structure due to seismic activity for each horizontal direction in which the building is analysed. For the effective modal mass m_k corresponding to a mode k, the base shear force is calculated using the formula in equation **(2.101)**.

$$F_{bki} = S_d(T_{ki}) \cdot m_k \quad \textbf{(2.101)}$$

Where:

F_{bk} is the base shear acting in the direction i of application of the seismic action;

$S_d(T_{ki})$ is the acceleration of the structure at the ground level for the mode k in the direction i; with T_{ki} the corresponding modal period of vibration in direction i;

ii. Internal forces in the structural elements

The structure here is considered as dissipative and the internal forces are obtained considering the ductility level of the structure given by its behaviour factor. For each ductility level considered, the corresponding seismic action and the vertical loads are applied, and the axial forces, bending moment and shear are determined at ULS in the structural elements.

iii. Displacement and inter-storey drift

The displacement of the structure induced by the seismic action is calculated at SLS based on ideally elastic behaviour of the structural system. The structure is considered non-dissipative hence a behaviour factor equal to 1 is considered.

The interstorey drift is evaluated as the difference of the average lateral displacement d_s at the top and bottom of the storey under consideration. The damage limitation requirement is considered to have been satisfied, for buildings having non-structural elements of brittle materials attached to the structure, if the interstorey drift are limited in accordance with equation **(2.102)**.

$$d_r \cdot \nu \leq 0.005h \quad \textbf{(2.102)}$$

Where:

d_r is the design interstorey drift;

h is the storey height;

ν is the reduction factor which considers the lower return period of the seismic action associated with the damage limitation requirements. The recommended values of ν are 0,4 for importance classes III and IV and ν = 0,5 for importance classes I and II.

Moreover, the criterion for not considering the second order effect is based on the interstorey drift sensitivity coefficient, which is defined in equation **(2.103)**.

$$\theta = \frac{p_{tot} \cdot d_r}{V_{tot} \cdot h} \leq 0.1 \qquad \textbf{(2.103)}$$

d. Combination of modal responses

The modal responses calculated for the different modes are combined to reconstruct the full effects of the actual earthquake. The Square Root of the Sum of Square (SRSS) and the complete quadratic combination (CQC) methods provide a better estimation of the response.

i. SRSS method

The SRSS is a method that takes the contributions of each mode instead of the sum of all the responses. This method gives excellent results when modal responses are independent (see equation **(1.3)**). The maximum acceleration response is obtained using equation **(2.104)**.

$$\boldsymbol{R_{max} \cong \sqrt{\sum R_i^2}} \qquad \textbf{(2.104)}$$

ii. CQC method

The CQC method considers a correlation between two responses to the difference in the two eigen periods using equation for the maximum response. The maximum acceleration response is obtained using equation **(2.105)**.**(2.104)**

$$\boldsymbol{R_{max} \cong \sqrt{\sum_i \sum_j \rho_{ij} \cdot R_i \cdot R_j}} \qquad \textbf{(2.105)}$$

e. Design of structural elements

Based on the internal forces obtained at the ULS, the structure is redesigned and the various SLS checks are carried out. The design of the structure in the seismic zone is closely related to the chosen ductility class. Athanasopoulou et al., (2012) summarised the design procedures for the different classes in table 2.3 and table 2.4.

Table 2.2. EN 1998 rules for design of primary beams (Athanasopoulou et al., (2012)

	DC H	DCM	DCL
"critical region" length	$1.5h_w$	h_w	
Longitudinal bars (l):			
ρ_{min}, tension side	$0.5f_{ctm}/f_{yk}$		$0.26f_{ctm}/f_{yk}$, 0.13%[0]
ρ_{max}, critical regions[1]	$\rho'+0.0018f_c/(\mu_\phi\varepsilon_{sy,d}f_{yd})$[1]		0.04
$A_{s,min}$, top & bottom	$2\Phi14$ ($308mm^2$)	-	
$A_{s,min}$, top-span	$A_{s,top\text{-}supports}/4$	-	
$A_{s,min}$, critical regions bottom	$0.5A_{s,top}$[2]		-
$A_{s,min}$, supports bottom		$A_{s,bottom\text{-}span}/4$[0]	
d_{bL}/h_c - bar crossing interior joint[3]	$\le \frac{6.25(1+0.8\nu_d)}{(1+0.75\frac{\rho'}{\rho_{max}})}\frac{f_{ctm}}{f_{yd}}$	$\le \frac{7.5(1+0.8\nu_d)}{(1+0.5\frac{\rho'}{\rho_{max}})}\frac{f_{ctm}}{f_{yd}}$	-
d_{bL}/h_c - bar anchored at exterior joint[3]	$\le 6.25(1+0.8\nu_d)\frac{f_{ctm}}{f_{yd}}$	$\le 7.5(1+0.8\nu_d)\frac{f_{ctm}}{f_{yd}}$	-
Transverse bars (w):			
(i) outside critical regions			
spacing $s_w\le$		0.75d	
$\rho_w\ge$	$0.08\sqrt{f_{ck}(MPa)}/f_{yk}(MPa)$[0]		
(ii) in critical regions:			
$d_{bw}\ge$		6mm	
spacing $s_w\le$	$6d_{bL}$, $\frac{h_w}{4}$, $24d_{bw}$, 175mm	$8d_{bL}$, $\frac{h_w}{4}$, $24d_{bw}$, 225mm	-
Shear design:			
V_{Ed}, seismic[4]	$1.2\frac{\sum M_{Rb}}{l_{cl}} \pm V_{o,g+\psi_2 q}$[4]	$\frac{\sum M_{Rb}}{l_{cl}} \pm V_{o,g+\psi_2 q}$[4]	from analysis for design seismic action plus gravity
$V_{Rd,max}$ seismic[5]	As in EC2: $V_{Rd,max}=0.3(1-f_{ck}(MPa)/250)b_{wo}zf_{cd}\sin2\delta$[5], $1\le\cot\delta\le2.5$		
$V_{Rd,s}$, outside critical regions[5]	As in EC2: $V_{Rd,s}=b_w z\rho_w f_{ywd}\cot\delta$[5], $1\le\cot\delta\le2.5$		
$V_{Rd,s}$, critical regions[5]	$V_{Rd,s}=b_w z\rho_w f_{ywd}$ ($\delta=45^o$)	As in EC2: $V_{Rd,s}=b_w z\rho_w f_{ywd}\cot\delta$, $1\le\cot\delta\le2.5$	
If $\zeta\equiv V_{Emin}/V_{Emax}$[6] <-0.5: inclined bars at angle $\pm\alpha$ to beam axis, with cross-section A_s/direction	If $V_{Emax}/(2+\zeta)f_{ctd}b_w d>1$: $A_s=0.5V_{Emax}/f_{yd}\sin\alpha$ & stirrups for $0.5V_{Emax}$	-	

Table 2.3. EN 1998 rules for design of primary columns (Athanasopoulou et al., (2012)

	DCH	DCM	DCL
Cross-section sides, h_c, $b_c \geq$	0.25m; $h_w/10$ if $\theta=P\delta/Vh>0.1$ [1]	-	
"critical region" length [1] $\geq$	$1.5h_c$, $1.5b_c$, 0.6m, $l_c/5$	h_c, b_c, 0.45m, $l_c/6$	h_c, b_c
Longitudinal bars (L):			
ρ_{min}	1%		$0.1N_d/A_cf_{yd}$, 0.2% [0]
ρ_{max}	4%		4% [0]
$d_{bL} \geq$		8mm	
bars per side $\geq$	3		2
Spacing between restrained bars	$\leq$150mm	$\leq$200mm	-
Distance of unrestrained bar from nearest restrained nearest restrained bar		$\leq$150mm	
Transverse bars (W):			
Outside critical regions:			
$d_{bw} \geq$		6mm, $d_{bL}/4$	
spacing $s_w \leq$	$20d_{bL}$, h_c, b_c	400mm	$12d_{bL}$, $0.6h_c$, $0.6b_c$, 240mm
at lap splices, if d_{bL}>14mm: $s_w \leq$	$12d_{bL}$, $0.6h_c$, $0.6b_c$, 240mm		
Within critical regions: [2]			
$d_{bw} \geq$ [3]	6mm, $0.4(f_{yd}/f_{ywd})^{1/2}d_{bL}$	6mm, $d_{bL}/4$	
$s_w \leq$ [3],[4]	$6d_{bL}$, $b_o/3$, 125mm	$8d_{bL}$, $b_o/2$, 175mm	-
$\omega_{wd} \geq$ [5]	0.08	-	
$\alpha\omega_{wd} \geq$ [4],[5],[6],[7]	$30\mu_\phi^* \nu_d \varepsilon_{sy,d} b_c/b_o$-0.035	-	
In critical region at column base:			
$\omega_{wd} \geq$	0.12	0.08	-
$\alpha\omega_{wd} \geq$ [4],[5],[6],[8],[9]	$30\mu_\phi \nu_d \varepsilon_{sy,d} b_c/b_o$-0.035		-

Capacity design check at beam-column joints: [10]	$1.3\sum M_{Rb} \geq \sum M_{Rc}$ No moment in transverse direction of column		-
Verification for M_x-M_y-N:	Truly biaxial, or uniaxial with (M_z/0.7, N), (M_y/0.7, N)		
Axial load ratio $\nu_d=N_{Ed}/A_cf_{cd}$	$\leq$ 0.55	$\leq$ 0.65	-
Shear design:			
V_{Ed} seismic [11]	$1.3\frac{\sum M_{Rc}^{ends}}{l_{cl}}$ [11]	$1.1\frac{\sum M_{Rc}^{ends}}{l_{cl}}$ [11]	from analysis for design seismic action plus gravity
$V_{Rd,max}$ seismic [12], [13]	As in EC2: $V_{Rd,max}=0.3(1-f_{ck}(MPa)/250)b_{wo}zf_c \sin2\delta$, $1\leq\cot\delta\leq2.5$		
$V_{Rd,s}$ seismic [12], [13], [14]	As in EC2: $V_{Rd,s}=b_w(\rho_w f_{ywd}\cot\delta+N_{Ed}(h-x)/l_c$ [13], $1\leq\cot\delta\leq2$ .5		

2.8.3. Pushover analysis

2.8.3.1. Principle and purposes

In the non-linear static (pushover) analysis, the structural model is subjected to an incremental lateral load representing the inertial forces which would be experienced by the structure when subjected to ground shaking. The structure is displaced until the target displacement is reached or structure collapses. The target displacement is intended to represent the maximum displacement likely to be experienced during the design earthquake (FEMA-356). Once the elastic limit is reached, the structure is further loaded which results in formation of cracks, plastic hinges and failure of structural components. The relation between base shear and displacement plotted is known as the pushover curve or capacity curve.

As mentioned in section 1.3.3.1, pushover analysis can be performed for several purposes but in this work, it will be used to estimate the plastic mechanisms, damage distribution of the structure and its ductility coefficient in order to come out the real behaviour of the building for the different levels of ductility.

2.8.3.2. Modelling of the structure

This analysis will be done on a 3D mathematical model using SAP2000 v22. The model of the building is done according to the results of the modal response spectrum analysis. The model is then converted from a linear model to a non-linear model by considering that the properties of some or all the components in the model include post-elastic strength and deformation characteristics in addition to the initial elastic properties. This is done by inserting plastic hinges at the two extremities of elements (inelastic deformation is assumed to be concentrated at the extremities of the element beam and column according to the concept of concentrated ductility). The inelastic deformation is represented by the inelastic rotation undergone by the two plastic hinges placed.

a. Plastic hinges

Plastic hinges are assigned in a structure where cracking and deformations are expected to occur with relatively higher intensity, so that the exhibit significant flexural (or shear) displacement as the structures approaches its ultimate strength under cyclic loading. These locations are found at both ends of beams and columns.

EC8 proposed various conditions while assigning hinges in the beams and columns. The critical insertion length of hinges is called critical length lcr and is defined by equations **(2.106)** and **(2.107)** for beams and columns respectively.

$$l_{cr,beam} = h_w \quad \textbf{(2.106)}$$

$$l_{cr,column} = max\left\{h_c; \frac{l_{cl}}{6}: 0.45\right\} \quad \textbf{(2.107)}$$

Where:

h_w is the beam depth;

h_c is the largest cross-section dimension of the column;

l_{cl} is the clear length of the column.

Following the critical length obtained, the hinges are assigned at relative distance in SAP2000 v22.

b. Plastic hinges properties

SAP2000 implements the properties of plastic hinges described in FEMA-356 (or ATC40). As shown in Figure 2.11, five points marked A, B, C, D and E define the force-deformations behaviour of a plastic hinges and are defined by different colours in SAP2000. The values assigned to each of these points vary depending on the type of member, material properties, longitudinal and transverse reinforcement, and the level of axial loading on the member. The point A represents the unloaded state A; the point B identifies the effective yielding state; the point C represents the nominal strength; and point D shows the deformation at which significant amount of strength degradations occurs. The section C-D shows the starting failure of an element and the strength of the strength of the element to resist lateral forces is unreliable after point C. The portion D-E on the curve shows that only the gravity loads are sustained by the frame element. After point E, the structure has no more capacity to sustain gravity loads.

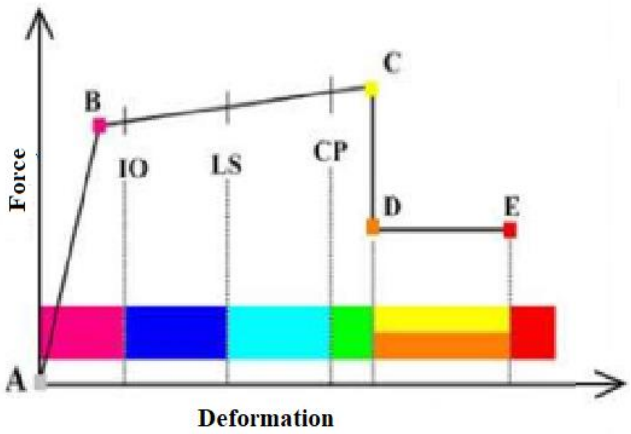

Figure 2.11. Force-deformation relationship of a typical plastic hinge (Meguellati, 2017)

Plastic hinges have non-linear states, known as performance levels, defined as "Immediate occupancy" (IO), "Life safety" (LS) and "Collapse prevention" (CP) within its ductile range used for the performance-bases design. According to FEMA-273, the performance levels:

- Immediate occupancy (IO) means the post-earthquake state in which only very limited structural damage has occurred. The basic vertical- and lateral-force-resisting systems of the building retain nearly their pre-earthquake strength and stiffness;
- Life safety (LS) means the post-earthquake damage in which significant damage to the structure has occurred, but some margin against either partial or total structural collapse remains;
- Collapse prevention (CP) means the post-earthquake damage in which the building is on the verge of the partial or total collapse, substantial damage has occurred to the building.

c. Assignment of hinges to the elements

The hinges assigned to an element is defined by the software according to the properties of the element, its behaviour with actions, the axial force behaviour (P), the bending moment behaviour (M), the axial force/moment interaction (P-M) or axial force/biaxial-moment behaviour (P-M-M). It is recommended that M3 hinges be assigned to beams and P-M2-M3 hinges to columns.

2.8.3.3. Lateral load patterns

According to EN 1998-1, at least two vertical distributions of the lateral loads should be applied:

- a "uniform" load pattern, based on lateral forces that are proportional to mass regardless of elevation (uniform response acceleration) and define using equation **(2.108)**;

$$P^2 = MR \qquad \textbf{(2.108)}$$

- a "modal" load pattern, proportional to the fundamental translational mode shape in each principal horizontal direction (x, y). This pattern has a triangular shape and is define using equation **(2.109)**;

$$P^1 = M\varphi_1 \qquad \textbf{(2.109)}$$

Where M is the mass matrix, φ_1 the first mode shape and R a vector of 1s corresponding to the degree of freedom parallel to the application of the ground motion.

Amongst the different loads patterns defined, the one to be considered is the one which gives unfavourable response of the structure.

2.8.3.4. Pushover curves and plastic mechanism

The application of incremental lateral loads in each principal direction allows to plastic mechanism to be identified and the behaviour of the building to be determined. The plastic mechanisms are characterised by changes in performance of the plastic hinges and the behaviour of the building is characterized by pushover curve, which related the base shear force to the displacement of the control node. The control node should be the one that gives the largest displacement; in most cases at the centre of mass at the roof of the building.

2.8.3.5. Determination of the capacity curve and the ductility coefficient

The pushover curve is obtained using the SAP2000 v22 software and is associated to the multi-degree-of-freedom (MDOF) system. The ductility coefficient is obtained from the capacity curve of the structure which is the pushover curve associated to the single-degree-of-freedom (SDOF) system (see Figure 2.12 left). This transformation is done according to the following steps in accordance with annex B of EN 1998-1.

a. Transformation of the structure to an equivalent SDOF system

The mass of an equivalent SDOF system m* is determined using equation **(2.110)**.

$$m^* = \sum m_i \phi_i = \sum \bar{F}_i \qquad \textbf{(2.110)}$$

Where:

ϕ_i are the normalized displacements in such a way that $\phi_n = 1$, with n the control node;

m_i is the mass in the i-th storey;

$\bar{F}_i$ are the normalized lateral forces.

The transformation factor is derived using equation **(2.111)**.

$$\Gamma = \frac{m^*}{\sum m_i \phi_i^2} = \frac{\sum \bar{F}_i}{\sum \left(\frac{\bar{F}_i^2}{m_i} \right)} \qquad \textbf{(2.111)}$$

Then the force Fb* and the displacement d* of an equivalent SDOF system are computed using equations **(2.112)** and **(2.113)** respectively**.**

$$F^* = F_b / \Gamma \qquad \textbf{(2.112)}$$

$$d^* = d_n / \Gamma \qquad \textbf{(2.113)}$$

Where Fb and dn are respectively the base shear force and the control node displacement of the MDOF system. The plot of the curve that connects F^* to d^* is the capacity curve.

b. Determination of the idealized elasto-perfectly plastic force-displacement relationship

The yield force Fy*, which also represents the ultimate strength of the idealized system, is equal to the base shear force at the formation of the plastic mechanism. The initial stiffness of the idealized system is determined in such a way that the areas under the actual and the idealized force–deformation curves are equal as shown in figure 2.12.

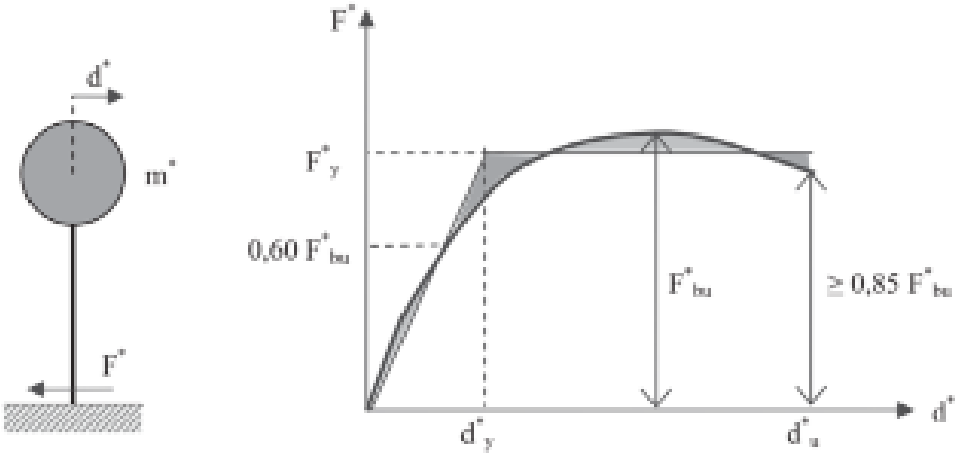

Figure 2.12. Bilinear idealisation of the capacity curve of the equivalent SDOF system (Dongmo B., 2018)

c. Determination of the ductility coefficient

Once the non-linear capacity curve of the structure has been bilinearized into the equivalent capacity curve of the SDOF system, the ductility coefficient μ, is obtained as the ratio between the maximum displacement d^* and the yield displacement d_y^* as shown in equation **(2.114)**.

$$\mu = \frac{d_u^*}{d_y^*} \qquad \textbf{(2.114)}$$

According to EC8, the ductility coefficient is related to the effective behaviour factor, which will be denoted as q_{eff}, of the building by the relationship given is equations **(2.115)** and **(2.116).**

$$If\ T_1 \geq T_C: \qquad q_{eff} = \mu \qquad \textbf{(2.115)}$$

$$If\ T_1 < T_C: \qquad q_{eff} = 1 + (\mu - 1)T_1/T_c \qquad \textbf{(2.116)}$$

Where:

T_1 is the fundamental period of the building taken within the vertical plane in which the bending takes place;

T_C is the period at the upper limit of the constant acceleration region of the spectrum.

Conclusion

The main objective of this chapter was to present the different analysis methods that will be used in this work. The vertical and horizontal loads that will be used have been clearly defined as well as the design standards. A detailed description of the linear static analysis of the different structural elements, under vertical loading only, as well as their design was given, followed by a description of the modal response spectrum analysis with consideration of the seismic action and finally the pushover analysis to determine the ductility coefficient of the structure for each level of ductility. The application of these different analyses and the presentation of the subsequent results will be the focus of the next chapter.

CHAPTER 3. PRESENTATION AND INTERPRETATION OF RESULTS

Introduction

This chapter aims to apply the different analyses presented in the previous chapter on a real case study and then present the different results. For this purpose, a general presentation of the case study, the material properties used, and the loads applied for the analysis will first be made. Then, the results of the different analyses performed, namely the linear static analysis, the modal response spectrum analysis, and the pushover analysis, for each ductility level, will be presented.

3.1. General presentation of the site

Yaoundé, also called the 'city of seven hill", is the political capital of Cameroon. With an estimated population of 4,1 million inhabitants in 2020, is the chief town of the Centre region and is home of Toutouli village where the project is located.

After the site visit and documentary research, the project site characteristics were obtained as the geographical location, climate, relief, population, and hydrology.

3.1.1. Geographical location

Toutouli is a village in the centre region of Cameroon located in the Centre region of Cameroon, located in the south of the municipality of Yaoundé IV, in the Mfoundi department. It has an elevation of 708 metres and is on 3.45° north latitude and 11.30° east longitude.

3.1.2. Geology

The bedrock in Yaoundé is mainly composed of gneiss. This rock is neither porous nor soluble, but it is its discontinuities (faults, diaclases) that give fissure permeability to the formation. The hydrogeology is characterized by continuous aquifers, approximately exploitable overlying water bearing fissures or fracture aquifers in the bedrock; these types of aquifers are superimposed or isolated.

3.1.3. Relief

Concerning the relief, the land rises gently in escarpments from the south-western coastal plain before joining the Adamawa Plateau via depressions and granite massifs. The field is irregular in certain places due to the presence of isolated hills or hills with variable slopes.

3.1.4. Climate

Yaoundé and its districts such as Toutouli features a tropical wet and dry climate, with record high temperatures of 36°C, an average of 23.8°c and a record low temperature of 14°C. Primarily due to the attitude, temperatures are not as high as would have been expected for a city located near the equator. The town of Yaoundé features a lengthy rainy season covering a nine-month span between March and November.

3.1.5. Hydrology

The hydrographic network of Yaoundé is very dense and composed permanent rivers such as the Mfoundi river which crosses the city from North to South, a few creeks, and lakes. Yaoundé is part of the western sector of the Southern Cameroon Plateau. The area is characterized by gentle rolling chains of hills, and numerous valleys and wetlands; this varied physical landscape permits a combination of streams, hydromorphic soils and a great variety of plants and Fauna.

3.2. Presentation of the project

3.2.1. Architectural data

From an architectural point of view, the case study is a residential building built in reinforced concrete and having a height of 28.8m above ground level. The building is divided into a ground level with 8 storeys, each level has a height of 3 m under a 20 cm thick floor and there is also a roof terrace. The different levels communicate each other with the staircases. The building is L-shaped and covers an area of 426.30m². It is divided into 2 blocks separated each other by a break joint as shown in figure 3.1.

The first block, named block A, is 28.40 m long and 7.80 m wide. It consists of 9 levels; the first level consists of 2 apartments and the recreation area while the other levels consist of apartments only. The various analyses will be carried out in this block.

The second block, named block B, is 28.05 m long and 7.30 m wide. It consists of 9 levels; level 1 is mainly provided for car park while the other levels consist of apartments only. The elevator of the building is in this block. The mane façade plan is presented in figure C.1 of Appendix C.

3.2.2. Structural data

From an structural point of view, it is a residential building and is therefore classified as Category A and Class II according to EN 1991-1 and EN 1998-1 respectively.

As the roof is accessible, it is classified as Category I according to EN 1991-1. All levels, except the ground floor, have the same distribution plan.

The building's framework is made up of a 20 cm thick hollow floor supported by a system of reinforced concrete column-beams which transfer the loads to isolated footings. The plan view for level 2 to 8 is presented in the figure 3.2.

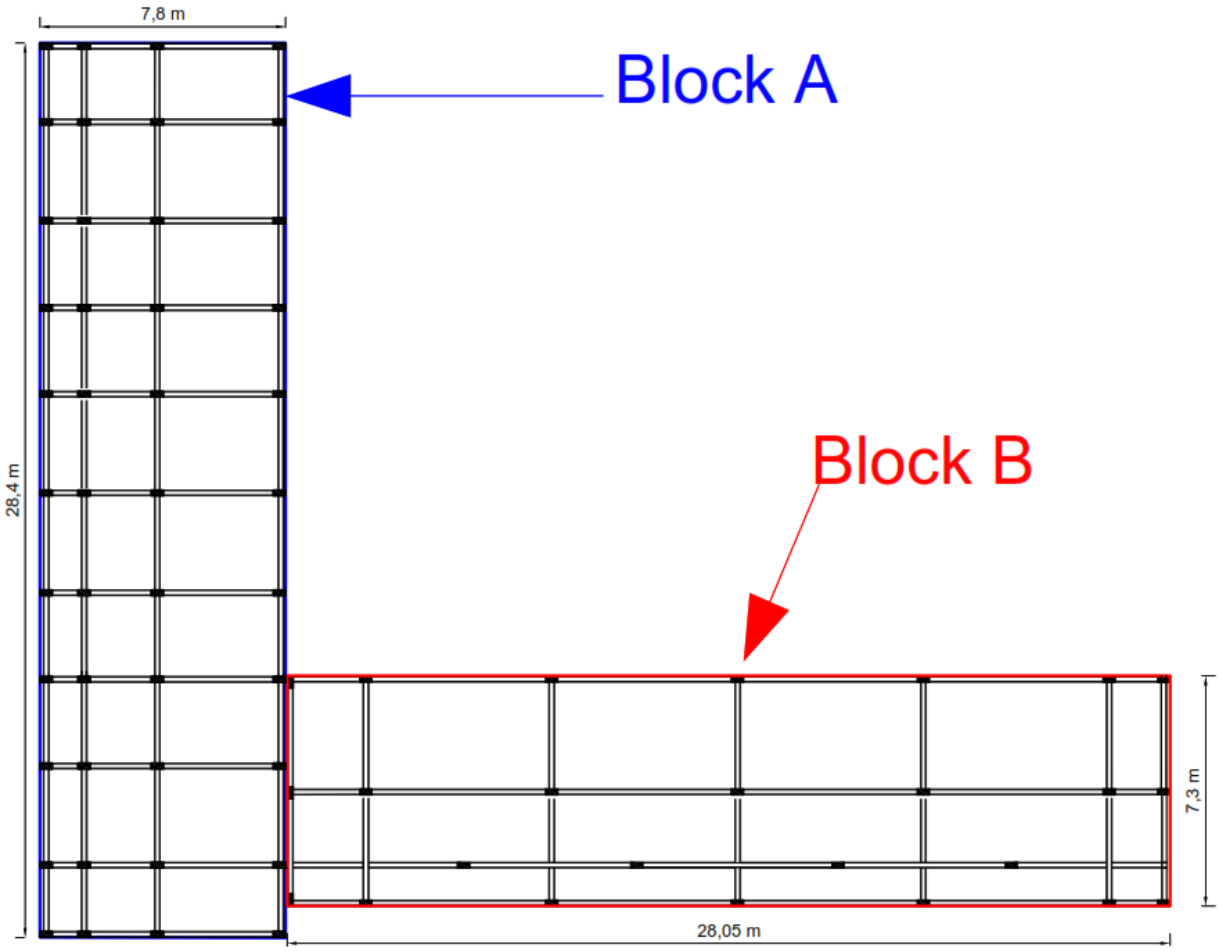

Figure 3.1. Repartition of the building

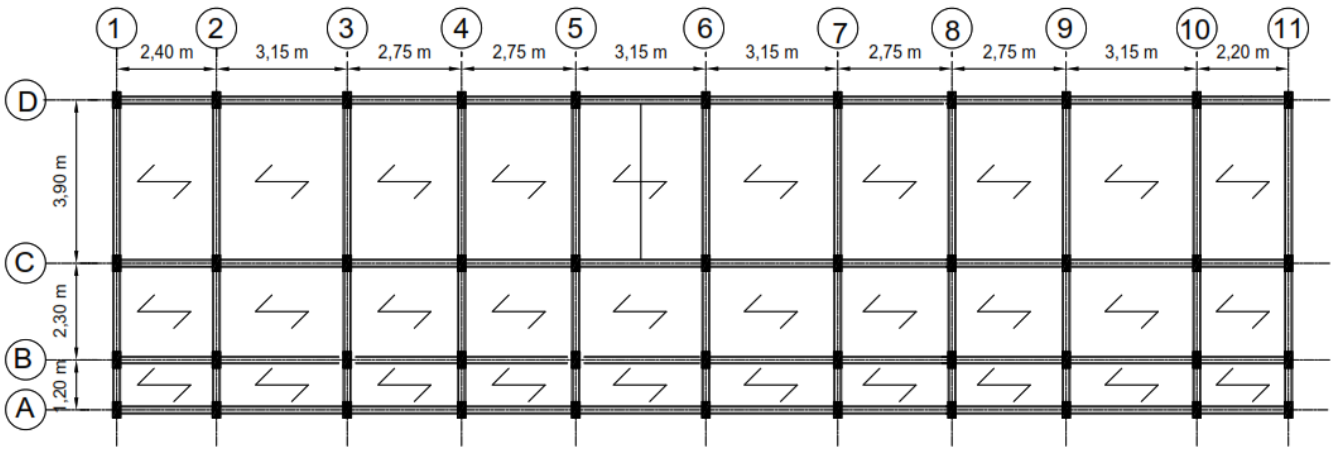

Figure 3.2. Structural plan of block A

3.2.3. Soil and material data

3.2.3.1. Soil properties

The main test carried out in this project was the heavy dynamic penetrometer type B investigation. For this study, six test points were used. The purpose of this test was to determine the admissible bearing capacity of the soil. The study report recommends the use of shallow foundations anchored at a depth of 2.50 m with an admissible soil bearing capacity of 3.50 bar.

3.2.3.2. Concrete

For the analysis and design, the concrete class chosen is C25/30. Table 3.1 gives the main characteristics for linear and design of our case study.

Table 3.1. Concrete characteristics

Property	Value	Unit	Definition
Grade	C25/30	-	Concrete class
f_{ck}	25	MPa	Characteristic cylindric compressive strength at 28 days
R_{ck}	30	MPa	Characteristic cubic compressive strength at 28 days
$f_{cm} = f_{ck}+8$	33	MPa	Mean compressive strength at 28 days
$f_{ctm}=0,3 \cdot fck^{2/3}$	2.56	MPa	Mean tensile strength
γ_c	1.5	-	partial safety factor of concrete
α_{cc}	0.85	-	The coefficient taking in account of long-term effects on the compressive strength and of unfavourable effects resulting from the way the load is applied
$f_{cd} = \frac{\alpha_{cc} \cdot fck}{\gamma_c}$	14.17	MPa	The value of the design compressive strength
$f_{ctd} = \frac{0,7 \cdot fctm}{\gamma_c}$	1.20	MPa	The value of the design tensile strength
$E_{cm}=22 \cdot (f_{cm}/10)^{0,3}$	31	GPa	Secant modulus of elasticity
γ	25	kN/m^3	Specific weight of concrete
ε_{cu2}	3.5	‰	The ultimate strain

3.2.3.3. Steel reinforcement

The steel reinforcement used in the project is Fe 500. It has been used for both longitudinal and transverse reinforcement. The table 3.2 presents the main characteristics of the steel reinforcement used for the analysis.

Table 3.2 . Reinforcement characteristics

Property	Value	Unit	Definition
Class	B500C	-	Longitudinal reinforcement class
fyk	500	MPa	Characteristic yield strength of longitudinal reinforcement
γ_s	1.15	-	Partial safety factor of steel
Es	200	GPa	Modulus of elasticity
$f_{yd}=f_{yk}/\gamma_s$	434.78	MPa	Design yield strain
$\varepsilon_s = f_{yd}/Es$	0.207	%	Yield strain
ε_{ud}	6.75	%	Ultimate strain
f_{ywk}	500	MPa	Characteristic yield strength of transversal reinforcement
$f_{ywd} = f_{ywk}/\gamma_s$	434.78	MPa	Design yield strength of transversal reinforcement
γ	78.5	kN/m^3	Specific weight of steel
v	0.3	-	Poisson ratio

3.3. Linear static analysis and design

Firstly, a linear static analysis will be carried out in order to determine the different solicitations on the structural elements when they are subjected to vertical loads and wind actions only. These solicitations are used to design the structure. The design will be carried out on the most loaded elements.

3.3.1. Actions on the building

As mentioned above, the loads used for the linear static analysis are grouped into three categories, namely permanent loads, variable-live loads and wind actions. These are determined for each of the project situations identified in accordance with EN 1990.

3.3.1.1. Permanent loads

The permanent loads are subdivided into structural permanent loads consisting of the self-weight of structural elements such as the slab, and non-structural permanent loads consisting in this case of architectural elements. These loads are defined in the table 3.3, table 3.4 and table 3.5.

- Structural permanent load at floor level and roof level

Table 3.3. Structural permanent load

Nature	Designation	Value	Unit
G_{1k}	Self-weight of slab (16+4 cm)	2.85	kN/m^2

The self-weight of the beams and columns are calculated automatically by the software.

- Non-structural permanent

Table 3.4. Non-structural permanent load at floors level and roof level due to slab

Nature	Designation	Value	Unit
G_{2k}	Paving	0.4	kN/m²
G_{2k}	Screed	0.5	kN/m²
G_{2k}	tiles	0.6	kN/m²
G_{2k}	waterproofness	0.5	kN/m²
Total		2	kN/m²

Table 3.5. Non-structural permanent load due to wall and exterior cladding

Nature	Designation	Value	Unit
G_{2k}	Exterior cladding	1.2	kN/m
G_{2k}	Partition walls	6	kN/m
Total		7.2	kN/m

3.3.1.2. Variable-live load

As the building is of category A and the roof is of category I, the values of the live loads assigned to them are well defined in EN 1991-1. They are presented in the table 3.6.

Table 3.6. Variable-live loads at floors levels and roof level

Nature	Designation	Value	Unit
Q_k	Floor	2	kN/m²
Q_k	Roof	1.5	kN/m²

3.3.1.3. Wind actions

The wind loads on the structure is determined for a terrain of category III (area with regular cover of buildings). Table 3.7 presents the wind loads parameters obtained.

Table 3.7. Wind load acting at each level

Designation	Symbol	Value	Unit
Basic wind velocity	v_b	22	m/s
Basic Velocity pressure	q_b	0.3	kN/m²
Reference height	z_e	27	m
Peak velocity pressure	$q_p(z)$	0.75	kN/m²
Wind pressure on the external surface	w_e	0.6	kN/m²

3.3.2. Durability and concrete cover

According to EN 1990, our building is of exposure class XC1 and structural class S4 as it is designed for a 50-year life span. Following the procedures presented in section **2.5.** of the methodology, we obtain:

From equation **(2.18)** Cmin = max (16; 15; 10 mm) = 16 mm

From equation **(2.17)** Cnom = 16 + 10 = 26 mm

The nominal concrete cover obtain is equal to 26 mm. So, for more security and for easy data handling, the value of the concrete cover use is c = 30 mm.

3.3.3. Design of beams

For an optimal design, the design of the beams of the project will done through the most solicited principal beam. Principal beams are the one parallel to y axis and secondary beams are the one parallel to x axis.

3.3.3.1. Preliminary design

The most solicited beam is the one with the largest area of influence (beam of line 6), as shown in figure 3.3.

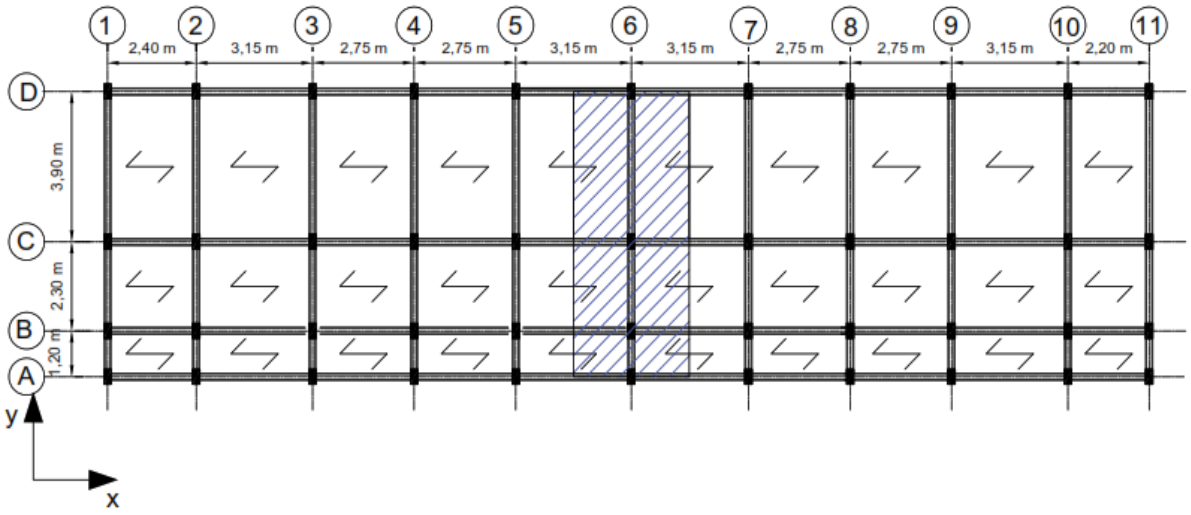

Figure 3.3. Beam selected for the design and its influence area

Following the procedure presented in section 2.6.1.1. of the methodology, and considering the beam is simply supported, the dimension of the beam is obtained.

The longest span of the beam has a length L = 3.90 m, from **(2.19)** we have:

$h \geq \frac{3.90}{14} = 0.28$ *and* $b \cong 0.5\ h$, we choose h= 40 cm and b= 20 cm.

3.3.3.2. Static scheme of beam and load arrangements

Once the cross-section is defined, the beam is modelled in the software SAP2000 v22 as a frame element with different restraint at the support as can be seen in figure 3.4. For the define static scheme, different load configurations necessary for the design of the beam at ULS are defined (see figure 3.5).

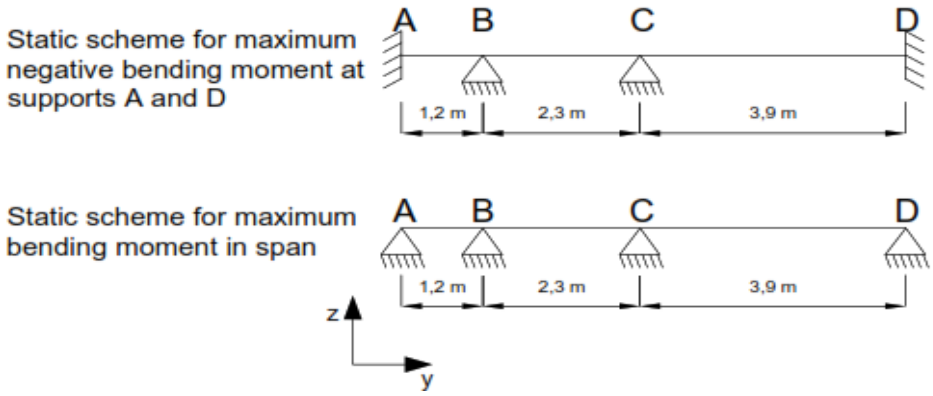

Figure 3.4. Static scheme of the considered beam

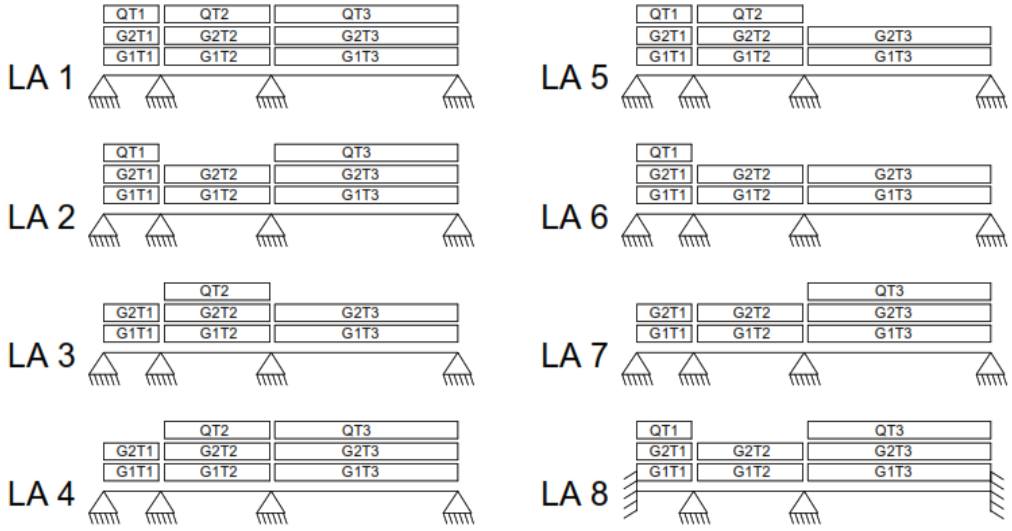

Figure 3.5. Load arrangements for the considered beam

From these load arrangements, solicitations are determined for each load arrangements, the envelope curves of the different solicitations are plotted, and the beam is designed at ULS for vertical actions only and verified at SLS, considering the horizontal action and the vertical actions.

3.3.3.3. Ultimate limit state design

a. Internal forces of the beam

The static scheme and loads were implemented in the calculation software SAP2000 v22. The 8 load arrangements were defined and the internal forces (bending moment and shear) at each point of the beam were obtained for each of the defined arrangements.

The analysis of these results, using Microsoft Excel, allowed to represent the diagrams of these internal forces for each of these arrangements as shown in figure 3.6 and figure 3.7.

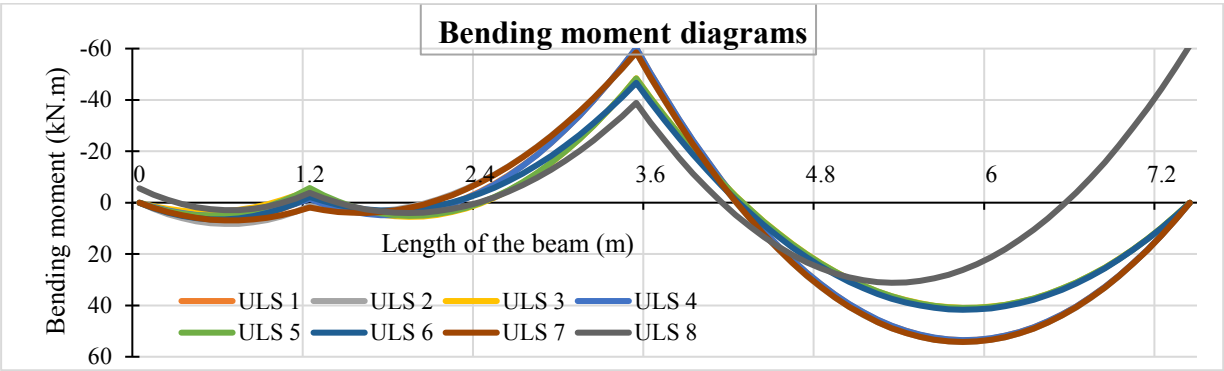

Figure 3.6. Bending moment diagrams for the 8 load arrangements on the beam

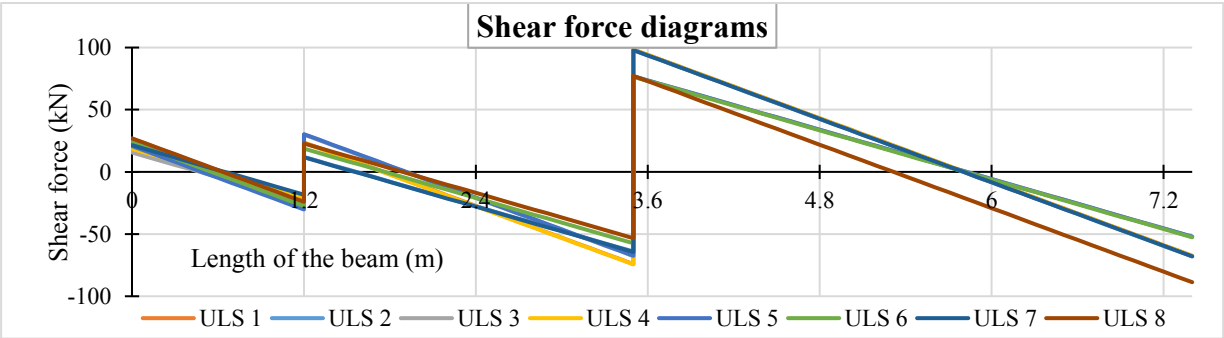

Figure 3.7. Shear force diagrams for the 8 load arrangements on the beam

Again, using Microsoft Excel, the envelope curve of each internal force was obtained and is illustrated in figure 3.8 and figure 3.9.

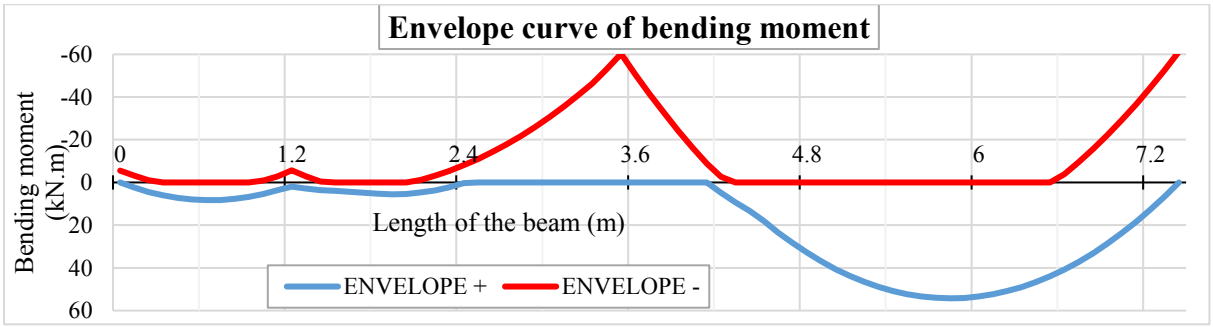

Figure 3.8. Envelope curve of bending moment on the beam

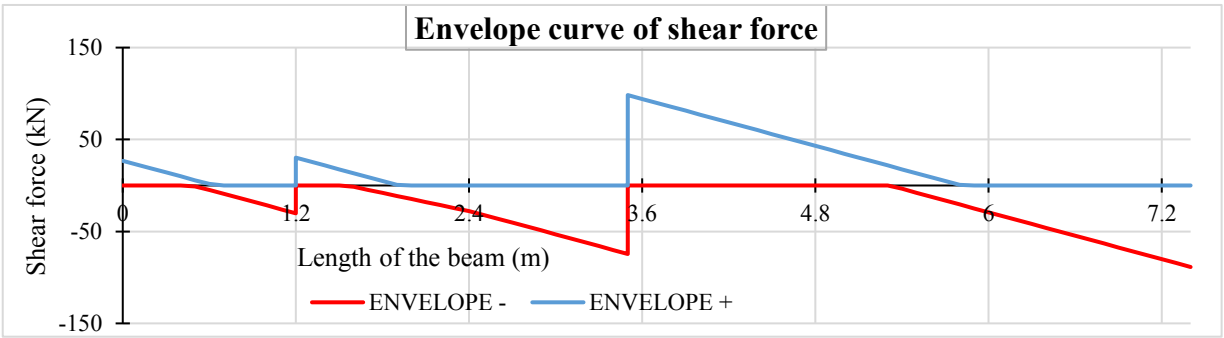

Figure 3.9. Envelope curve of shear force on the beam

b. Longitudinal reinforcement

Following the procedure described in section **2.6.1.2.a.i** of the previous chapter, the design diagram is plotted in figure 3.10.

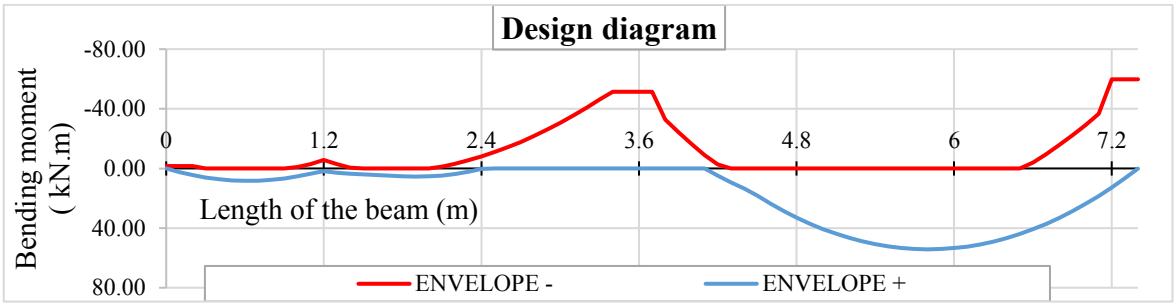

Figure 3.10. Design diagram for longitudinal reinforcement

This curve is used to determine the longitudinal reinforcement of the beam according to the procedure presented in section **2.6.1.2.a.ii** of chapter 2. Figure 3.11 presents the longitudinal reinforcement according to the resisting moment at each point of the beam.

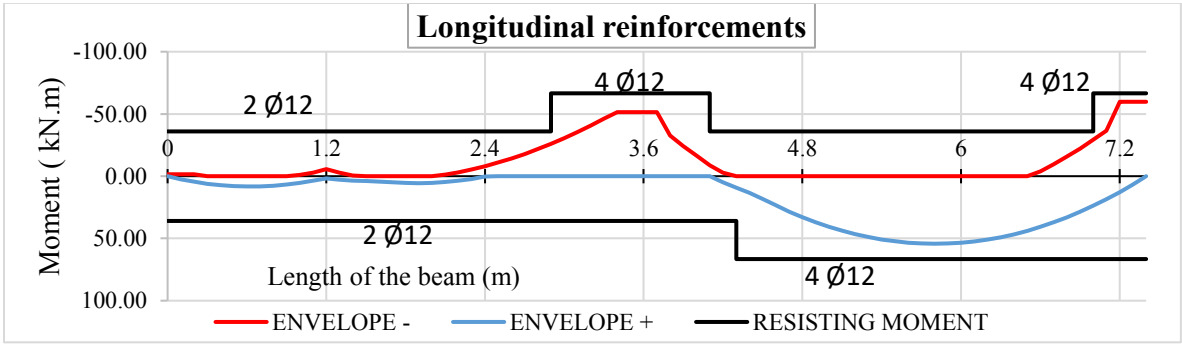

Figure 3.11. Longitudinal reinforcement provided with resisting moment on the beam

c. Shear reinforcement

Following the procedure described in section **2.6.1.2.b**, the shear reinforcement distribution has been plotted in the same diagram as envelope curve of shear in order to show that at each point of the beam, the resisting shear is greater than the shear force. The transverse reinforcements represented in figure 3.12 are made of **Ø8** and the number of legs of stirrups is 2.

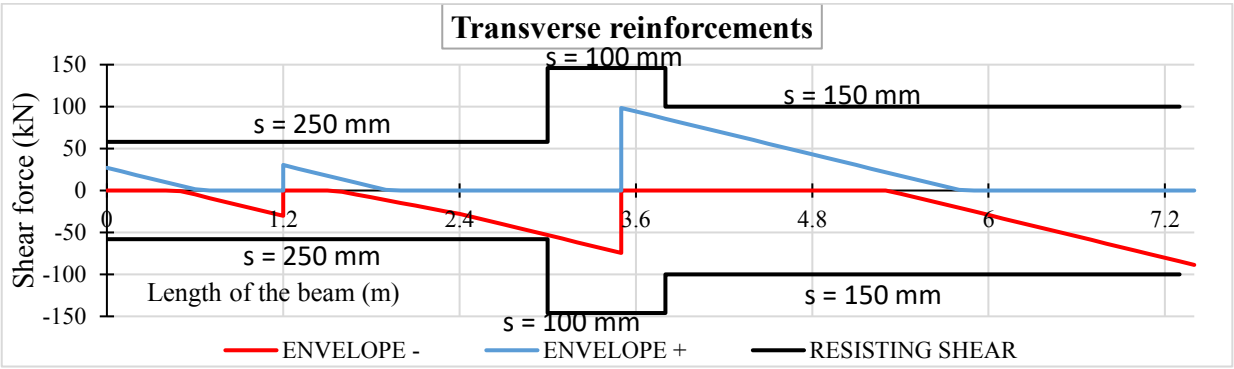

Figure 3.12. Transversal reinforcement provided with resisting shear on the beam

3.3.3.4. Serviceability limit state verifications

a. Combinations for SLS verifications

The SLS verifications were carried out considering the characteristic (rare) loading condition. Two load combinations were used. The first load combination given by equation **(3.1)** was used for SLS verifications under vertical actions and the second one given by equation **(3.2)** was used for SLS verifications under horizontal actions.

$$G_k + Q_k + 0.3w_e \quad \textbf{(3.1)}$$

$$G_k + w_e + 0.3Q_k \quad \textbf{(3.2)}$$

b. Internal forces

The application of the rare loading condition was carried out on the different load arrangements defined in figure 3.13 which allowed to represent the envelope diagram of the bending moment for vertical actions in figure 3.14. It also permits to determine the bending moment for horizontal actions as represent in figure 3.15.

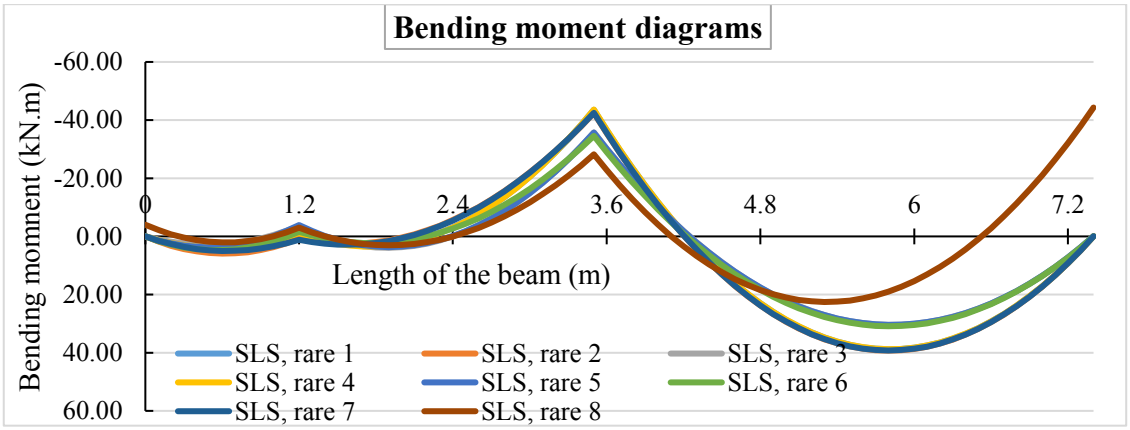

Figure 3.13. Bending moment diagrams for SLS rare combination

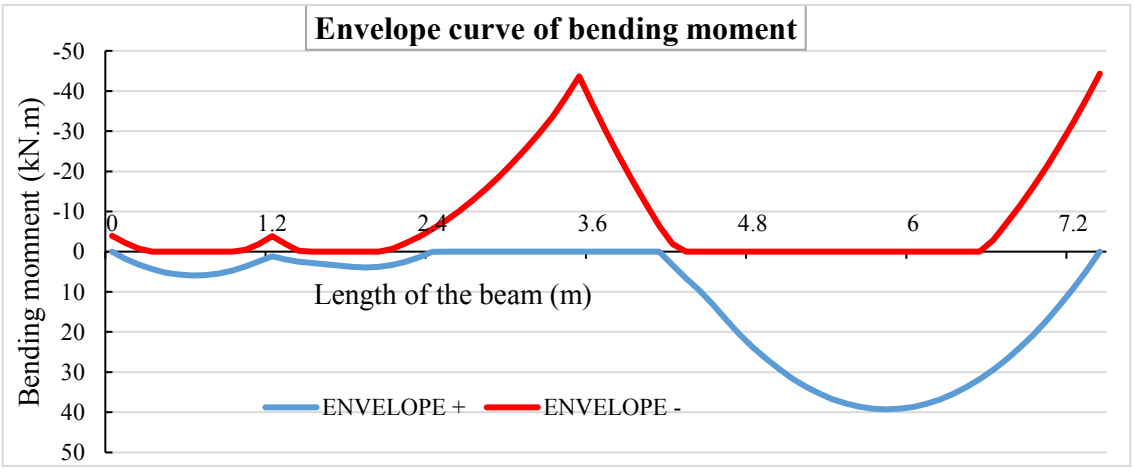

Figure 3.14. Envelope curve of SLS bending moment for vertical actions

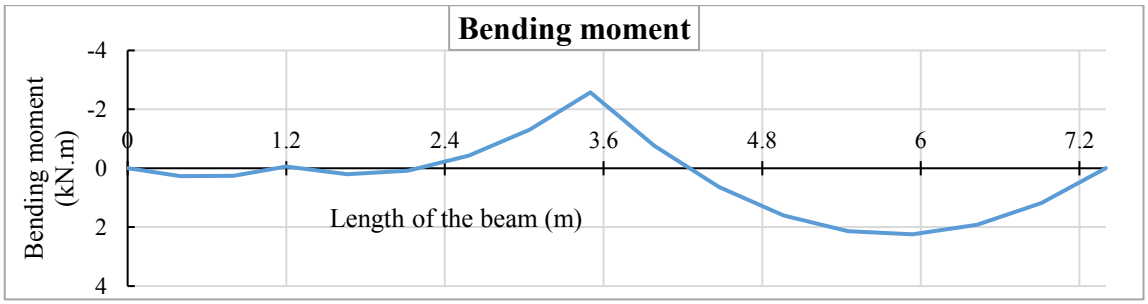

Figure 3.15. SLS bending moment for horizontal action

c. Stress limitation

Following the procedure described in section **2.6.1.3.a,** the stress distribution in concrete and in longitudinal reinforcement is plotted to check the stress limitation. They are presented in figure 3.16 and figure 3.17 for vertical actions and figure 3.18 and figure 3.19 for horizontal action. As can be seen from the graphs, the stress in concrete and steel are under the limit values.

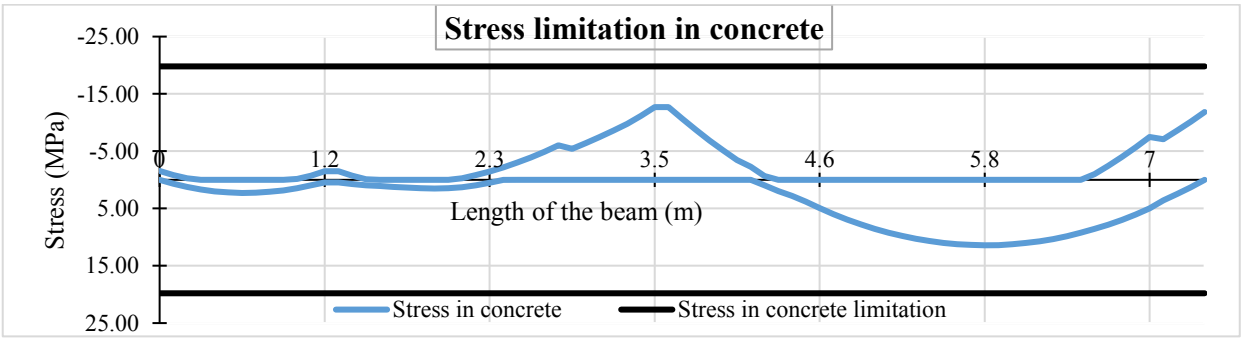

Figure 3.16. Stress limitation in concrete for vertical actions

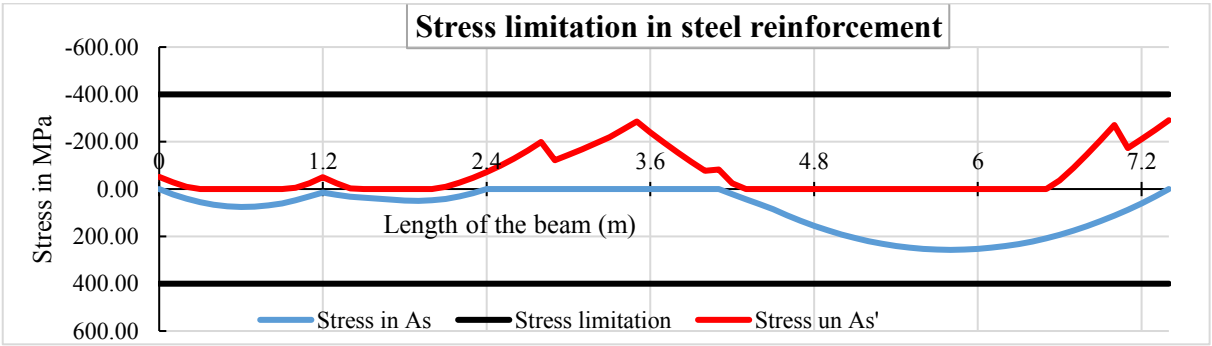

Figure 3.17. Stress limitation in steel reinforcement for vertical actions

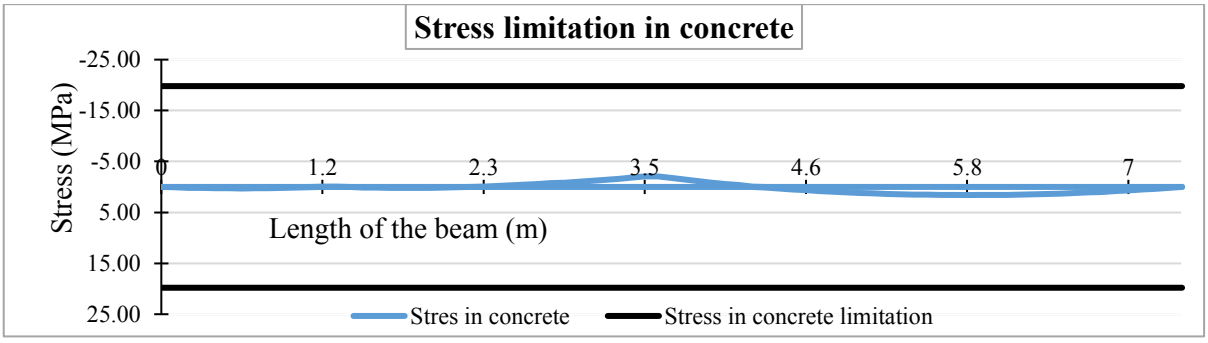

Figure 3.18. Stress limitation in concrete for horizontal action

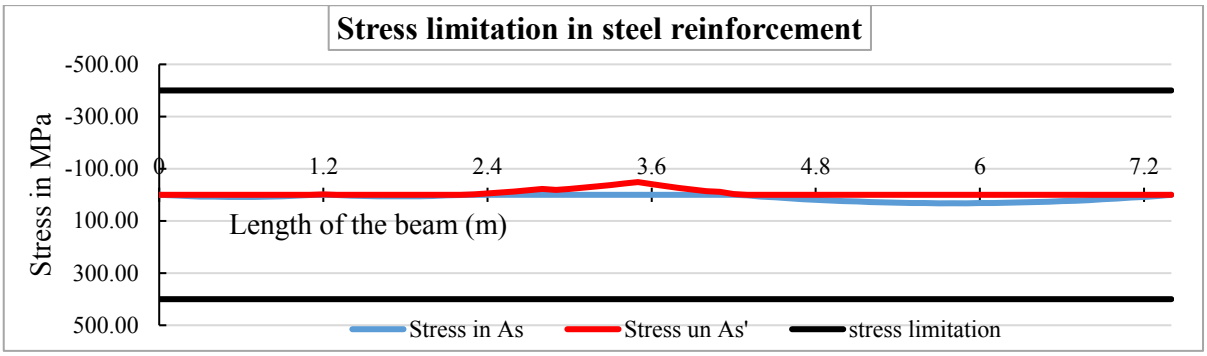

Figure 3.19. Stress limitation in steel reinforcement for horizontal action

d. Deflection control

The deflection control was carried out in the middle of each span (SC1, SC2 et SC3) as this is where the maximum deflection is likely to occur. The application of the procedure described in section **2.6.1.3.b** gives the following results which are presented in the table 3.8 and table 3.9. As we can see from the tables, the deflection of the beam at each span is tolerable.

Table 3.8. Deflection control for vertical actions

Span	Length L (mm)	Depth d (mm)	As provided	As' provided	L/d	$(L/d)_{lim}$	Verification
AB	1200	370	2 Ø 12	2 Ø 12	3.2	42.4	Deflection tolerable
BC	2300	370	2 Ø 12	2 Ø 12	6.2	51.0	Deflection tolerable
CD	3900	370	4 Ø 12	2 Ø 12	10.5	25.7	Deflection tolerable

Table 3.9. Deflection control for horizontal action

Span	Length L (mm)	Depth d (mm)	As provided	As' provided	L/d	$(L/d)_{lim}$	Verification
AB	1200	170	2 Ø 12	2 Ø 12	7.1	42.4	Deflection tolerable
BC	2300	170	2 Ø 12	2 Ø 12	13.5	51.0	Deflection tolerable
CD	3900	170	3 Ø 12	3 Ø 12	22.9	33.4	Deflection tolerable

e. Crack control

Following the procedure of crack control described in section **2.6.1.3.c,** a maximum reinforcement diameter of **25 mm** and a maximum reinforcement spacing of **235 mm** were obtained to ensure a maximum cracks width of **0.4 mm**. In this work the longitudinal reinforcement has maximum diameter of **12 mm** and the maximum spacing between bars is **100 mm**. Hence the necessary condition for crack control is fulfilled.

3.3.3.5. Structural detailing of the beam

With respect to the results of the design of the beam, the structural detailing of the principal beams was plotted and presented in figure 3.20.

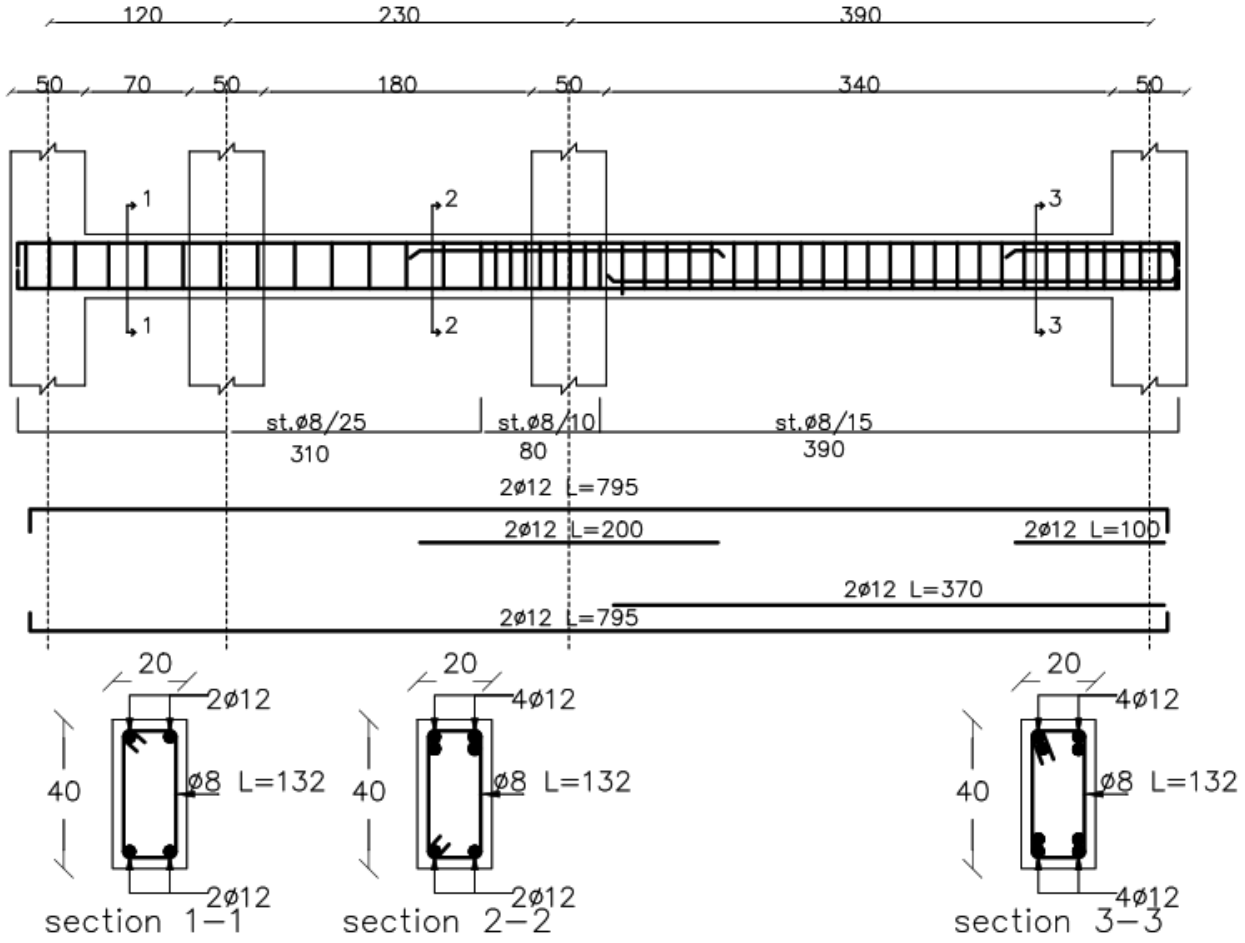

Figure 3.20 Structural detailing of the principal beams

3.3.4. Design of column

3.3.4.1. Preliminary design

The column chosen for the design is the most loaded column, C6 (see figure 3.21). The influence area of the column A_i is equal to 3.15*3.1=9.8m². It is too onerous to load all the floors with full load because there is a low probability of finding all the floors loaded at the same time. Hence one single floor (top floor) is loaded with maximum values, while a reduction coefficient ψ_0=0.7 can be applied for others. This coefficient considers the probability of contemporary loads.

Using equation **(2.54)**, the minimum cross-sectional area of the columns was determined. With this minimum area, the column sections were selected, considering the slenderness. For this study, a single column section for all levels will be adopted. The checks have been reduced to those of the first level and are presented in tables 3.10.

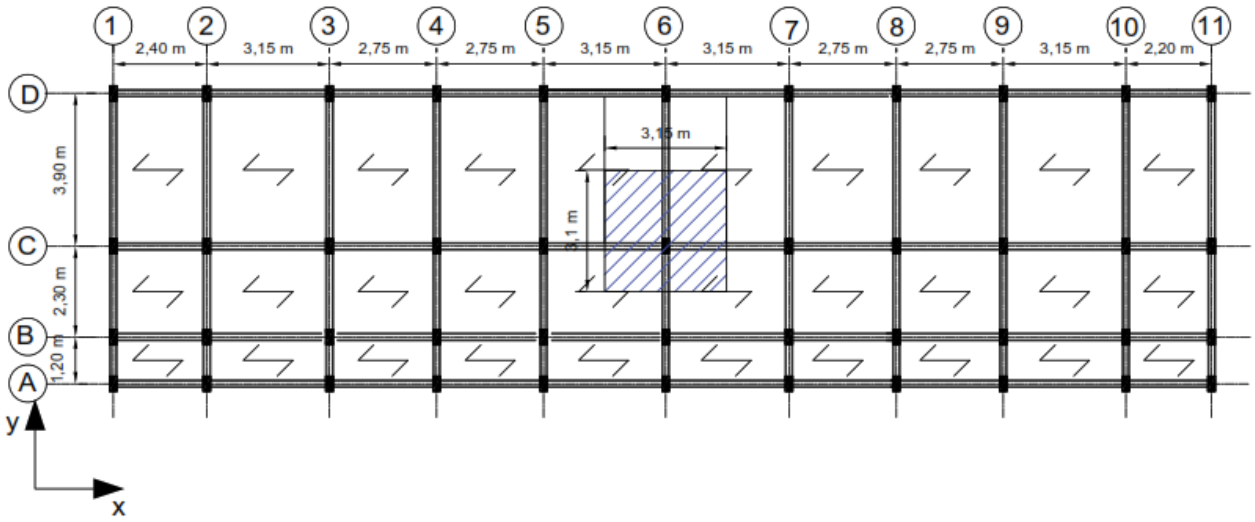

Figure 3.21. Influence area of the chosen column

Table 3.10. Preliminary design of columns

LEVELS	Max N_{ed} (kN)	Ac,min (mm^2)	a(y) (mm)	b(x) (mm)	Ac (mm^2)	λy	λx	λlim
1 to 9	1267.93	137 693.7	500	300	150 000	24.34	14.60	53.83

Table 3.10 shows that λx and λy are lower than λl_{im}, so all these columns are classified as short column. Therefore, the second order effect can be neglect during the design of the longitudinal reinforcement.

3.3.4.2. The internal forces on columns

The static analysis was carried out using SAP2000 v22 to determine the internal forces acting on the columns at ULS load combination. For this analysis we first identified the most stressed columns in the building and then applied different load arrangements to these columns to obtain the maximum solicitations. The most stressed columns in terms of axial force are columns in row C-6 and the most stressed columns in terms of bending moments and shear are columns in rows D-1.

Figure 3.22 shows on the left the numerical model of the structure on SAP2000 v22 and on the right the most stressed columns in terms of bending moment.

To determine the loads in the columns, the load arrangements defined above must also consider the secondary beams. The loads to be considered on these beams are only the self-weight of the walls and the beam itself. Therefore, only one load arrangement has to be considered for the secondary beams (see figure 3.23).

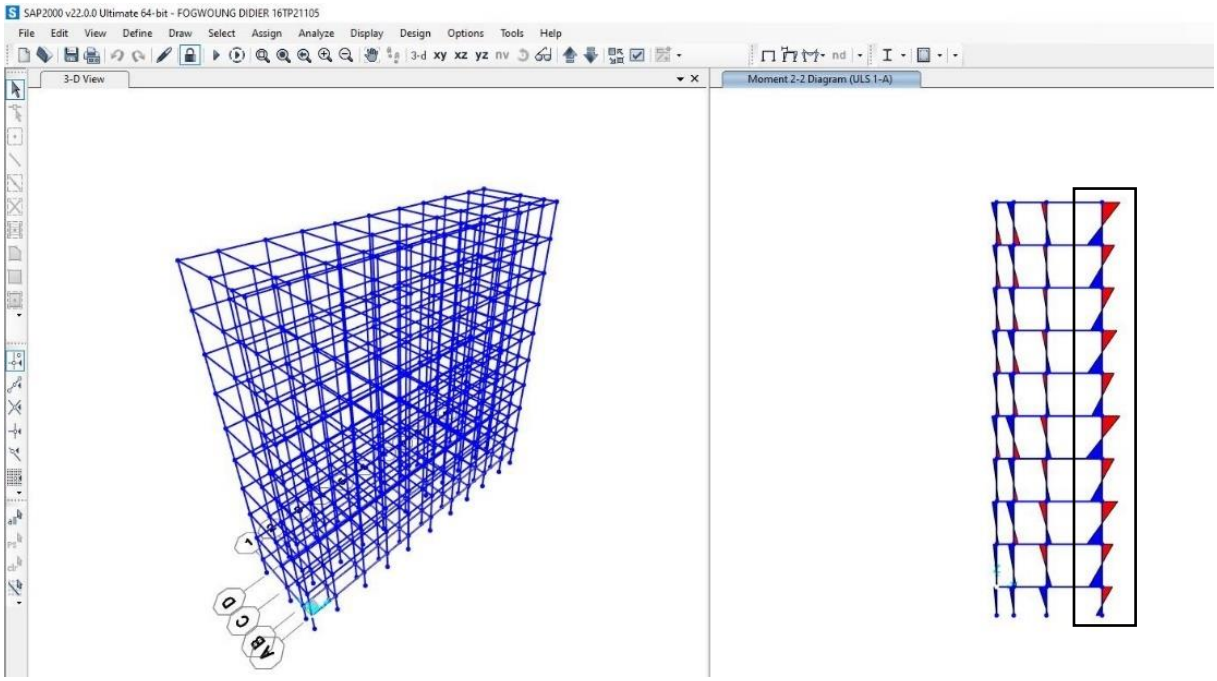

Figure 3.22. Numerical modelling and analysis of columns in SAP2000 v22

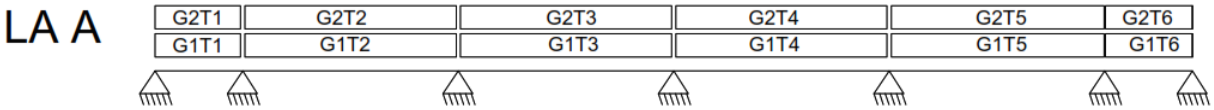

Figure 3.23. Load arrangement for secondary beams

The solicitations that result from these new loads arrangements are presented in figure 3.24, figure 3.25 and figure 3.26. It is important to note that the shear along the x-axis and the bending moment around the y-axis are not presented because the values are the same for all load arrangements.

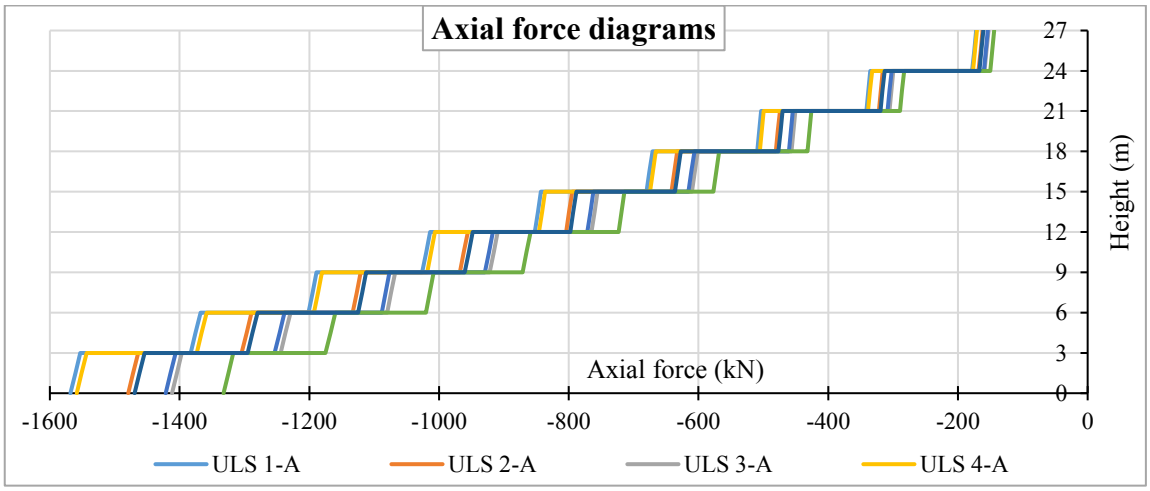

Figure 3.24. Axial force diagrams for columns in row C-6

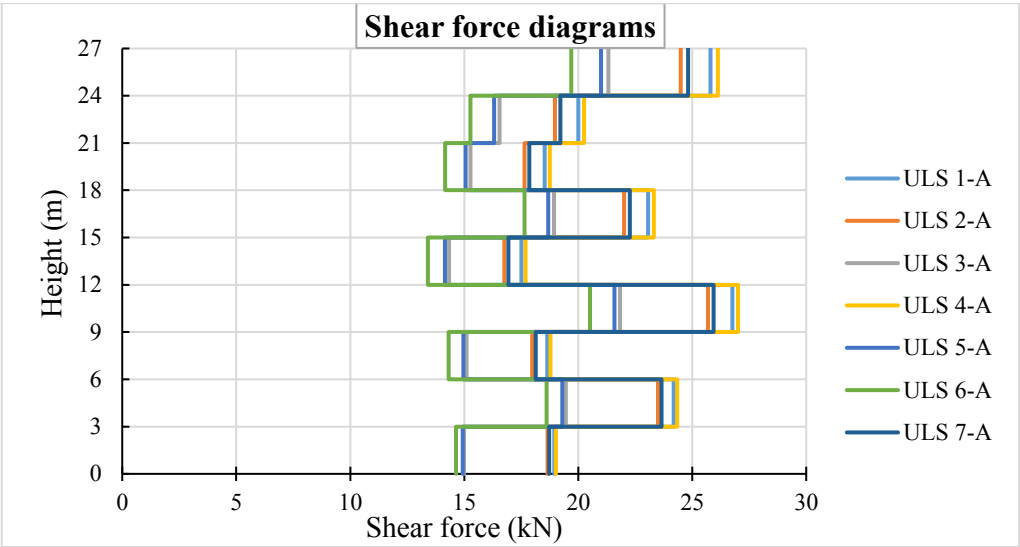

Figure 3.25. Shear force diagrams Vy-y for columns in row D-1

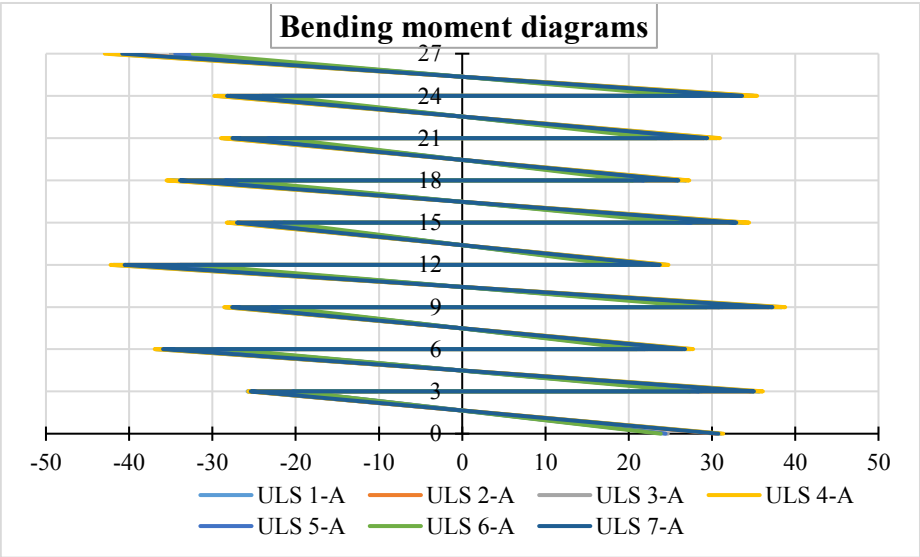

Figure 3.26. Bending moment diagrams Mx-x around x axis in columns D-1

Based on the diagrams of the different solicitations obtained from the 7 load arrangements, the envelope curves for each solicitation were drawn as shown in figure 3.27 to figure 3.30.

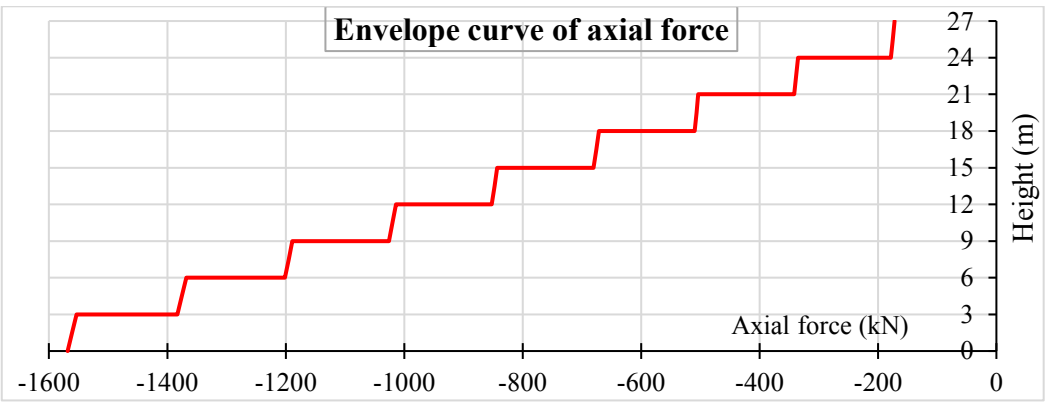

Figure 3.27. Envelope curve of axial force in column C-6

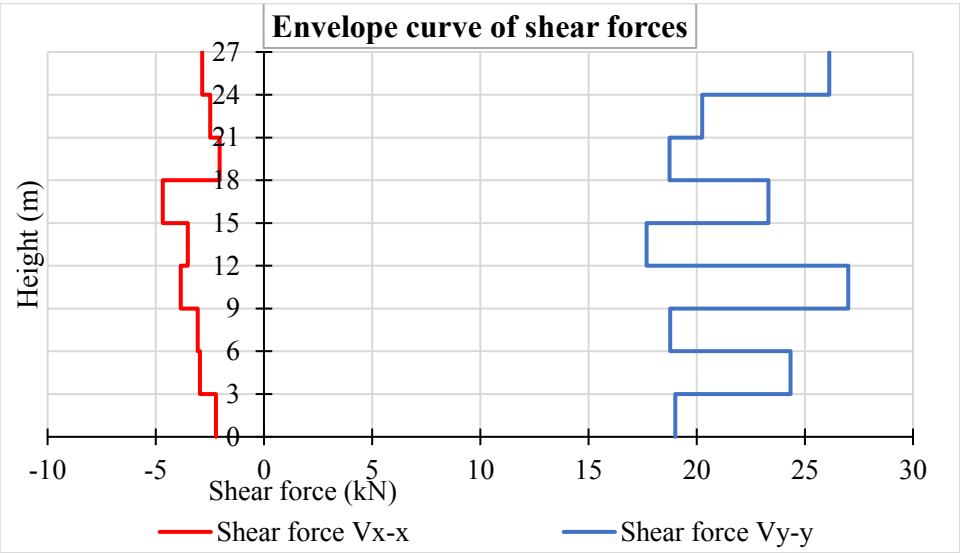

Figure 3.28. Envelope curve of shear forces for columns in row D-1

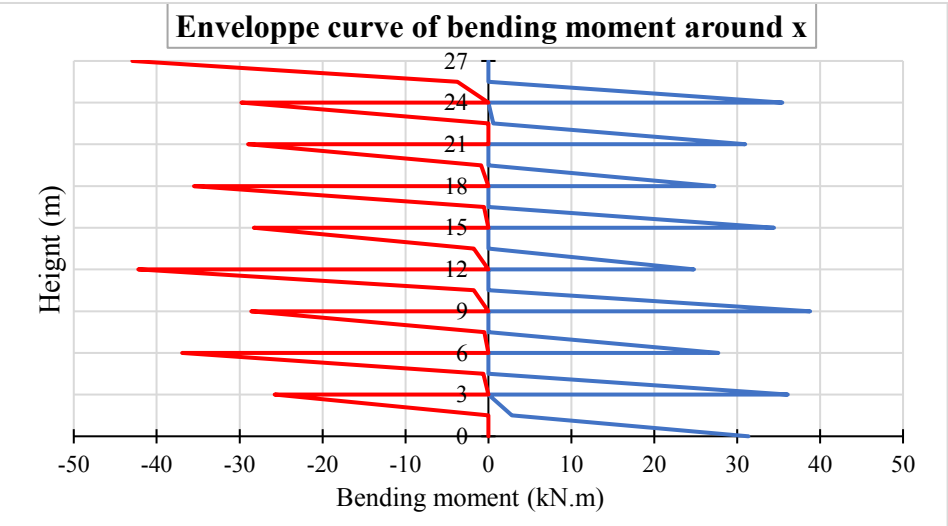

Figure 3.29. Envelope curve of bending moment Mx around x axis for columns in row D-1

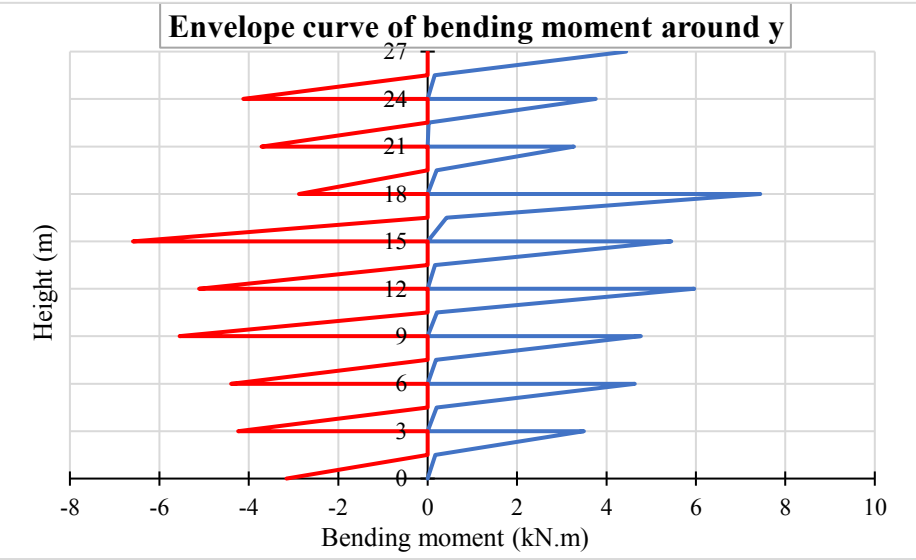

Figure 3.30. Envelope curve of bending moment My around y axis for columns in row D-1

3.3.4.3. Longitudinal reinforcement

In accordance with the procedure described in sections **2.6.2.3** of the Methodology chapter, the longitudinal reinforcement of the columns was determined, and the results are presented in table 3.11. Moreover, verification for the maximum and minimum quantity of reinforcement according to equations **(2.66)** and **(2.67)** has been done. This verification is presented is Table 3.12.

Table 3.11. Longitudinal reinforcements for columns

LEVELS	a(y) (mm)	b(x) (mm)	c(y) (mm)	c(x) (mm)	Asy=Asy'		Asx=Asx'	
					(mm²)	Ø	(mm²)	Ø
1 TO 9	500	300	30	30	339	3 Ø 12	339	3 Ø 12

Table 3.12. Columns verification for maximum and minimum steel quantity

LEVELS	As total		As,min	As,max	Verification
	Ø	(mm²)	mm²	mm²	
1 TO 9	8 Ø 12	905	361	60000	Verified

3.3.4.4. M-N interaction diagram

Once the steel sections were determined, the M-N interaction diagram was plotted for both directions of the columns. Table 3.13 presents the maximum solicitations in columns at each level and figure 3.31 and figure 3.32 present the different M-N interaction diagrams for the columns. As can be seen from those figures, all the points are inside the corresponding M-N diagram, so the section is correct.

Table 3.13. Maximum solicitations in columns at each level

Storeys	Ned (kN)	Mx (kN.m)	My (kN.m)
1	1568.33	3.4953	31.3393
2	1382.875	4.6348	36.9348
3	1201.17	4.766	28.6014
4	1025.92	5.9669	42.2299
5	852.15	5.4453	28.2669
6	680.107	7.4385	35.495
7	509.467	3.2717	28.9926
8	341.199	3.7615	30.972
9	177.998	4.4367	40

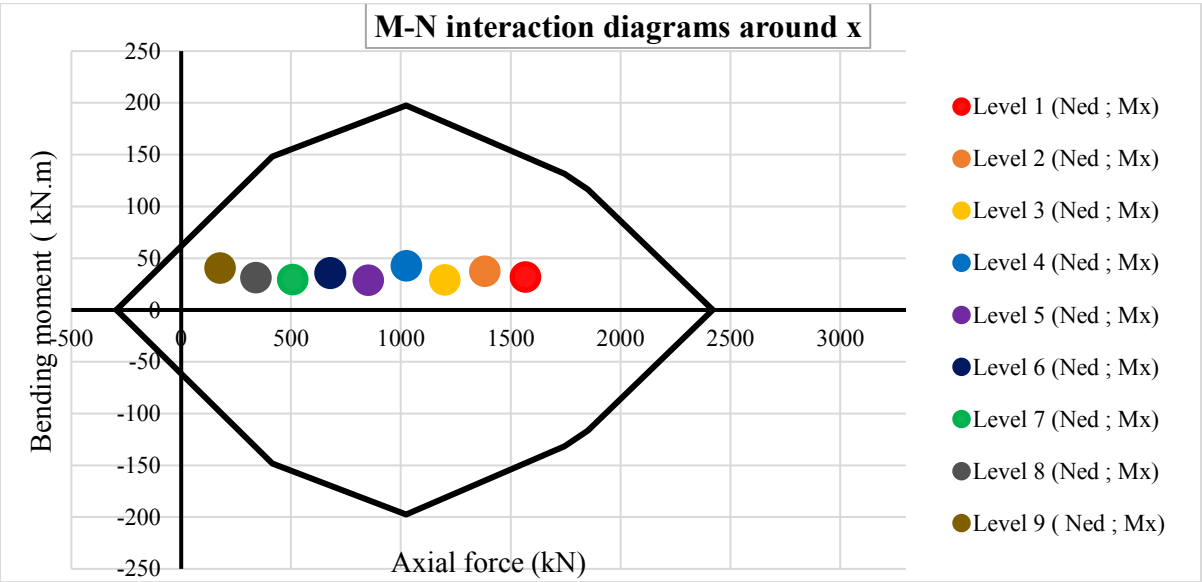

Figure 3.31. Columns verification with M-N interaction diagram around x axis

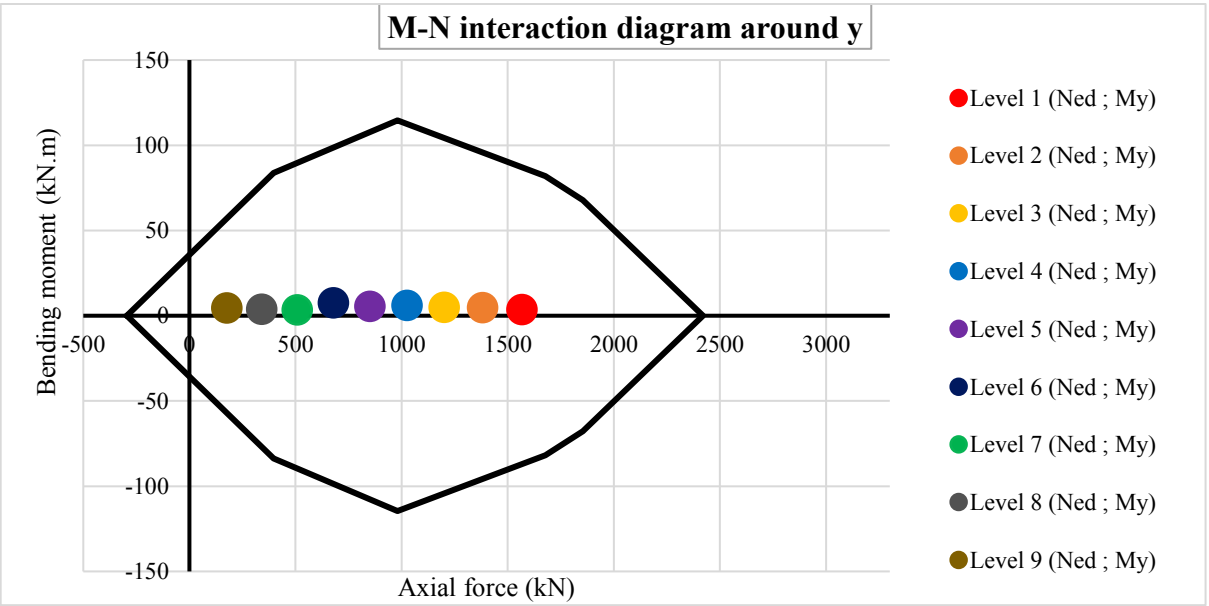

Figure 3.32. Columns verification with M-N interaction diagram around y axis

3.3.4.5. Design for shear

The calculation of the shear reinforcement according to the procedure described in section **2.6.1.2.b** shows that the cross-section of the column is capable of withstanding the shear force. Therefore, the minimum area and maximum spacing of the transverse reinforcement is provided. According to section **2.6.2.5.,** the transverse reinforcements are made of **Ø8** with maximum spacing of **250 mm**. This spacing is reduced to **150 mm,** 50cm above and below the beam.

3.3.4.6. Structural detailing of the column

With respect to the results of the design of the column, the structural detailing of the columns was plotted and presented in figure 3.33.

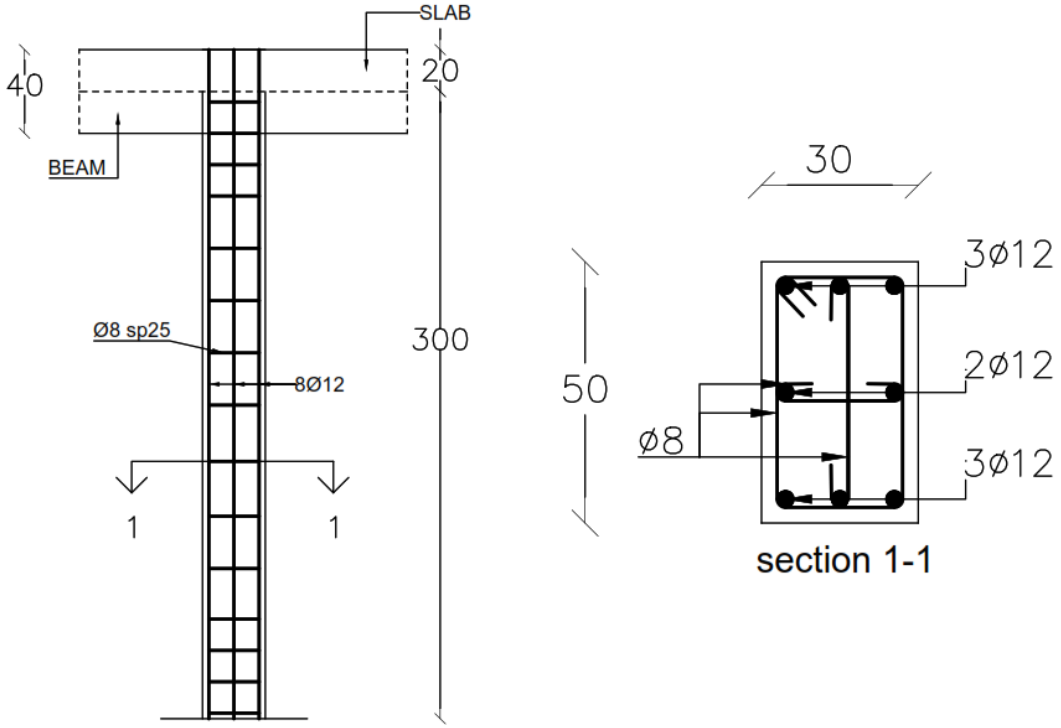

Figure 3.33. Structural detailing of the column

3.3.5. Design of footings

3.3.5.1. Preliminary design

The preliminary design of the footings was done following the procedure given in section 2.6.3.1 and three types of footing were considered. F1 corresponds to a combine footing which supports columns along A and B grid. F2 and F3 are isolated footings which supports columns along C and D grid respectively. The maximum vertical load in the footing at SLS is determined in SAP2000 v22 considering all the load arrangement defined previously. Assuming a soil bearing capacity of 0.35 MPa (see section **3.2.3.1**), the minimal base area of each footing was determined by applying equation **(2.80)**. The results of the preliminary design are reported in table 3.14 and table 3.15. The foundation plan is presented in figureFigure C. 2 of Appendix C.

Table 3.14. Minimum base area of the footings

FOOTING TYPE	soil characteristics	columns properties		Axial Load	Minimum Area		
	sigma soil	a (y)	b (x)	Nsls	Areq	A,min	B,min
	N/mm2	mm	mm	kN	mm²	mm	mm
F1	0.35	500	300	674	3 897 143	2 362	1 650
	0.35	500	300	879			
F2	0.35	500	300	1 280	3 645 714	2 465	1 479
F3	0.35	500	300	1 052	3 082 857	2 267	1 360

Table 3.15. Provided sizes for the footings

FOOTING TYPE	Columns properties		Provided sizes				
	a (y)	b (x)	A	B	h	d	Aprov
	mm	mm	mm	mm	mm	mm	mm²
F1	500	300	2400	1650	550	500	3 960 000
	500	300					
F2	500	300	2500	1500	550	500	3 750 000
F3	500	300	2300	1400	550	500	3 220 000

The foundation plan of the building is illustrated in Figure C. 2 of Appendix C.

3.3.5.2. Longitudinal reinforcement

In accordance with the procedure described in section **2.6.3.3**, the longitudinal reinforcement of the footing F2 was determined and the results are presented in table 3.16. Moreover, verification for the minimum quantity of reinforcement according to equations **(2.87)** has been done.

Table 3.16. Longitudinal reinforcement for footing F2

A mm	B mm	Gk kN	P_{ULS} kN	q' N/mm²	$M_{ED,x}$ kN.m	As,y mm²	As, provided		
							Ø 16	mm²	sp (mm)
2 500	1 500	51.56	1 797.56	0.479	360	1 838	10	2 020	250
					$M_{ED,y}$ kN.m	As,x mm²	As, provided		
							Ø 14	mm²	sp (mm)
					215.71	1 103	8	1 232	200

3.3.5.3. Structural detailing of the footing

With respect to the results of the design of the footing, the structural detailing of the footing F2 was plotted and presented in figure 3.34.

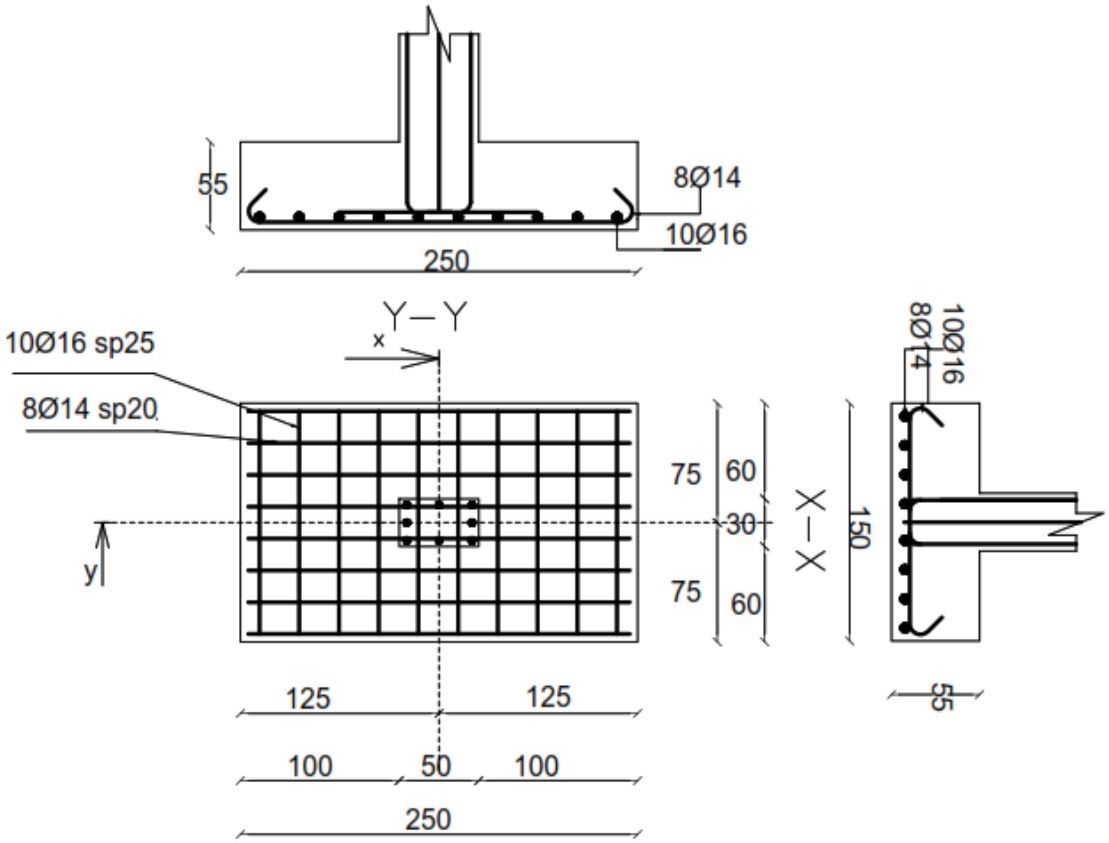

Figure 3.34. Structural detailing of the footing F2

3.4. Regularity of the structure

3.4.1. Centre of mass and centre of rigidity of the structure

The position of the centre of mass CM and the centre of rigidity CR of the structure were determined following the procedure described in section **2.7.1** Table C. 1 and table C.2 of Appendix C present the data used to determine the position of CM and CR respectively.

Hence, the position of the centre of mass is:

$$\begin{Bmatrix} X_{CM} = 14.1\ m \\ Y_{CM} = 3.70\ \mathrm{m} \end{Bmatrix}$$

Using equation **(2.89)**, the position of the centre of rigidity is equal to:

$$\begin{Bmatrix} X_{CR} = \Sigma(K_{yi} * x_i)/\Sigma K_{\mathrm{yi}} = 14.18\ m \\ Y_{CR} = \Sigma(\mathrm{K_{xi}} * y_i)/\Sigma K_{\mathrm{xi}} = 3.03m \end{Bmatrix}$$

The position of the centre of mass and centre of rigidity are illustrated in figure 3.35.

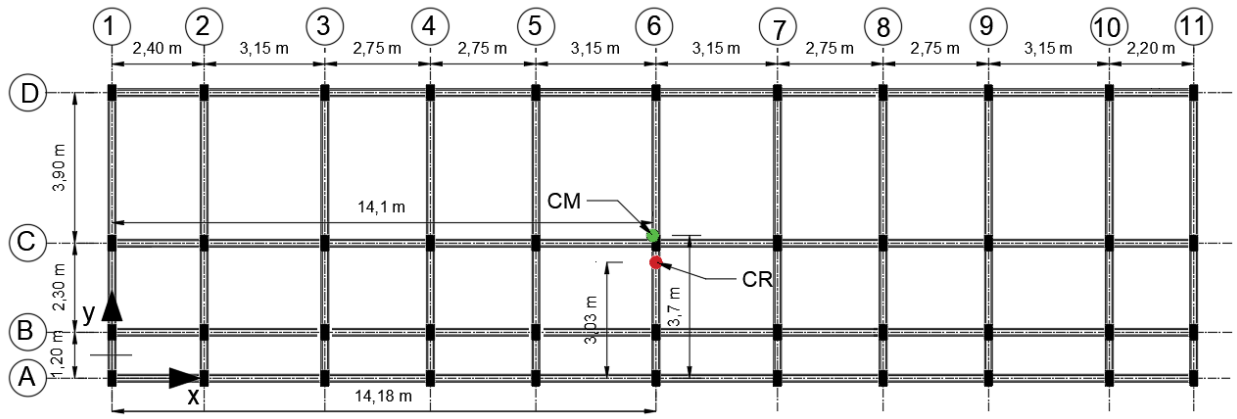

Figure 3.35. Illustration of the position of the CM and CR

The centre of mass and centre of rigidity are not located at the same position, thus there is a structural eccentricity. The value of structural eccentricity along x and y axis were determined according to equation **(2.91)**.

$$\begin{cases} e_x = 14.1 - 14.18 = -0.08\text{m} \\ e_y = 3.70 - 3.03 = 0.67\ \text{m} \end{cases}$$

The value of the accidental eccentricity is determined using equation **(2.92)** and its value is:

$$\begin{cases} e_{ax} = \pm 0.05 \cdot 28.2 = \pm 1.41\ m \\ e_{ay} = \pm 0.05 \cdot 7.40 = \pm 0.37\ m \end{cases}$$

3.4.2. Regularity in plan and in elevation

The criteria for regularity in plan are described in section **2.7.2.1.** Concerning the first condition given, the building is approximately symmetric in plan with respect to the two orthogonal directions according to the mass distribution, but it is not symmetric with respect to the x axis according to the lateral stiffness. Since this necessary condition for regularity in plan is not satisfied, the building is irregular in plan. The other conditions are not evaluated since a necessary condition is not satisfied.

Moreover, the building evidently fulfils all requirements for regularity in elevation state in section **2.7.2.2.** Hence the building is regular in elevation and the value of the behaviour factor adopted is the reference value.

3.5. Modal analysis and seismic weight of the building

To understand the dynamic behaviour of the building, a modal analysis was performed. The first step is to define the building model in SAP2000 software.

3.5.1. Modelling of the building

For this study, a three-dimensional (spatial) structural model is used. This model is based on the requirements of EN 1998-1/4.3.1. The infill walls are not included in the model, assuming their influence on lateral load stiffness and strength on the building structure negligible. Beams and columns are modelled as frame elements connected together by means of rigid diaphragms (in horizontal plane) at each floor level. The slabs are not modelled. The foundations are modelled as shell elements supported by springs (see figure 3.36) in order to take into account, the soil-structure interaction which is an important parameter in the dynamic response of the building.

The cross-sections of beams and columns used in the model are those obtained in the sections **3.3.3** and **3.3.4** respectively. As for the footings, the springs stiffnesses used are presented in the table 3.17.

Table 3.17. Spring stiffness for foundations

Footing	Subgrade modulus of the soil	Section		Discretized section		kx	ky	kz
	C (kN/m^3)	A (m)	B (m)	a (m)	b (m)	kN/m	kN/m	kN/m
F1	120 000	2.4	1.65	0.3	0.165	2 970	2 970	5 940
F2	120 000	2.5	1.5	0.25	0.15	2 250	2 250	4 500
F3	120 000	2.3	1.4	0.23	0.14	1 932	1 932	3 864

Figure 3.36 shows the model used for the analysis with a special emphasis on the foundation.

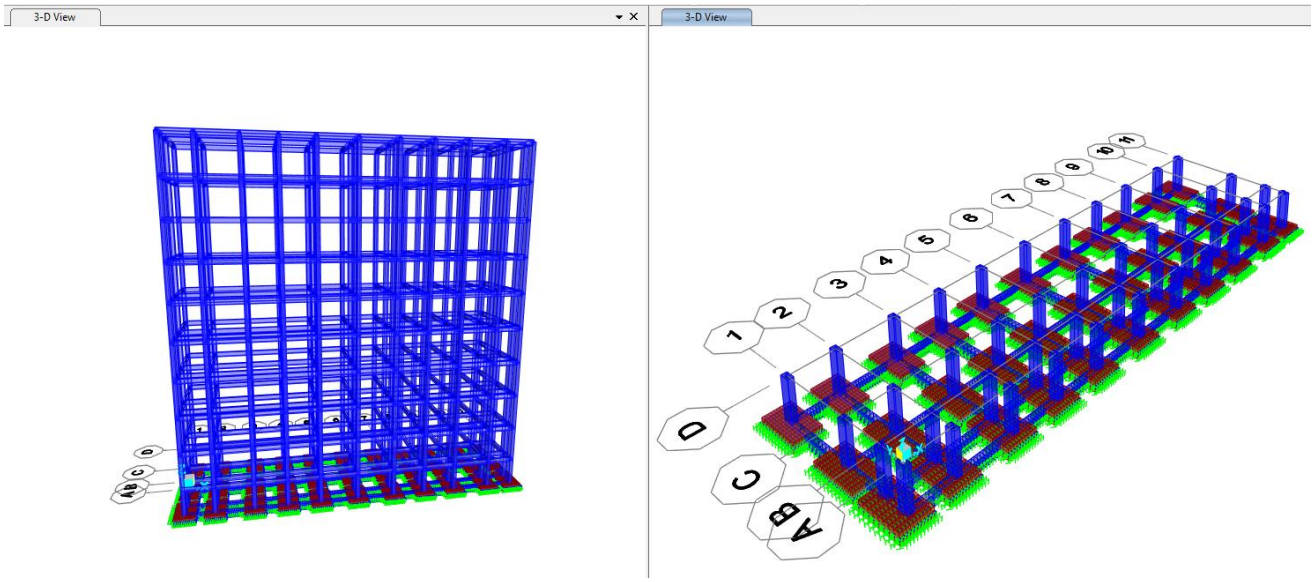

Figure 3.36. 3D view of the model in SAP2000 v22 (Left) and the foundation model (Right)

3.5.2. Modal properties

Several modes of vibration result from the modal analysis of the previous model. These modes differ from each other mainly by their periods. For this analysis we will first look at the first 16 vibration modes. Figure 3.37 shows these modes according to their period.

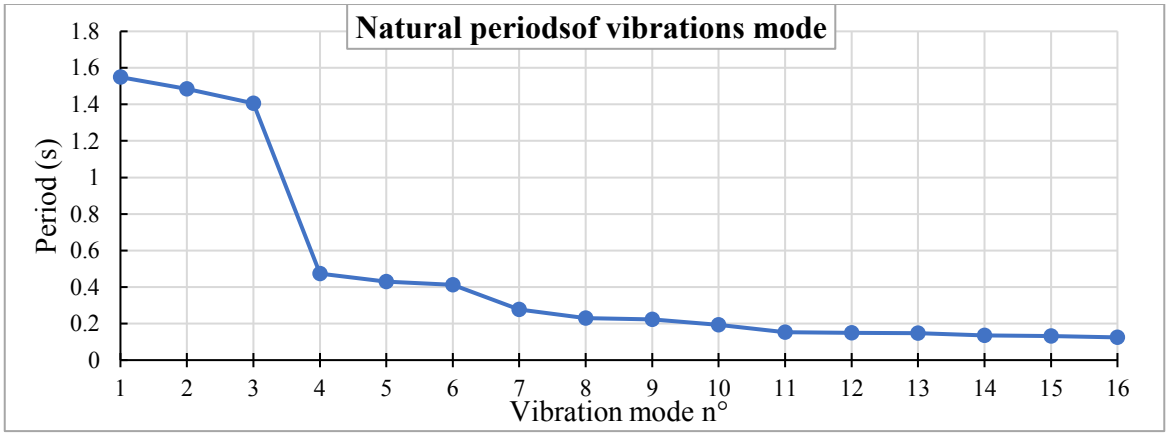

Figure 3.37. Natural periods of the building for each vibration mode

Not all modes participate to the same degree in the deformation of the structure under dynamic loading, the importance of each mode is determined from the modal participation mass ratio or its effective modal mass. Figure 3.38 presents the modal participating mass ratio of the main directions in the different vibration mode of the building.

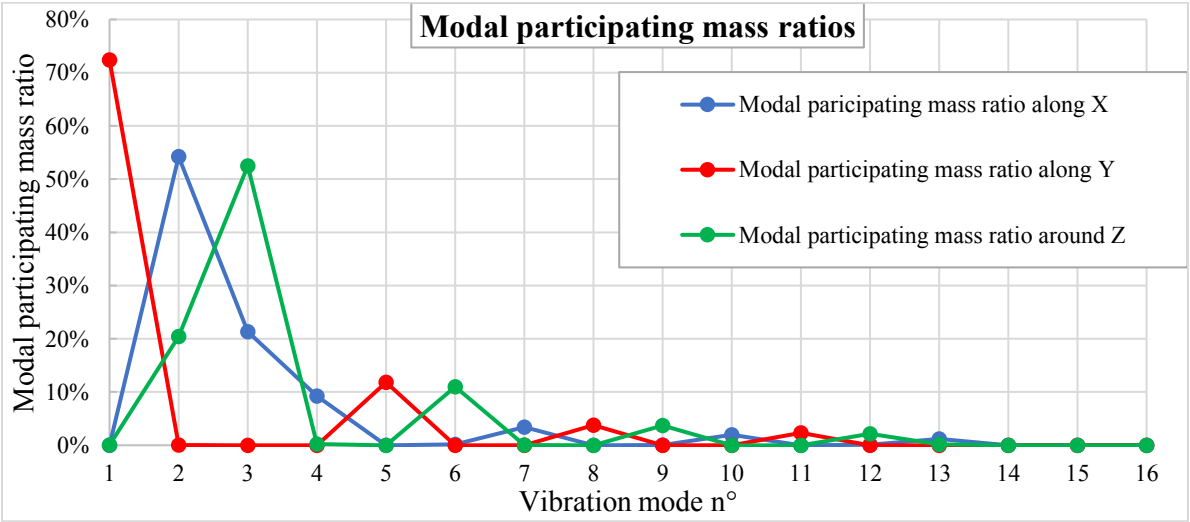

Figure 3.38. Modal participating mass ratios

3.5.3. Selection of useful modes

The response of all modes of vibration contributing significantly to the global response shall be taken into account. Those modes verified that the sum of the effective modal mass accounts to at least 90% of the total mass of the structure. Figure 3.39 shows a cumulation of the mass

participation ratio of the vibration modes along x and y directions and around z direction in order to make the selection.

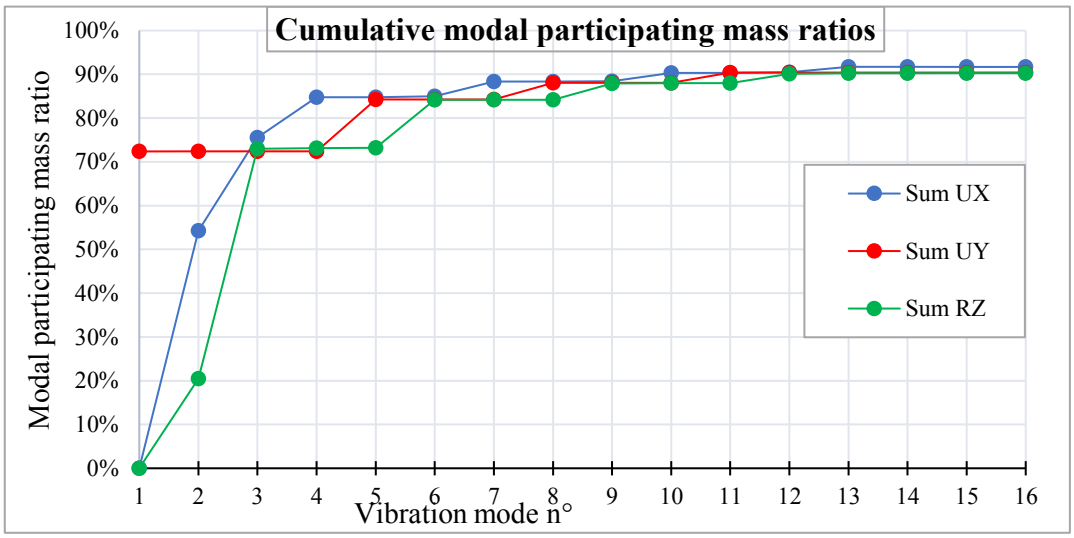

Figure 3.39. Cumulative modal participating mass ratios

From the examination of the previous curve, it can be seen that the first 12 vibration modes satisfy the above condition and their modal percentage mass ratio for each direction is given in the table 3.18.

Table 3.18. Useful modes

Mode	Period (s)	Modal participating mass ratios		
		UX (%)	UY (%)	RZ (%)
1	**1.549**	0.005	72.386	0.023
2	**1.486**	54.234	0.019	20.425
3	**1.406**	21.327	0.008	52.512
4	**0.473**	9.230	0.000	0.210
5	**0.430**	0.000	11.846	0.009
6	**0.412**	0.169	0.010	11.002
7	**0.276**	3.399	0.000	0.028
8	**0.230**	0.000	3.777	0.007
9	**0.224**	0.029	0.007	3.726
10	**0.193**	1.966	0.000	0.013
11	**0.152**	0.000	2.348	0.008
12	**0.149**	0.130	0.007	2.128
SUM		**90.489**	**90.409**	**90.091**

These results represent the intrinsic properties of the structure and are not function of the level of ductility. They have an important role to play in the evaluation of the response of the structure to the earthquake through the modal response spectrum analysis.

The first three vibration modes are presented in figure 3.40, figure 3.41 and figure 3.42.

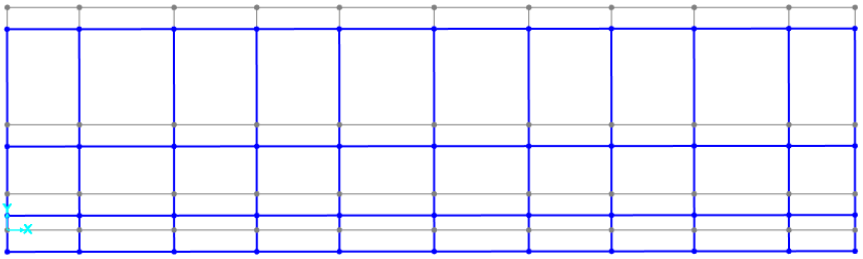

Figure 3.40. 1st vibration mode : Translation along y axis

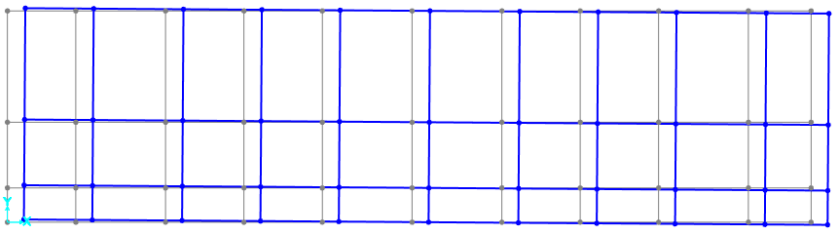

Figure 3.41. 2nd vibration mode: Translation along x axis with a slightly torsion

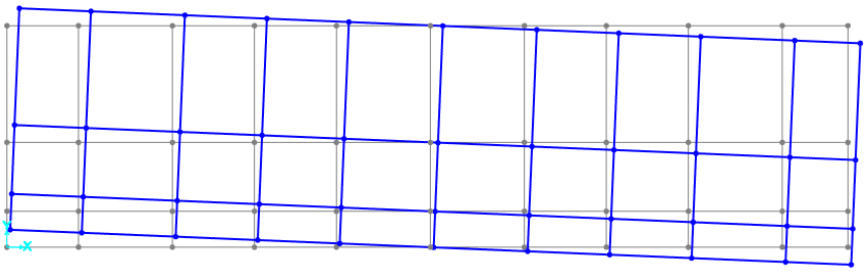

Figure 3.42. 3rd vibration mode: Rotation around z axis

3.5.4. Seismic weight of the building

The total seismic weight of the building is computed and the results are presented in table 3.19. The combination used to determine the weight is the one given by equation

Table 3.19. Seismic weight of the building

Storeys	Permanent load Gk	Variable load Qk	ψ_2	ϕ	ψ_E	$G_k + \psi_E.Q_k$	Mass
	kN	kN				kN	t
Ground (0)	1723.42	417.36	0.3	0.8	0.24	1823.59	182.36
1	3653.18	417.36	0.30	0.80	0.24	3753.34	375.33
2	3653.18	417.36	0.3	0.8	0.24	3753.34	375.33
3	3653.18	417.36	0.3	0.8	0.24	3753.34	375.33
4	3653.18	417.36	0.3	0.8	0.24	3753.34	375.33
5	3653.18	417.36	0.3	0.8	0.24	3753.34	375.33
6	3653.18	417.36	0.3	0.8	0.24	3753.34	375.33
7	3653.18	417.36	0.3	0.8	0.24	3753.34	375.33
8	3653.18	417.36	0.3	0.8	0.24	3753.34	375.33
Roof (9)	1723.42	313.02	0.3	1	0.3	1817.33	181.73
TOTAL	30948.844	3651.9				**33 668**	**3 416**

3.6. Results of the analysis

As mentioned in section **1.4.3**, the basic parameter used to define a level of ductility is the behaviour factor and from this, the design spectrum of the seismic action is derived. For this work, due to the lack of sufficient data to establish the exact spectrum for our study area, the spectrum used will be that of the locality of Belluno in Italy. This is an area of moderate seismicity and the elastic response spectrum is presented in figure 3.43.

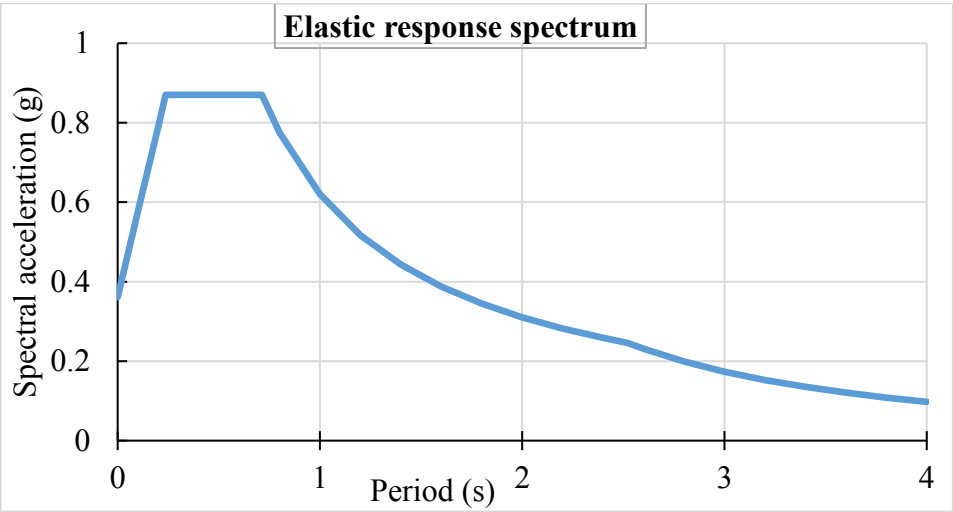

Figure 3.43. Belluno elastic response spectrum

3.6.1. Behaviour factor and design spectrum

For this analysis, the ULS and SLS limit states were considered by the associated behaviour factors. For the SLS verifications, the structure was considered non dissipative and the behaviour factor considered was equal to 1 for both ductility levels.

For the ULS analysis, the procedure for determining the behaviour coefficient was described in section **2.7.3**. The first step is to identify the structural type of the building. The building to be analysed is a frame system with multistorey and multi-bay frames. For this analysis, two levels of ductility were considered and therefore two behaviour coefficients have been chosen.

The maximum allowable behaviour factor in DCM was determined by applying the equation **(2.95)**:

$$\boldsymbol{maxq_{all}} = q_0 \cdot k_w = (3 \cdot 1.3) \cdot 1 = \mathbf{3.9}$$

With respect to this maximum value, two behaviour factors were adopted. The first one is given by **q = 2.5** in order to have an idea of the behaviour of the building at low level of ductility and the second one is given by **q = 3.9** in order to have an idea of the behaviour of the building at a higher level of ductility. These behaviour factors were used in both directions.

The SLS and design spectra are plot in figure 3.44.

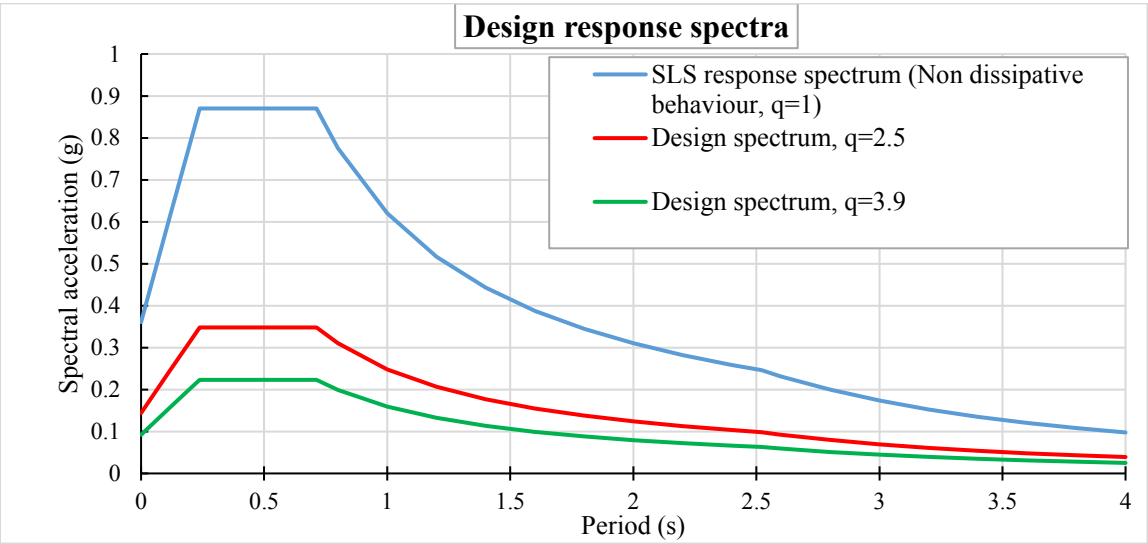

Figure 3.44. Response spectra of earthquake motion

3.6.2. Results of modal response spectrum analysis

3.6.2.1. Combination of seismic action

Equation **(2.16)** allows the establishment of 8 seismic load combinations (SLC):

- **SLC 1:** $\sum_k G_k + 0.3\sum_k Q_k + E_x + 0.3E_y$
- **SLC 2:** $\sum_k G_k + 0.3\sum_k Q_k + E_x - 0.3E_y$
- **SLC 3:** $\sum_k G_k + 0.3\sum_k Q_k - E_x + 0.3E_y$
- **SLC 4:** $\sum_k G_k + 0.3\sum_k Q_k - E_x - 0.3E_y$
- **SLC 5:** $\sum_k G_k + 0.3\sum_k Q_k + 0.3E_x + E_y$
- **SLC 6:** $\sum_k G_k + 0.3\sum_k Q_k - 0.3E_x + E_y$
- **SLC 7:** $\sum_k G_k + 0.3\sum_k Q_k + 0.3E_x - E_y$
- **SLC 8:** $\sum_k G_k + 0.3\sum_k Q_k - 0.3E_x - E_y$

3.6.2.2. Response of the structure

After running the modal response spectrum analysis for all the combination defined and for each ductility levels, several results were obtained. The most important were the base shear, the new internal forces on the structural elements and the displacement of each storey.

a. The base shear forces

In accordance with section **2.8.2.2.c.i**, the base shear force which represent the total lateral seismic force, was determined for each seismic combination in each direction. The results are presented in table 3.20 and table 3.21.

Table 3.20. The base shear forces for q = 2.5

Seismic load combination	Base shear force (kN)	
	In x direction	In y direction
SLC 1	5165.632	1544.647
SLC 2	5165.632	-1544.647
SLC 3	-5165.632	1544.647
SLC 4	-5165.632	-1544.647
SLC 5	1572.92	5071.388
SLC 6	-1572.92	5071.388
SLC 7	1572.92	-5071.388
SLC 8	-1572.92	-5071.388
Maximum value	5165.632	5071.388
Minimum value	-5165.632	-5071.388

Table 3.21. The base shear forces for q = 3.9

Seismic load combination	Base shear force (kN)	
	In x direction	In y direction
SLC 1	3310.212	989.668
SLC 2	3310.212	-989.668
SLC 3	-3310.212	989.668
SLC 4	-3310.212	-989.668
SLC 5	1007.916	3249.383
SLC 6	-1007.916	3249.383
SLC 7	1007.916	-3249.383
SLC 8	-1007.916	-3249.383
Maximum value	3310.212	3249.383
Minimum value	-3310.212	-3249.383

As can be seen, the base shear force is lower for a higher behaviour factor. An increase in the behaviour factor of **56%** produces a reduction in the base shear force of **35.9%** in the case of this study. This result is due to a higher energy dissipation for a higher behaviour factor, resulting in a lower design seismic action.

In addition, the base shear force is directly related to the solicitations in the different structural elements. Hence, the structural elements designed for q = 2.5 will have higher solicitations and therefore a larger concrete and steel section to resist these solicitations.

b. The new internal forces in the structural elements

The seismic action will generate new solicitations in the different structural elements. Attention will be paid on the beams and columns only.

i. Beams

The solicitations in the beams under the different seismic combinations were determined using the SAP2000 v22 software. The results were exported to Excel in order to derive the maximum values for the design of the beams and are presented in figure 3.45 to figure 3.48.

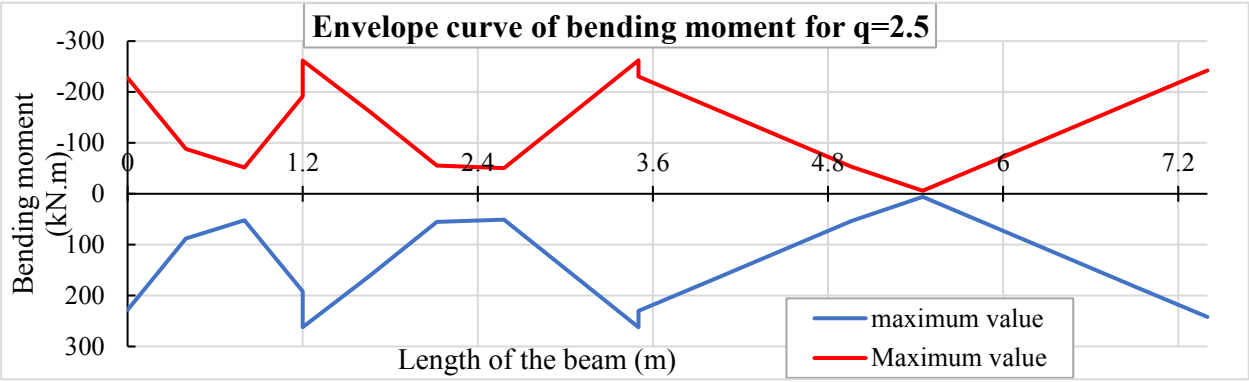

Figure 3.45. New envelope curve of bending moment on the beam for q = 2.5

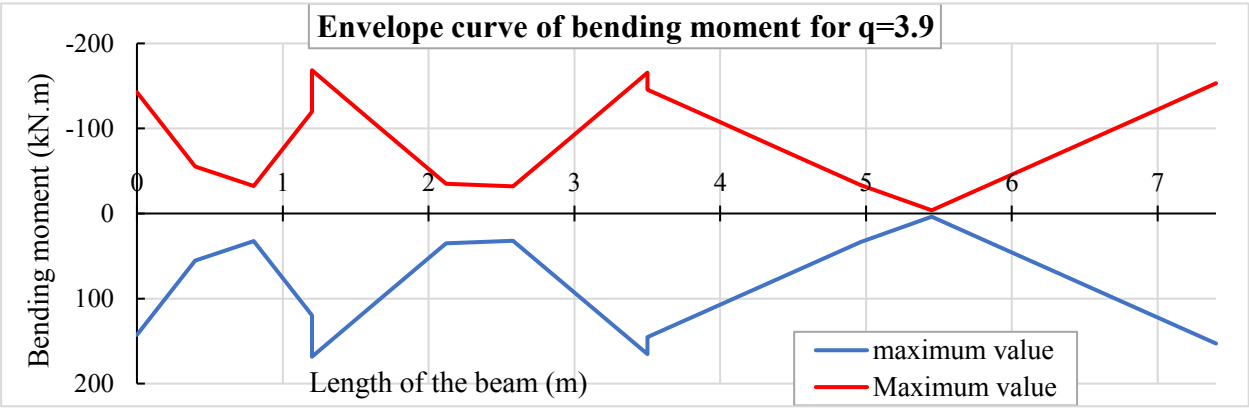

Figure 3.46. New envelope curve of bending moment on the beam for q = 3.9

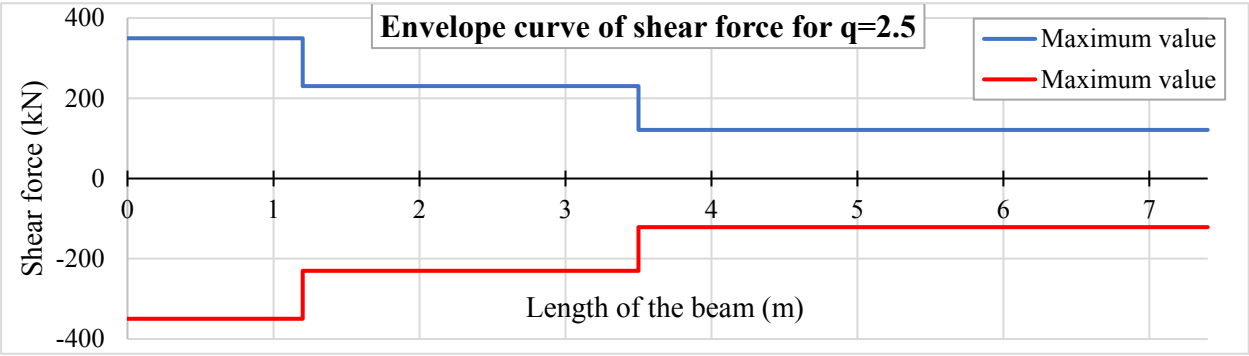

Figure 3.47. New envelope curve of shear force on the beam for q = 2.5

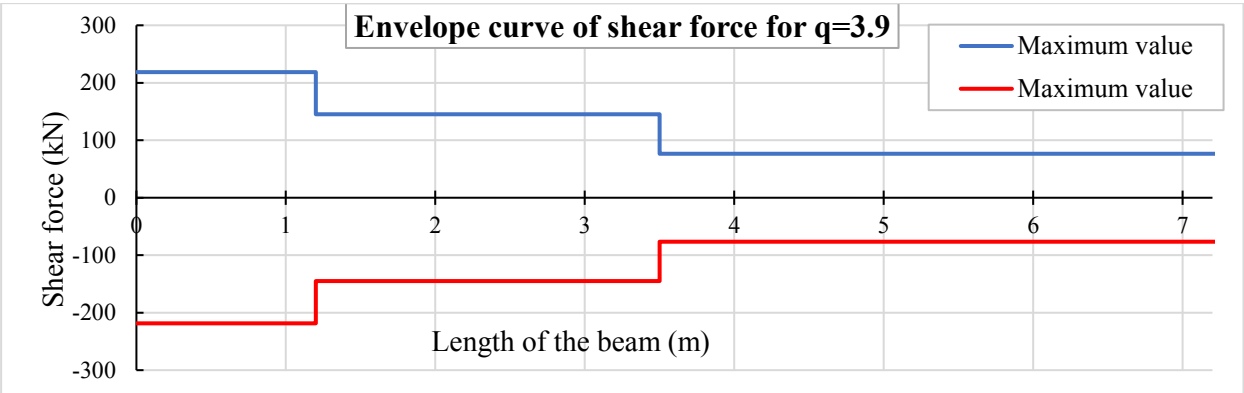

Figure 3.48. New envelope curve of shear force on the beam for q = 3.9

ii. Columns

The internal forces in the columns under the different seismic combinations were determined using the SAP2000 v22 software. Different columns were selected in order to obtain the maximum solicitations. The obtained internal forces were exported to MS Excel in order to better visualise and are presented in figure 3.49 to figure 3.54.

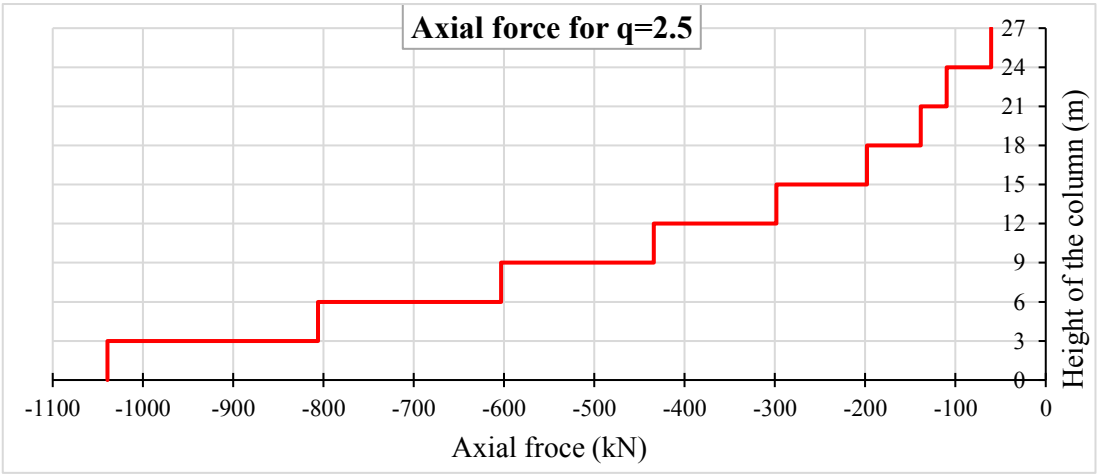

Figure 3.49. New envelope curve of axial force on the columns for q = 2.5

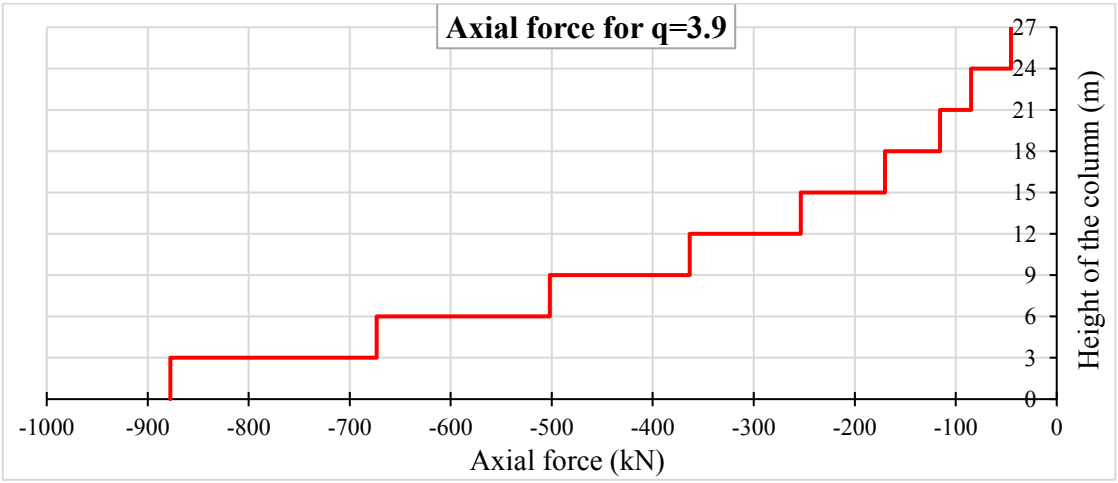

Figure 3.50. New envelope curve of axial force on the columns for q = 3.9

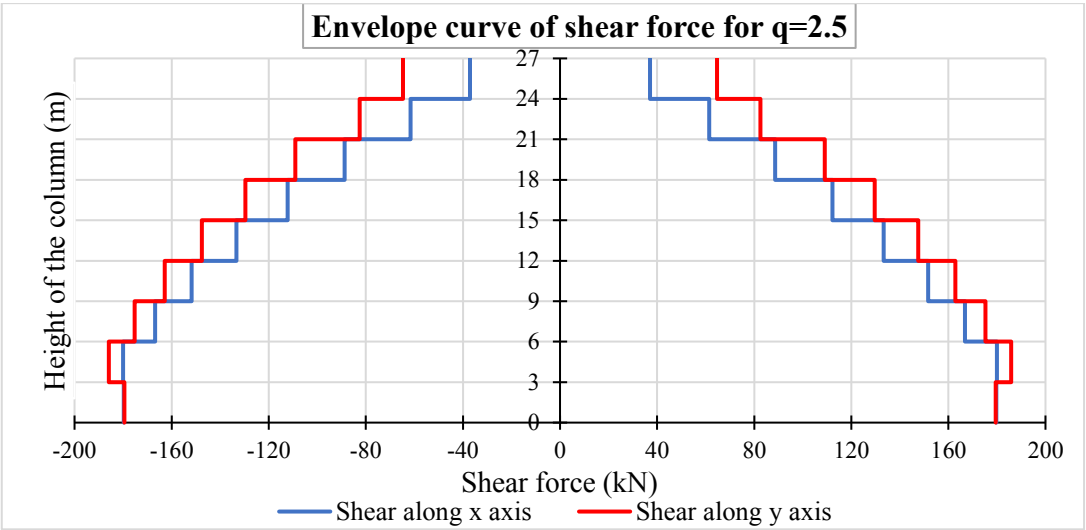

Figure 3.51. New envelope curve of shear force on the columns for q = 2.5

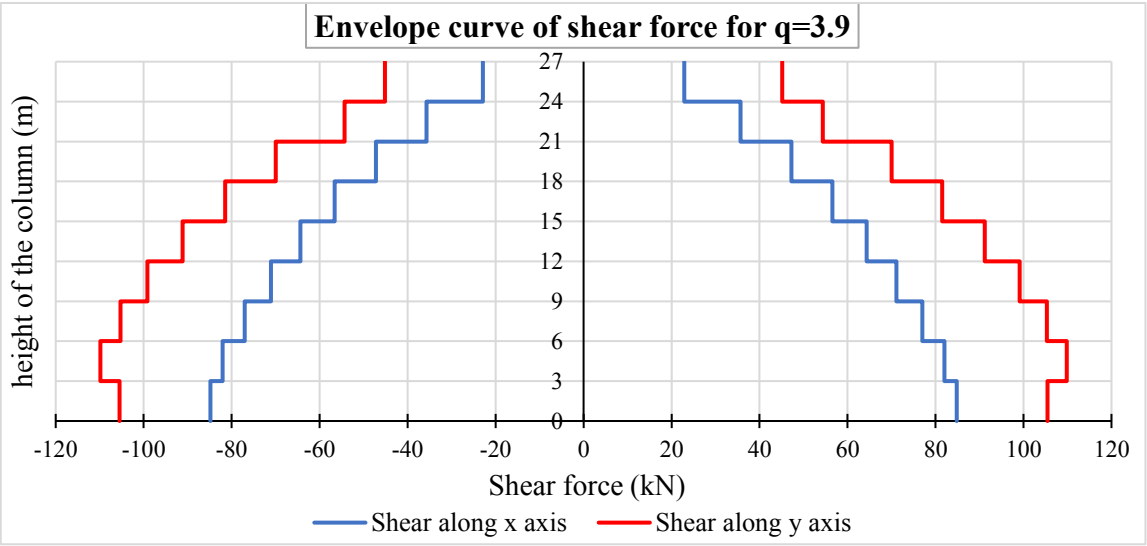

Figure 3.52. New envelope curve of shear force on the columns for q = 3.9

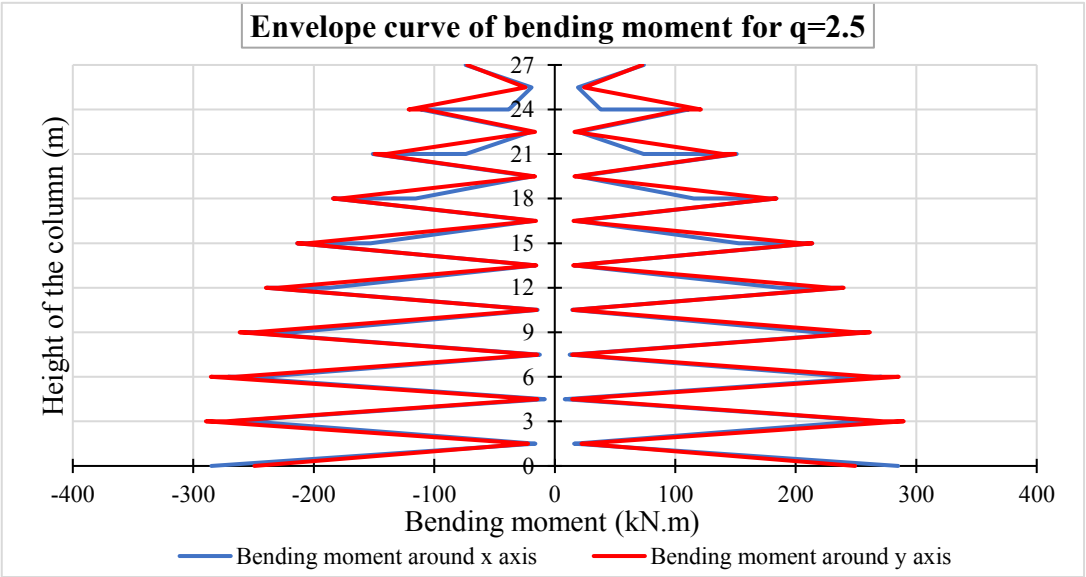

Figure 3.53. New envelope curve of bending moment on the columns for q = 2.5

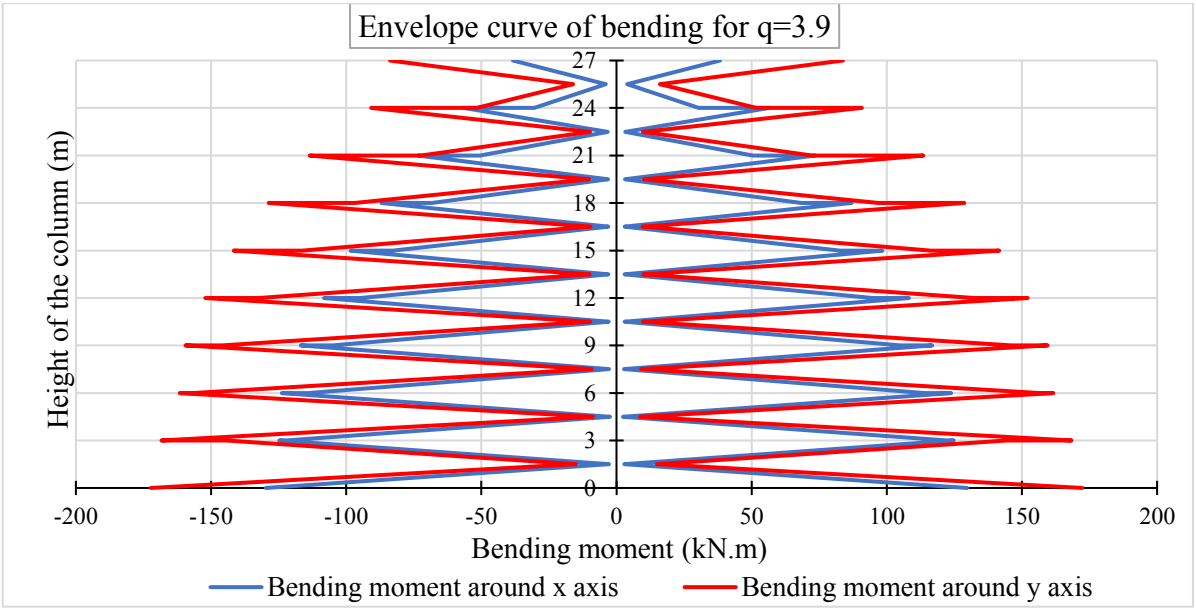

Figure 3.54. New envelope curve of bending moment on the columns for q = 3.9

c. Displacement and interstorey of the structure

Using the SLS response spectrum presented in figure 3.44, the displacement of the structure was determined. Figure 3.55 and figure 3.56 present the maximum deformed shape of the structure on different reference plane.

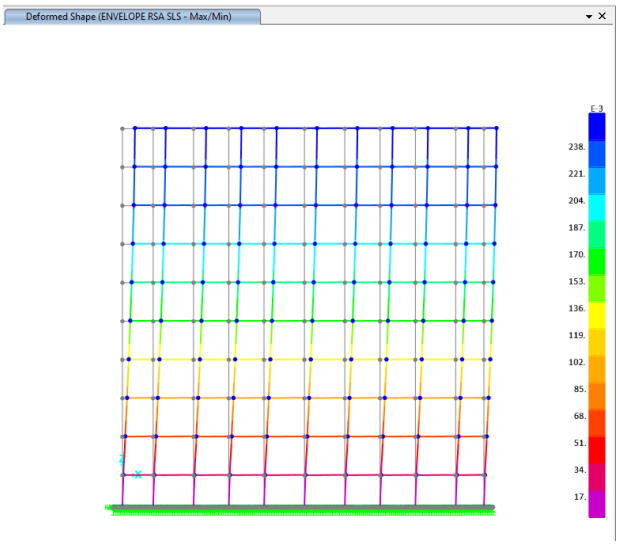

Figure 3.55. Deformed shape of the structure on the X-Z reference plan

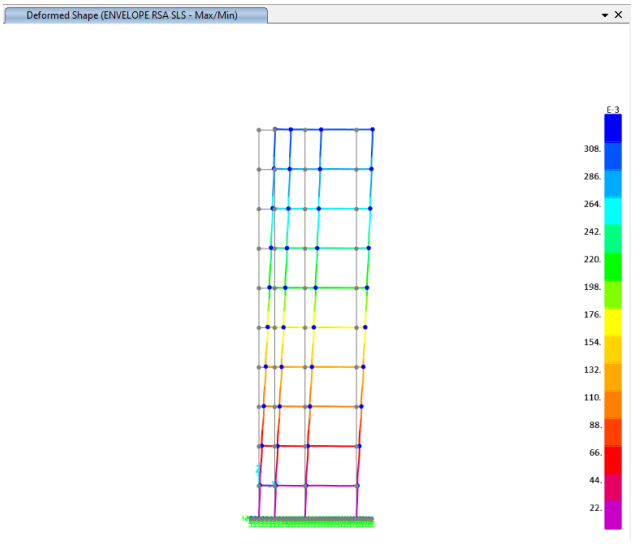

Figure 3.56. Deformed shape of the structure on the Y-Z reference plan

As we can observe from the previous figures, the displacements are practically equal at the nodes located at the same floor and it increases with the height. The displacements being maximal at the centre of mass, the analysis of the displacements at each storey and the interstorey drift will be done considering the column closest to the centre of mass (see figure 3.57).

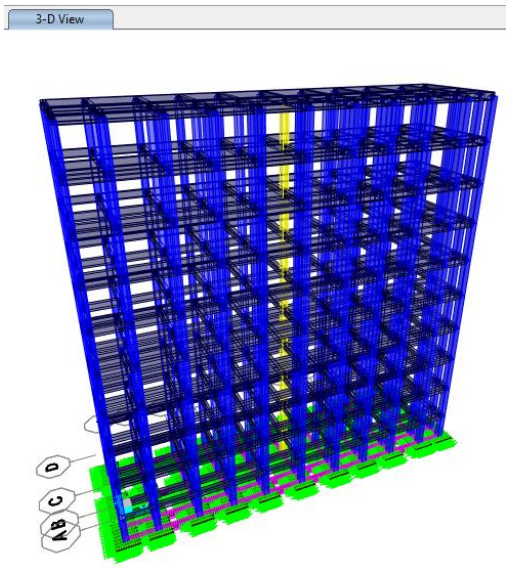

Figure 3.57. Reference vertical element (in yellow) for displacement analysis

The results obtained from this element for each seismic load combination allowed us to plot the displacement diagram along x and y direction as shown in figure 3.58 and figure 3.59 respectively.

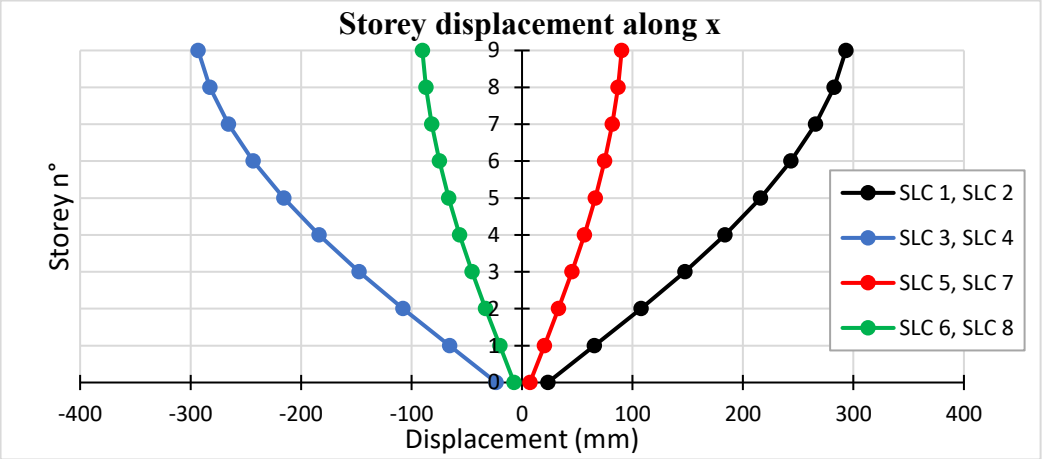

Figure 3.58. Storey displacement along x direction

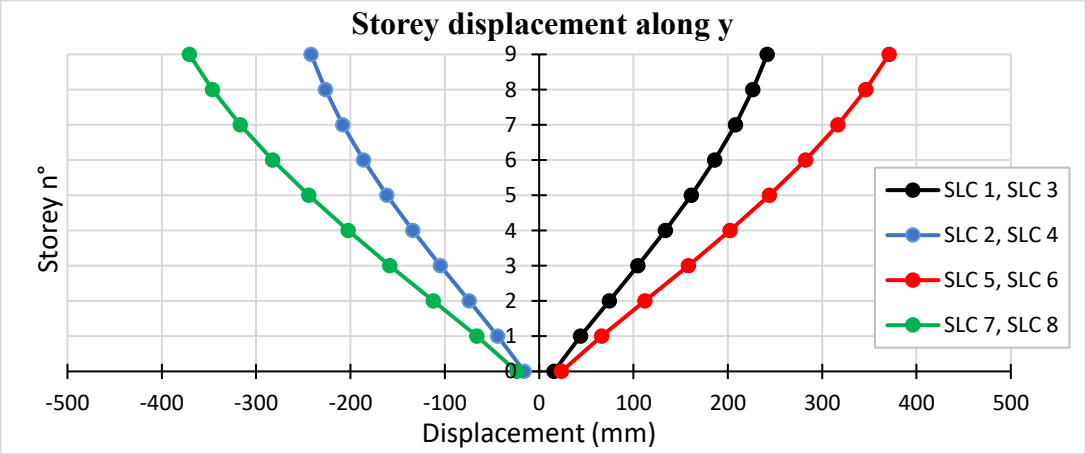

Figure 3.59. Storey displacement along y direction

Through these displacements, the interstorey drift have been determined and compared to the limit inter-storey drift for damage limitation given in equation **(2.102).** The results are presented in table 3.22.

Table 3.22. Storey drift control for both direction

Storeys	Max. displacement (m)		Storey drift (m)		H (m)	ν	ν*dr/h		Limit value
	dx	dy	dr,x	dr,y			Direction X	Direction Y	
0	23.341	23.724	23.341	23.724	3000	0.5	0.0039	0.0040	0.005
1	65.582	66.153	42.241	42.429	3000	0.5	0.0070	0.0071	0.005
2	107.846	112.24	42.264	46.087	3000	0.5	0.0070	0.0077	0.005
3	147.45	158.192	39.604	45.952	3000	0.5	0.0066	0.0077	0.005
4	183.588	202.483	36.138	44.291	3000	0.5	0.0060	0.0074	0.005
5	215.71	244.17	32.122	41.687	3000	0.5	0.0054	0.0069	0.005
6	243.3	282.487	27.59	38.317	3000	0.5	0.0046	0.0064	0.005
7	265.783	316.726	22.483	34.239	3000	0.5	0.0037	0.0057	0.005
8	282.526	346.284	16.743	29.558	3000	0.5	0.0028	0.0049	0.005
9	293.147	370.885	10.621	24.601	3000	0.5	0.0018	0.0041	0.005

As can be seen, the different responses of the structure following the analysis of the modal response spectrum reveal that the choice of the behaviour factor which implies the level of ductility has a great impact on the solicitations and displacements obtained in the structural elements. The previous results show that for q=2.5, all the solicitations on the beams and columns are higher compared to those obtained for q=3.9.

Based on these results, a new design of the different structural elements will be carried out taking into account the capacity design rules in ULS and the limits on displacements in SLS.

3.6.2.3. New design of structural element

The design of the structural elements was carried out in accordance with the procedures described in the sections **2.6** and **2.8.2.2.e.**

a. Beams

By applying the procedures described in section **2.6.1.2** to determine the longitudinal and transverse reinforcement in the beams, while respecting the rules of the constructional provisions, the diagrams presented in figure 3.60 to figure 3.63 have been drawn. These diagrams also highlight the increase in cross-sections required to resist seismic action.

For q=2.5, the new cross-section of the beam is **30 x 60 cm²** and a 12 mm diameter bars are inserted in the middle of the cross-section due to its significant height. In addition, the transverse reinforcements are made of **Ø8** and the number of legs for stirrups is 3.

For q=3.9, the new cross-section of the beam is **30 x 50 cm²** and a 12 mm diameter bars are inserted in the middle of the cross-section due to its significant height. In addition, the transverse reinforcements are made of **Ø8** and the number of legs for stirrups is 3.

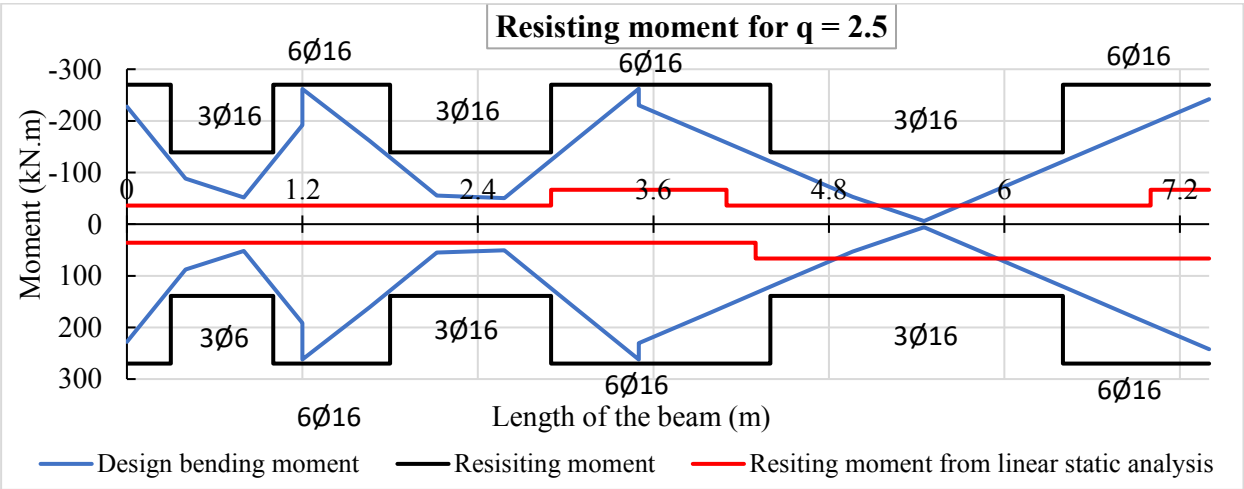

Figure 3.60. Verification of the new section under bending moment for q = 2.5

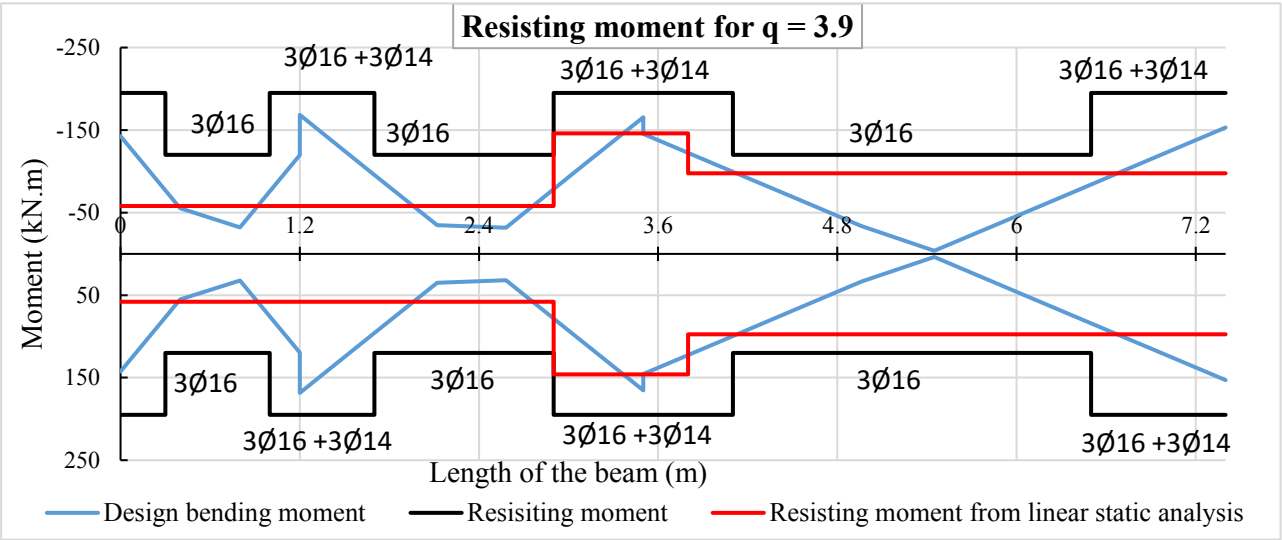

Figure 3.61. Verification of the new section under bending moment for q = 3.9

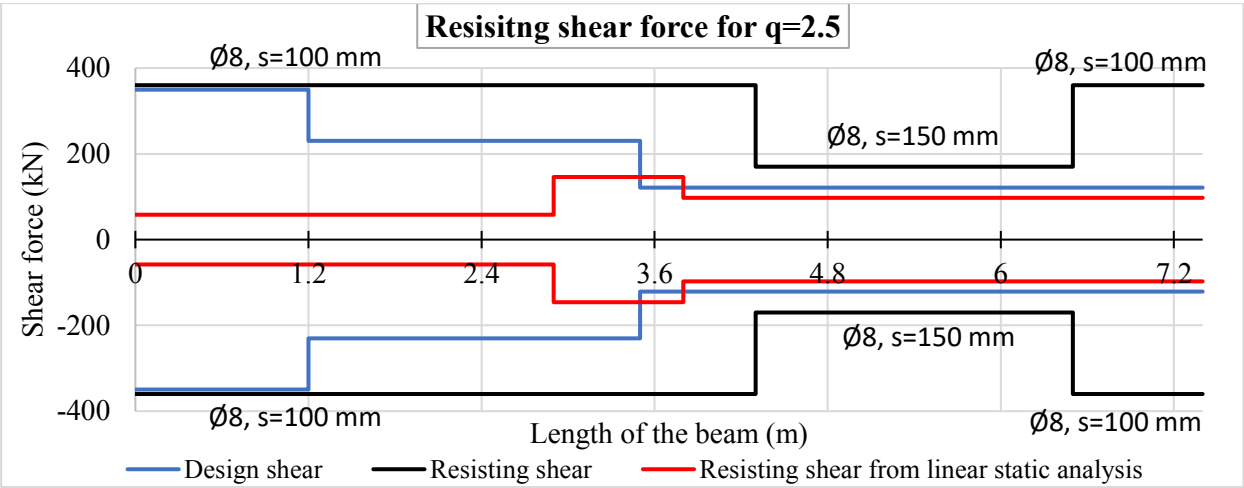

Figure 3.62. Verification of the new section under shear force for q = 2.5

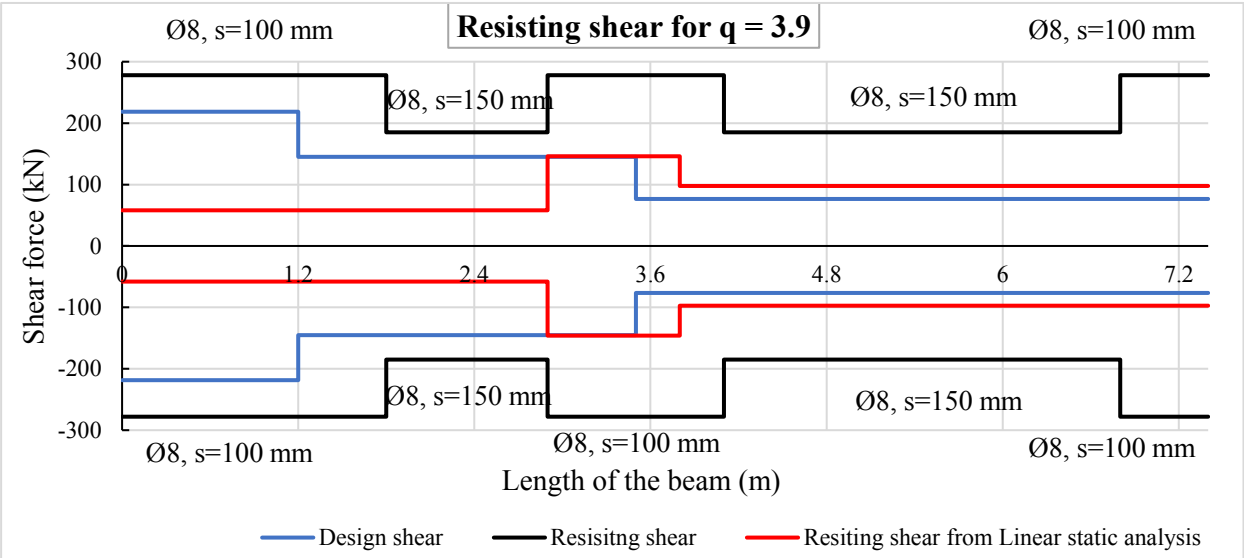

Figure 3.63. Verification of the new section under shear force for q = 3.9

b. Columns

By applying the column design procedure and taking into account the capacity design rules which impose bending resistances of columns connected to the node greater than 1.3 times that of the beams, the cross-section and the longitudinal reinforcement of the columns were determined. For q = 2.5, the cross-section adopted is **65 x 65 cm²** with **16Ø16** and for q = 3.9, the cross-section adopted is **50 x 50 cm²** with **12Ø16**. From those sections, the interaction diagrams between bending moment and axial force were plotted and presented in figure 3.64 to figure 3.67. The solicitations in the columns for each level of ductility are reported in table 3.23 and table 3.24.

Table 3.23. Maximum solicitations in columns for q=2.5

Storeys	Ned (kN)	Mx (kN.m)	My (kN.m)
1	1050	285	290
2	806	271.2	286
3	603	260	265
4	434	240	250
5	298	215	230
6	198	184	206
7	139	151	178
8	110	112	140
9	60	75	122

Table 3.24. Maximum solicitations in columns for q=3.9

Storeys	Ned (kN)	Mx (kN.m)	My (kN.m)
1	878	130	172
2	673	124	168
3	502	117	159
4	363	108	152
5	253	98	142
6	170	87	129
7	116	73	113
8	85	57	91
9	45	38	84

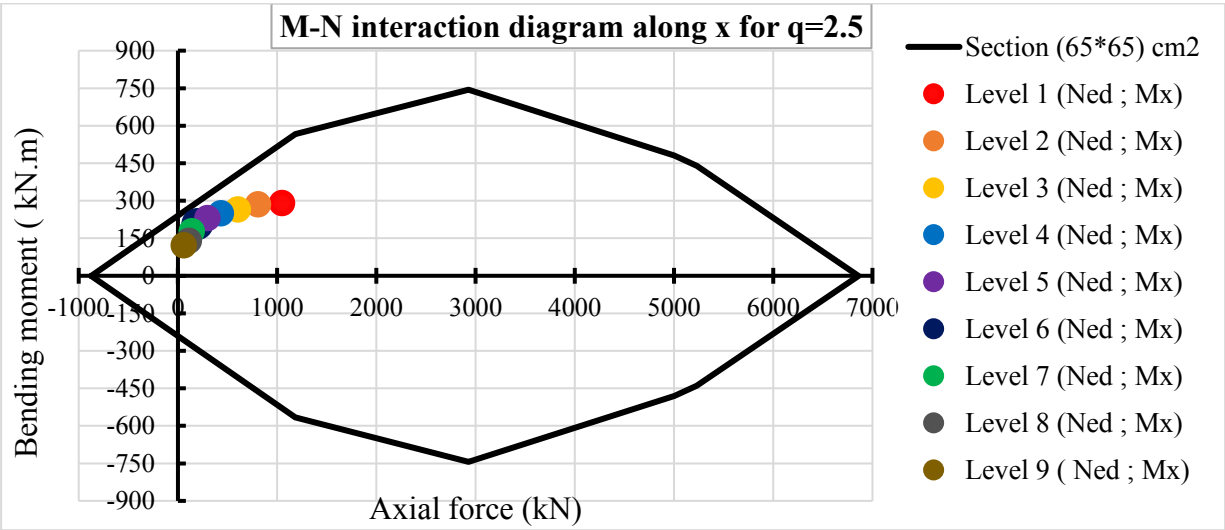

Figure 3.64. M-N interactions diagram around x direction for q = 2.5

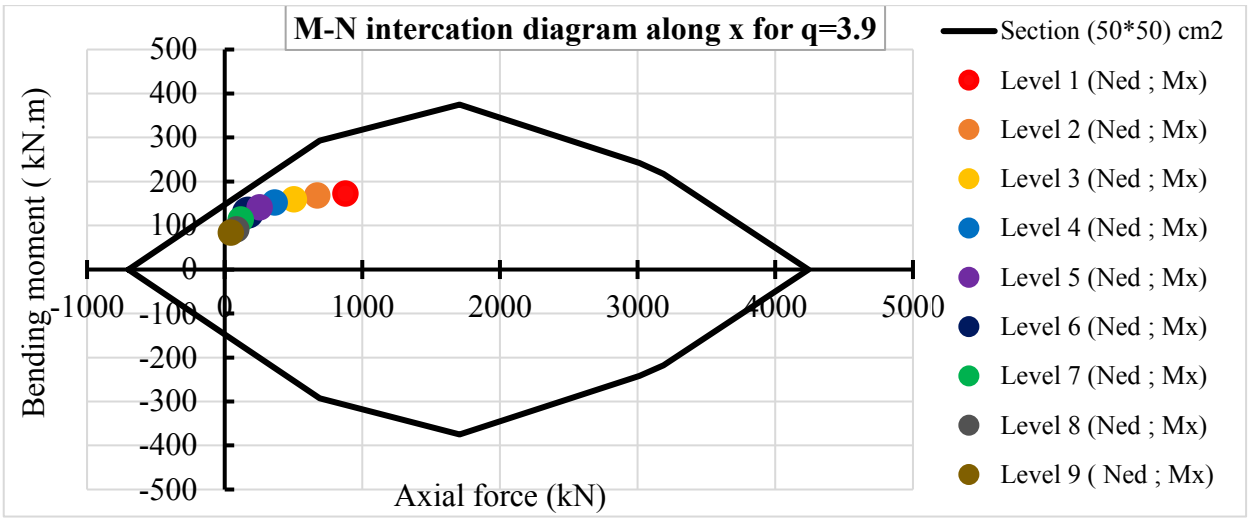

Figure 3.65. M-N interactions diagram around x direction for q = 3.9

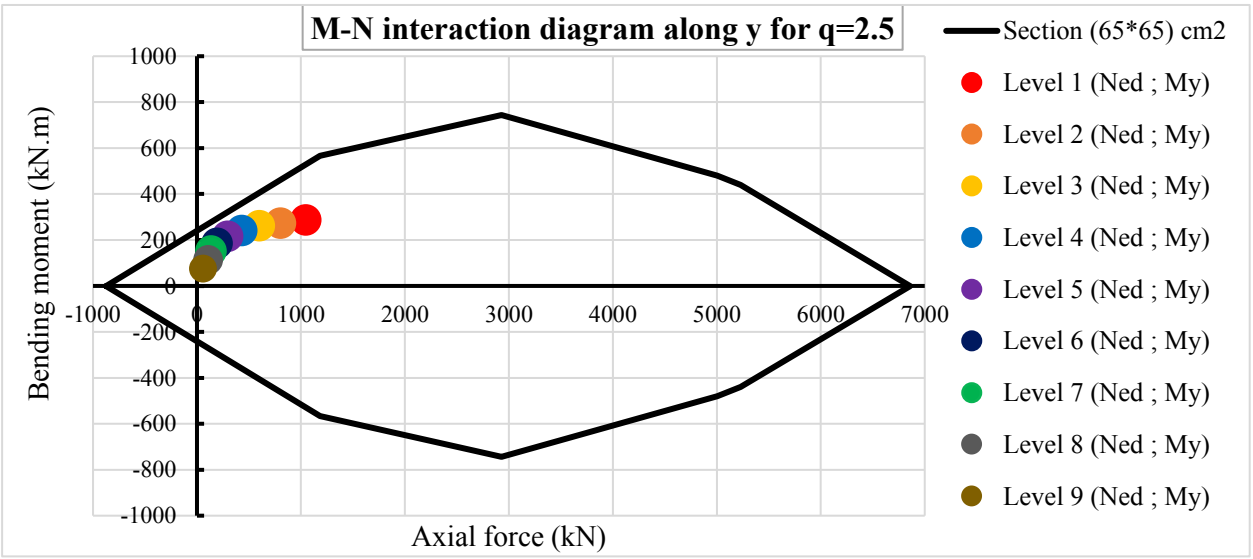

Figure 3.66. M-N interaction diagram around y direction for q = 2.5

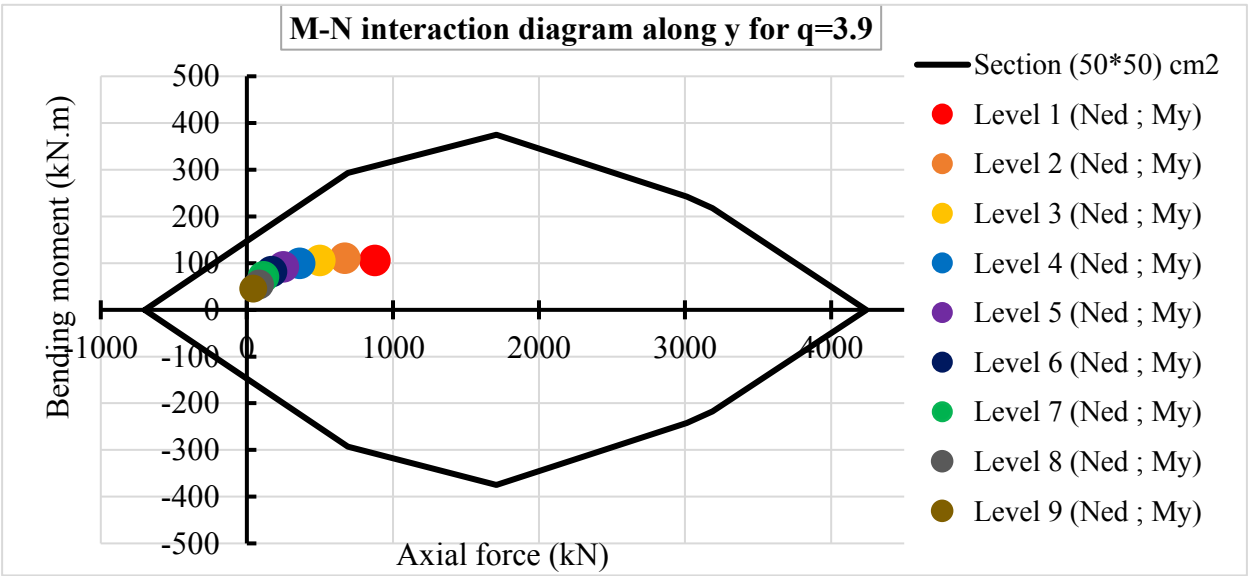

Figure 3.67. M-N interactions diagram around y direction for q = 3.9

For the transverse reinforcement, according to the procedure described in section **2.6.1.2.b** and the precision given in table 2.4, shear reinforcements provided within the critical regions are made of Ø**8** with spacing of **100 mm** for q = 2.5 and q = 3.9**.** Outside the critical regions, the shear reinforcement provided are made of Ø**8** with spacing of **150 mm**.

c. SLS verifications

Once the design of the beams and columns has been carried out, it is therefore necessary to check that the displacement due by the seismic effect remains below a tolerable limit. The results of this verification for each ductility level are reported in table 3.25 and table 3.26.

Table 3.25 New storey drift control in both direction for q = 2.5

Storeys	Max. displacement (mm)		Storey drift (mm)		h (mm)	ν	ν*dr/h		Limit value
	dx	dy	dr,x	dr,y			Direction X	Direction Y	
0	11.953	17.235	11.953	17.235	3000	0.5	0.0020	0.0029	0.005
1	26.927	39.839	14.974	22.604	3000	0.5	0.0025	0.0038	0.005
2	42.452	63.68	15.525	23.841	3000	0.5	0.0026	0.0040	0.005
3	57.319	87.508	14.867	23.828	3000	0.5	0.0025	0.0040	0.005
4	71.076	110.772	13.757	23.264	3000	0.5	0.0023	0.0039	0.005
5	83.435	133.101	12.359	22.329	3000	0.5	0.0021	0.0037	0.005
6	94.156	154.188	10.721	21.087	3000	0.5	0.0018	0.0035	0.005
7	103.027	173.761	8.871	19.573	3000	0.5	0.0015	0.0033	0.005
8	109.885	191.61	6.858	17.849	3000	0.5	0.0011	0.0030	0.005
Roof (9)	114.775	207.689	4.89	16.079	3000	0.5	0.0008	0.0027	0.005

Table 3.26 New storey drift control for both direction for q = 3.9

Storeys	Max. displacement (mm)		Storey drift (mm)		h (mm)	ν	ν*dr/h		Limit value
	dx	dy	dr,x	dr,y			Direction X	Direction Y	
0	13.886	18.079	13.886	18.079	3000	0.5	0.0023	0.0030	0.005
1	34.896	45.239	21.01	27.16	3000	0.5	0.0035	0.0045	0.005
2	56.435	73.784	21.539	28.545	3000	0.5	0.0036	0.0048	0.005
3	76.938	102.101	20.503	28.317	3000	0.5	0.0034	0.0047	0.005
4	95.855	129.512	18.917	27.411	3000	0.5	0.0032	0.0046	0.005
5	112.799	155.55	16.944	26.038	3000	0.5	0.0028	0.0043	0.005
6	127.432	179.813	14.633	24.263	3000	0.5	0.0024	0.0040	0.005
7	139.439	201.923	12.007	22.11	3000	0.5	0.0020	0.0037	0.005
8	148.546	221.542	9.107	19.619	3000	0.5	0.0015	0.0033	0.005
9	154.7	238.449	6.154	16.907	3000	0.5	0.0010	0.0028	0.005

In order to better analyse the difference in building displacements between the two ductility levels, figure 3.68 and figure 3.69 show the evolution of the interstorey drift in each direction and for each ductility level. These curves show an increase in the interstorey drift for q = 3.9 compared to those for q = 2.5. This is due to a decrease in cross-sectional area as the behaviour coefficient increases.

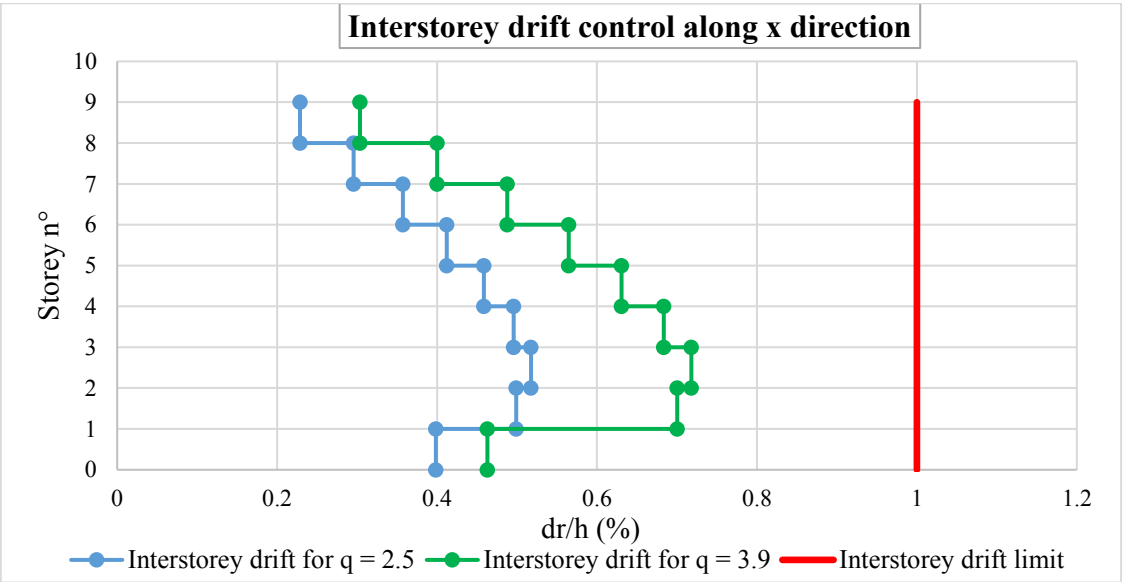

Figure 3.68. Interstorey drift control along x direction

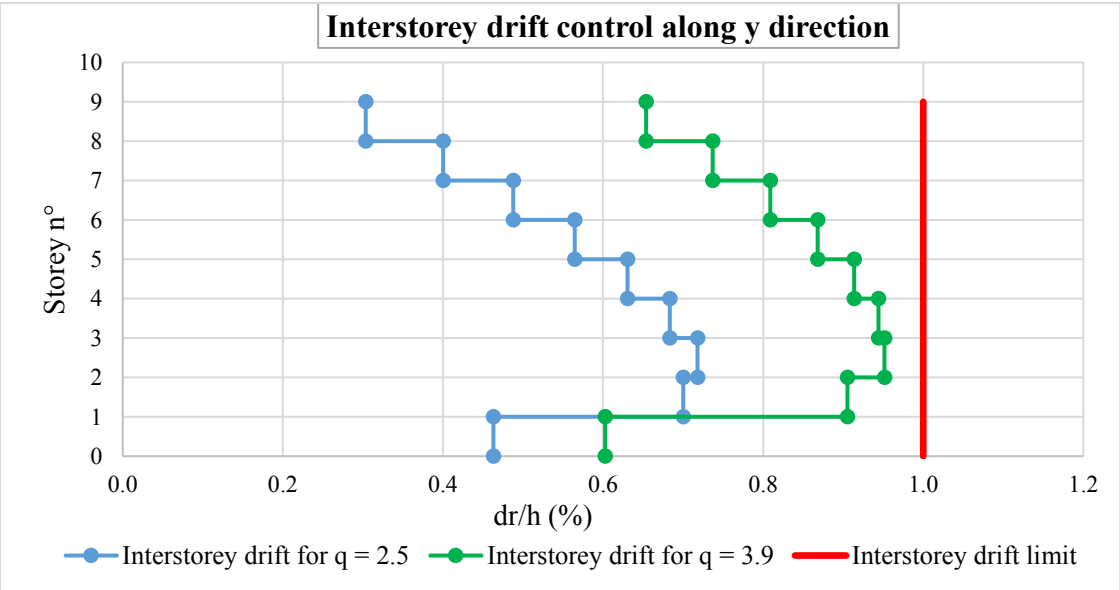

Figure 3.69. Interstorey drift control along y direction

Moreover, in the investigated building, the second order effects needed not be taken into account for both cases, because the interstorey drift coefficient **θ** is smaller than 0.1 in all storeys in both directions as shown in table 3.27 and table 3.28.

Table 3.27. Interstorey drift sensitivity coefficient for q = 2.5

Storey	Ptot (kN)	dr (mm)		V (kN)		h (mm)	θx	θy
		dr,x	dr,y	Vx	Vy			
1	1039.3	14.97	22.60	179.789	179.49	3000	0.029	0.044
2	806.1	15.53	23.84	180.004	185.874	3000	0.023	0.034
3	603.5	14.87	23.83	166.823	175.217	3000	0.018	0.027
4	434.2	13.76	23.26	151.722	162.909	3000	0.013	0.021
5	298.3	12.36	22.33	133.35	147.576	3000	0.009	0.015
6	197.9	10.72	21.09	112.233	129.641	3000	0.006	0.011
7	138.5	8.87	19.57	88.677	109.033	3000	0.005	0.008
8	109.8	6.86	17.85	61.514	82.51	3000	0.004	0.008
9	60.5	4.89	16.08	37.085	64.689	3000	0.003	0.005

Table 3.28. Interstorey drift sensitivity coefficient for q = 2.5

Storey	Ptot (kN)	dr (mm)		V (kN)		h (mm)	θx	θy
		dr,x	dr,y	Vx	Vy			
1	877.6	21.01	27.16	84.826	105.467	3000	0.072	0.075
2	673.3	21.54	28.55	82.029	109.84	3000	0.059	0.058
3	501.8	20.50	28.32	77.015	105.281	3000	0.045	0.045
4	363.3	18.92	27.41	71.094	99.156	3000	0.032	0.033
5	253.5	16.94	26.04	64.354	91.168	3000	0.022	0.024
6	170.2	14.63	24.26	56.562	81.498	3000	0.015	0.017
7	115.6	12.01	22.11	47.22	70.005	3000	0.010	0.012
8	84.9	9.11	19.62	35.688	54.352	3000	0.007	0.010
9	45.3	6.15	16.91	22.892	45.154	3000	0.004	0.006

As can be seen from the previous results, the sections adopted for each ductility level allow the structure to resist the solicitations generated by the seismic action while respecting the displacement restrictions. These cross-sections will be used in the subsequent work for the pushover analysis.

3.6.3. Results of pushover analysis

The pushover analysis was carried out according to the procedure described in section **2.8.3**. The first step was to model the building. It was modelled in the same way as the one used in the elastic analysis but with the addition of the plastic hinges as defined in section **2.8.3.2.c**, to mark the non-linearities in the structures.

3.6.3.1. Plastic mechanism and pushover curve

a. Plastic mechanisms

The incremental loading of the structure gives rise to the formation of plastic hinges in the structure. These hinges are presented in the SAP2000 v22 software and the change in colour of these hinges reflects the transition from one performance level to another (see figure 2.11).

Figure 3.70 and figure 3.71 show examples of the last plastic mechanisms occurring in the building when subjected to incremental loading in the x direction. Figure 3.70 shows the state of the building at the end of the analysis (the 13th step) for q=2.5. It corresponds to a roof displacement of 132 mm and a base shear force of 16631kN. As can be seen from the figure, the plastic hinges formed on the beams and columns are in the elastic domain (IO level). One hinge in the base of ground level column is in the CP-C zone which means substantial damage has occurred to the building but no collapse.

Figure 3.71 illustrates the 18th step (end of the analysis) of the building when designed for q=3.9. It corresponds to a roof displacement of 220 mm and a base shear force of 9628 kN. As can be seen from the figure, most of the plastic hinges formed on the beams are in the LS level and those of the columns are in the IO level. Two hinges in the base of foundation column and one in the column are in the CP-C zone which means substantial damage has occurred to the building but no collapse.

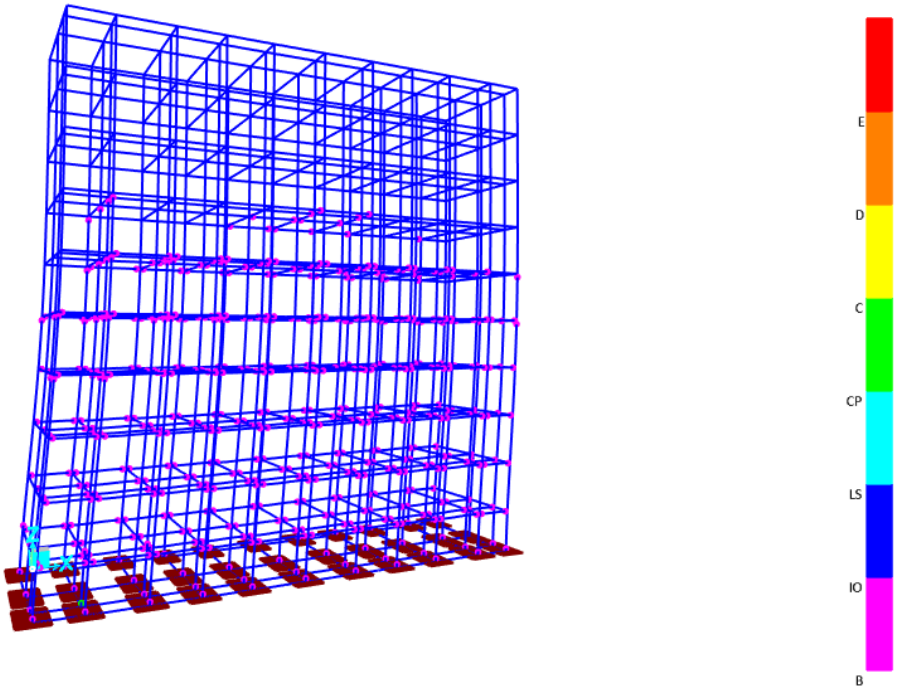

Figure 3.70. Plastic mechanism along x direction for q=2.5

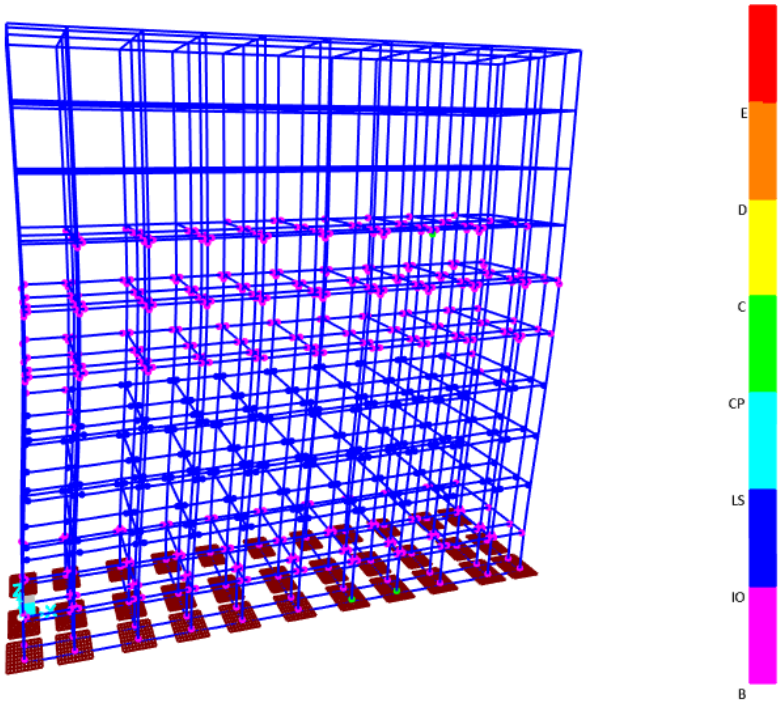

Figure 3.71. Plastic mechanism along x direction for q=3.9

The recordings of all the different states of the structure made it possible to draw the curve linking the shear force at the base of the structure to its displacement, the pushover curve.

b. Pushover curves

As descried in the section **2.8.3.4,** the pushover curve describes the behaviour of the building under incremental lateral load in x and y directions of the building. The pushover curves along x direction and y direction are presented in figure 3.72 and figure 3.73 respectively.

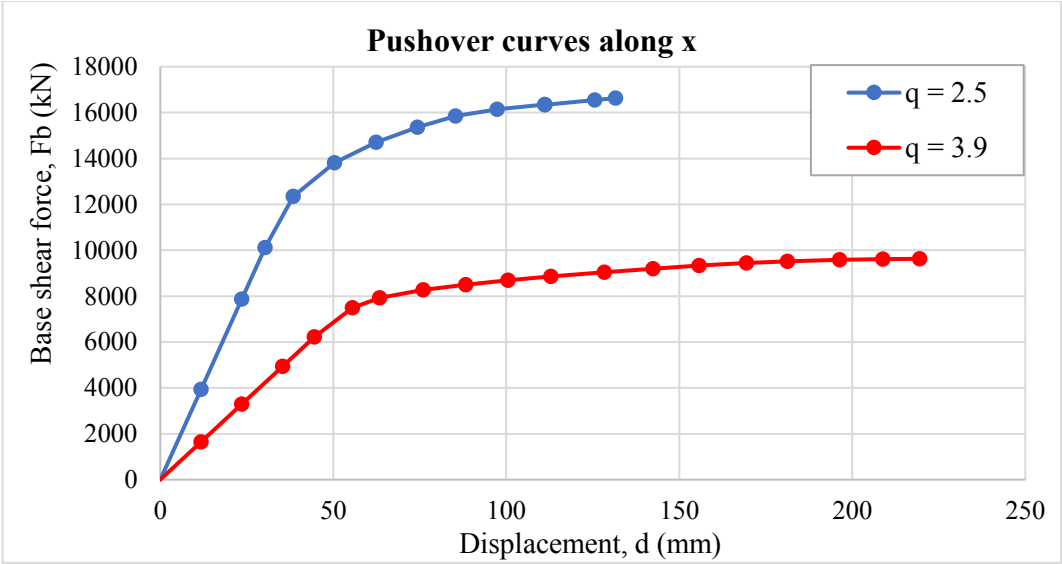

Figure 3.72. Pushover curve along x direction

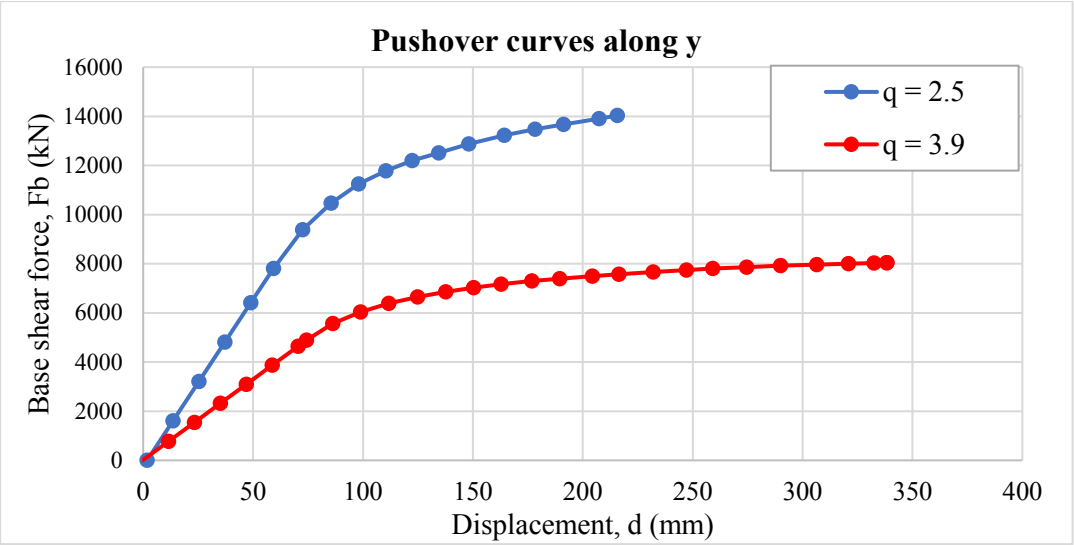

Figure 3.73. Pushover curve along y direction

As mentioned in the methodology chapter, EC8 considers the building by its equivalent SDOF model. The pushover curves obtained above are associated to the MDOF model. Therefore, these curves must be transformed into the capacity curve of the equivalent SDOF model.

3.6.3.2. Capacity curves and ductility coefficient

As mentioned in Section **2.8.3.5.a**, the transformation from a multi-degree-of-freedom (MDOF) system to a single-degree-of-freedom (SDOF) system is done through the transformation factor Γ. Its value is determined and presented for each ductility level in table 3.29 and table 3.30.

Table 3.29. Transformation factor for q=2.5

Storey	ϕi displacement vector	ϕi normalized	mi	mi*ϕi	mi*ϕi^2
9	21.772	1.00	2 752.45	2 752.45	2 752.45
8	20.063	0.92	5 138.09	4 734.78	4 363.12
7	18.175	0.83	5 138.09	4 289.22	3 580.59
6	16.107	0.74	5 138.09	3 801.18	2 812.13
5	13.880	0.64	5 138.09	3 275.62	2 088.26
4	11.525	0.53	5 138.09	2 719.85	1 439.75
3	9.078	0.42	5 138.09	2 142.37	893.28
2	6.586	0.30	5 138.09	1 554.27	470.16
1	4.108	0.19	5 138.09	969.47	182.92
0	1.770	0.08	2 758.71	224.28	18.23
Sum				26 463.47	18 600.89
				Γ	1.42

Table 3.30. Transformation factor for q=3.9

Storey	ϕi displacement vector	ϕi normalized	mi	mi*ϕi	mi*ϕi^2
9	23.121	1.00	2 322.18	2 322.18	2 322.18
8	21.466	0.93	4 423.19	4 106.58	3 812.63
7	19.552	0.85	4 423.19	3 740.42	3 163.04
6	17.392	0.75	4 423.19	3 327.20	2 502.78
5	15.013	0.65	4 423.19	2 872.08	1 864.91
4	12.458	0.54	4 423.19	2 383.29	1 284.16
3	9.770	0.42	4 423.19	1 869.06	789.79
2	7.029	0.30	4 423.19	1 344.69	408.80
1	4.290	0.19	4 423.19	820.70	152.28
0	1.710	0.07	2 328.44	172.21	12.74
Sum				22 958.43	16 313.30
				Γ	1.41

These factors allow us to draw the capacity curves presented in figure 3.74 and figure 3.75. These graphs are bilinearized in order to calculate the ductility coefficients.

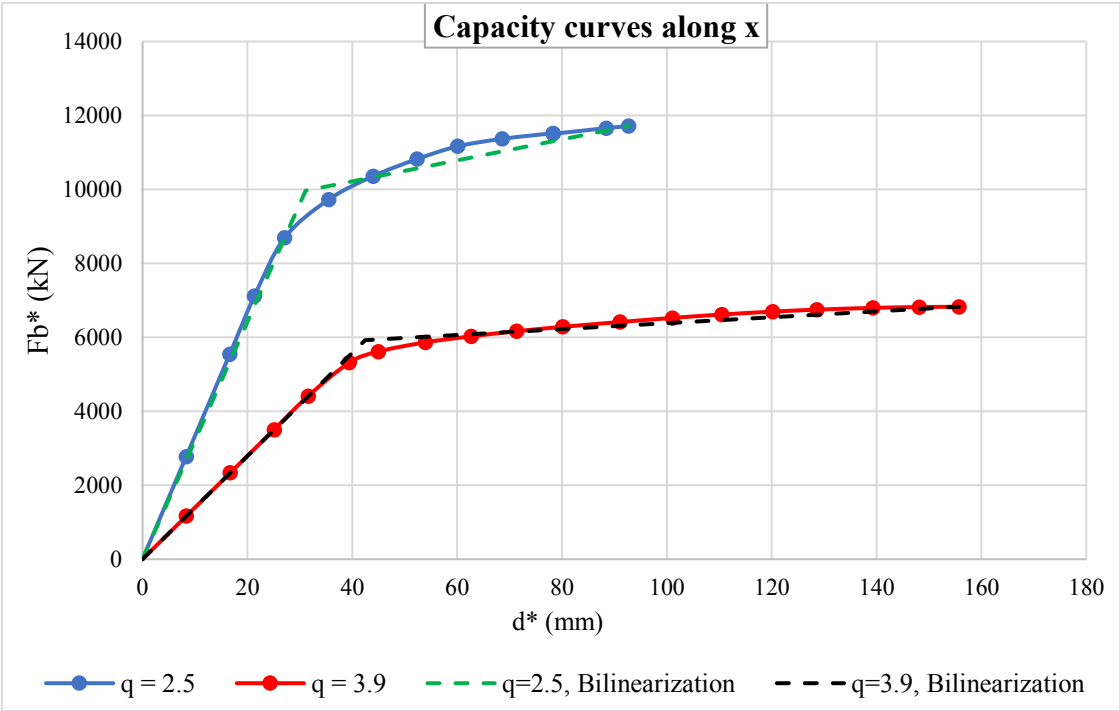

Figure 3.74. Capacity curves and bilinearization along x direction

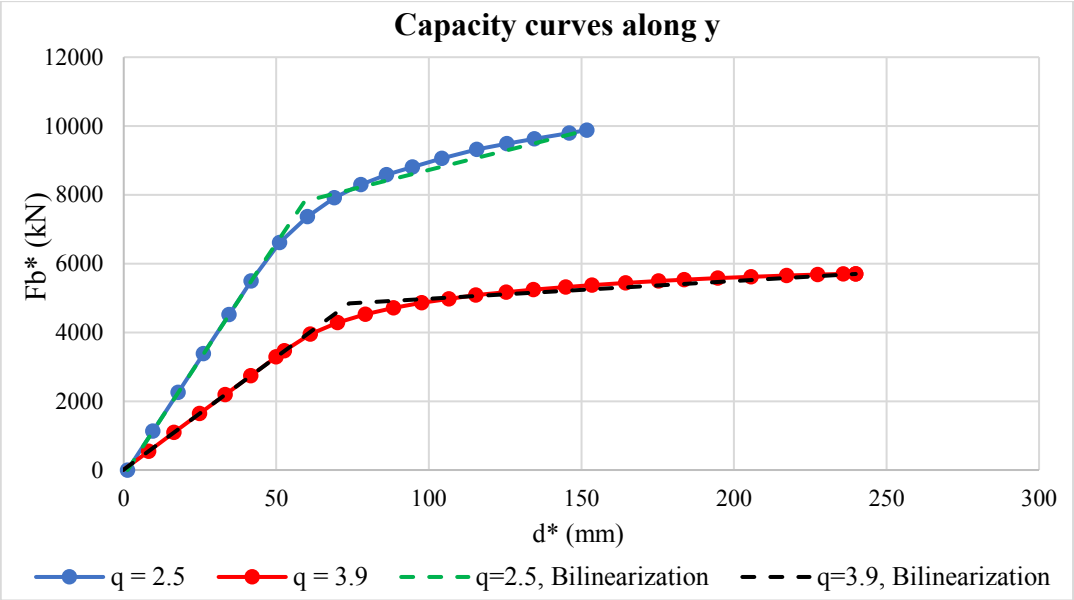

Figure 3.75. Capacity curves and bilinearization along y direction

The above graphs reveal that the building designed for a higher behaviour factor, which implies higher level of ductility, develops more in the non-linear domain compared to the one design for a lower behaviour factor. As a result, the building can withstand larger displacements without failure compared to the one with lower level of ductility.

In addition, the bilinearization of the capacity curves allows the ductility coefficient of the structure to be derived according to equation **(2.114)**. The results of the computations are presented in table 3.31 and as can be seen form this table, the yield displacement, the ultimate displacement, and the ductility coefficient are larger for higher level of ductility.

Table 3.31. Determination of the ductility coefficient

Direction	Behaviour factor	Yield displacement	Ultimate displacement	Ductility coefficient
X	2.5	31.07	92.69	**2.98**
	3.9	42.46	155.70	**3.67**
Y	2.5	59.31	151.85	**2.56**
	3.9	73.84	239.93	**3.25**

As mentioned in section 1.4.1.2, the behaviour factor can be considered as the ductility demand and the ductility coefficient as the ductile capacity of the structure. According to EC8, the effective behaviour factor of the building is given by $q_{eff} = \mu$ for $T_1 \geq T_C$ (see equation **(2.116)** which is the case for most of tall buildings. Table 3.32 shows the different fundamental periods of the building in each direction and for each chosen ductility level.

Table 3.32. Fundamentals periods of the building

Behaviour factor	**q = 2.5**		**q = 3.9**	
Directions	**x**	**y**	**x**	**y**
T_1	0.75	1.08	0.89	1.23
Tc	0.72	0.72	0.72	0.72

This table shows that the condition $T_1 \geq T_C$ is indeed verified and therefore $q_{eff} = \mu$.

Figure 3.76 and table 3.33 present the correlation between the values of the ductility coefficient (effective behaviour factor) obtained in this study and the values of the behaviour factor chosen (predicted) according to EC8.

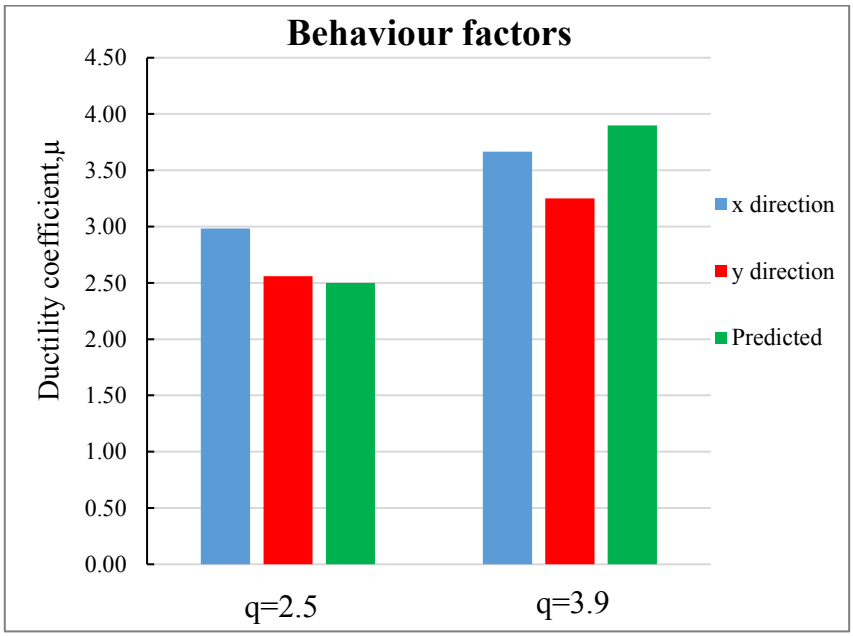

Figure 3.76. Comparison between the ductility coefficient and the behaviour factor

Table 3.33. Comparison between the ductility coefficient and the behaviour factor

	q =2.5		**q = 3.9**	
Direction	**μ**	**μ/q (%)**	**μ**	**μ/q (%)**
x	2.98	119.31	3.67	94.02
y	2.56	102.41	3.25	83.31

From figure 3.76 and table 3.33, it can be seen that the effective behaviour coefficient is higher than that predicted for q=2.5. An increase of 19.31% in the x direction and 2.41% in the y direction

is obtained. Conversely, for q=3.9, the effective behaviour factor obtained is 5.98% lower in the x direction and 16.69% lower in the y direction than the predicted one.

These results show a limit of the chosen ductility level according to EC8 on the actual behaviour of the structure. For a relatively low chosen ductility level (low behaviour factor according to EC8), the building has a better ductile behaviour than predicted and therefore can resist larger seismic actions than those used for its design. The higher the ductility level, the less the building is able to guarantee the predicted ductile behaviour and therefore the choice of the behaviour factor according to the Eurocode 8 is no longer conservative.

Hypotheses can be formulated to explain these results:

a. The height of the building

Studies conducted by Tirca and Tremblay (2004) and Mourad and Hassan (2019) have shown that height has a significant influence on the seismic behaviour of buildings. It has been shown that the behaviour coefficient decreases with increasing building height. However, the height of the building is not a parameter considered in EC8 when choosing the behaviour factor, which may lead to a lower actual behaviour factor obtained by the pushover method than the one initially chosen.

b. Soil-structure interaction

The response of the structure to seismic action is affected by 3 related systems: the structure, the foundations, and the soil. Soil-structure interaction (SSI) analysis evaluates the collective response of these systems to a specified ground motion. One of the limitations of most structural design codes, including EC8, is that the behaviour of the substructure (foundation and soil) is completely ignored and assumed to be perfectly rigid. This may be true for a relatively flexible structure located on stiff soil or rock, but for a heavy structure on soft soil, the flexibility of the soil causes the motion on the foundation to differ from the field motion (ground motion when the structure is not present). Hence, the SSI has a significant effect on the seismic behaviour of the structure especially for soft soils

This hypothesis was verified by the research of Eser et al. (2011) who demonstrated that the SSI reduces the strength reduction factor (behaviour factor q) for soft soils.

c. The SDOF model used by the EC8

Furthermore, the model used in EC8 for the analysis is an SDOF model. This model does not consider, or at least in a rather limited way, two important facts in the seismic behaviour of the

building: the interaction between different structural elements present on the same plane and the interaction between structural elements present in different planes. For this study, the modelled building is an MDOF system and therefore the interaction between the different structural elements has a considerable influence on the seismic behaviour of the structure.

Conclusion

The main objective of this chapter was to present, analyse and interpret the results of the different analyses carried out on the tall building chosen for this study. The first analysis carried out was the static linear analysis, which allowed to obtain the different sections of the structural elements necessary to resist to the vertical and wind actions. Subsequently, an elastic response spectrum representing the action of the earthquake was defined and based on Eurocode 8, two behaviour factors were chosen which characterise two levels of ductility. The results of the modal response spectrum analysis show an increase in the base shear force when the behaviour factor decreases and consequently an increase in the solicitations in the various structural elements, accompanied by an increase in the cross-sections necessary to resist the design seismic action. The increase in the cross-section of the elements increases the stiffness of the structure, which results in a reduction of the inter-storey drift when the ductility level decreases. The pushover analysis shows an increase in the ductility coefficient as the ductility level increases. However, the results of this analysis showed a decrease between the behaviour factor chosen according to Eurocode 8 and that obtained by the pushover method for higher ductility level. This reflects a lower effective seismic performance of the structure than predicted when the ductility level increases.

GENERAL CONCLUSION

Throughout this thesis, the main objective was to analyse the behaviour of a tall reinforced concrete building when the level of ductility increases and to evaluate the correlation between its predicted behaviour and the obtained one. The case study is a residential building constituting a ground level with 8 storeys at Toutouli in Yaoundé, Cameroon.

The first step consisted in designing the building using linear static analysis, considering only the vertical loads (permanent and variable-live loads) and wind load acting on it. This design made it possible to obtain the concrete and reinforcement sections on the beams, columns and footings necessary to resist these actions both in the ultimate and serviceability limit states.

The second step consisted in the design of the building taking into account the seismic action and the level of ductility. Through the modal analysis, it was possible to determine the modal properties of the building especially the natural periods and frequencies and the modal participating mass ratios of each vibration mode of the building. This analysis revealed that the first 12 vibration modes were required to study the linear dynamic behaviour of this building. Furthermore, staying in the medium ductility class, two behaviour factors were chosen, specifically q=2.5 in order to have an idea of the behaviour of the structure at low level of ductility and q=3.9 in order to have an idea of the behaviour of the structure at a higher level of ductility. Using the characteristics of the 12 vibration modes and the design response spectrum derived from the reduction of the elastic response spectrum by the different behaviour factors, it was possible to determine the response of the building by means of modal response spectrum analysis. The most important results were the base shear, the new internal forces on the structural elements and the displacement of each storey. These results revealed that the base shear force is lower for a higher behaviour factor. An increase in the behaviour factor of 56% produces a reduction in the base shear force of 35.9% in the case of this study and therefore reduces the solicitations in the structural elements. Moreover, this study showed an increase in displacement for q = 3.9 compared to those for q = 2.5. This is due to a decrease in cross-sectional area as the level of ductility increases.

Finally, in order to evaluate the correlation between the predicted behaviour of the building and the obtained one, a non-linear static analysis (pushover analysis) was carried out. This analysis resulted in the capacity curve of the building, showing its actual behaviour. It was observed that the building designed with a higher behaviour factor, which implies higher level of ductility, has a higher deformation capacity in the non-linear domain as compared to the one

designed with a lower behaviour factor. Hence, the building can withstand larger displacements without failure as compared to the one with lower level of ductility. The use of the capacity curve allowed to obtain the ductility coefficients related to the chosen levels of ductility. According to EC8, this coefficient is equal to the effective behaviour factor of the building. This study showed that the effective behaviour factor is higher than that predicted for q=2.5. An increase of 19.31% in the x direction and 2.41% in the y direction were obtained. Conversely, for q=3.9, the effective behaviour factor obtained is 5.98% lower in the x direction and 16.69% lower in the y direction than the predicted one. These results show a limitation in the Eurocode 8 in terms of ductile design. For a relatively low chosen ductility level (low behaviour factor), the building has a better ductile behaviour than predicted and therefore can resist larger seismic actions than those used for its design. The higher the ductility level, the less the building is able to guarantee the predicted ductile behaviour and therefore the choice of the behaviour factor according to the Eurocode 8 is no longer conservative. Some assumptions were made to explain these results, concerning the height of the building, the soil-structure interaction, and the use of the SDOF model.

However, this analysis was performed using two levels of ductility and considering only one structural type of building. Further studies can be eventually carried out with more levels of ductility and in a different structural type of building. The absence of data especially seismic data of the construction site is one of the main limitations of this analysis. The seismic data considered in this analysis were taken in Belluno in Italy. Also, non-linear static analysis was used in this work to obtain the real behaviour of the structure. However, more accurate results could be obtain using a non-linear dynamic analysis.

BIBLIOGRAPHY

BOOKS

Athanasopoulou, A., Fardis, M., Pinto, P., Aucun, B., Tsionis, G., Somja, H., Plumier, A., Pecker, A., Franchin, P., Carvalho, E., Fajfar, P., Degee, H., Kreslin, M., Bisch, P., & European Commission. Joint Research Centre. (2012). *Eurocode 8: seismic design of buildings - Worked examples*. Publications Office.

Avramidis, I., Athanatopoulou, A., Morfidis, K., Sextos, A., & Giaralis, A. (2016). Eurocode-compliant seismic analysis and design of R/C buildings. In *Geotechnical, Geological and Earthquake Engineering* (Vol. 38). Springer.

Balandier, P. (2004). *Sismologie appliquée : à l'usage des architectes et ingénieurs*. Les Grands ateliers de L'Isle-d'Abeau.

Beeby, A. W., & Narayanan, R. S. (2005). *Designers' Guide to EN 1992-1-1 and EN 1992-1-2. Eurocode 2: Design of Concrete Structures: General Rules and Rules for Buildings and Structural Fire Design* (Vol. 17). Thomas Telford.

Corvez, D., & Davidovici, V. (2016). *Pratique du calcul sismique : Guide d'application de l'Eurocode 8*. Editions Eyrolles.

Elnashai, A. S., & di Sarno, L. (2015). *Fundamentals of earthquake engineering: from source to fragility*. John Wiley & Sons.

Fajfar, P., & Krawinkler, H. (1992). *Nonlinear Seismic Analysis and Design of Reinforced Concrete Buildings: Workshop on Nonlinear Seismic Analysis of Reinforced Concrete Buildings*, Bled, Slovenia, Yugoslavia, 13-16 July 1992. CRC Press.

Gioncu, V., & Mazzolani, F. (2010). *Earthquake engineering for structural design*. CRC Press.

Giresini, L., & Butenweg, C. (2019). *Earthquake resistant design of structures according to Eurocode 8*. In Structural Dynamics with Applications in Earthquake and Wind Engineering: Second Edition (pp. 197–358). Springer Berlin Heidelberg. https://doi.org/10.1007/978-3-662-57550-5_4

Krawinkler, H., & Seneviratna, G. (1998). *Pros and cons of a pushover analysis of seismic performance evaluation*. Engineering Structures, 20(4–6), 452–464.

Lestuzzi, P., Sellami, S., & Badoux, M. (2008). *Génie parasismique : Conception et dimensionnement des bâtiments*. PPUR presses polytechniques.

Mosley, W. H., Hulse, R., & Bungey, J. H. (2012). Reinforced concrete design: to Eurocode 2. Macmillan International Higher Education.

Moussard, M., Garibaldi, P., & Curbach, M. (2017). The invention of Reinforced concrete (1848-1906). High Tech Concrete: Where Technology and Engineering Meet - Proceedings of the 2017 Fib Symposium, 2785–2794. https://doi.org/10.1007/978-3-319-59471-2_316

Taranath, B. S. (2009). Reinforced Concrete Design of Tall Buildings. CRC Press. https://doi.org/10.1201/9781439804810

van Damme, H. (2018). Concrete material science: Past, present, and future innovations. Cement and Concrete Research, 112(April), 5–24. https://doi.org/10.1016/j.cemconres.2018.05.002

NORMS

EN 1990*, Basis of structural design*, 2002, (Eurocode 0).

BS EN 1991-1-1, *General actions densities, self-weight, imposed loads for buildings*, 2002, (Eurocode 1: Actions on structures)

BS EN 1992-1-1, *General rules and rules for buildings, 2004*, (Eurocode 2: Design of concrete structures)

BS EN 1998-1-1, *General rules, seismic actions and rules for buildings, 2002*, (Eurocode 8: Design of structures for earthquake resistance)

FEMA 356, *Prestandard and commentary for the seismic rehabilitation of buildings*, November 2000

ARTICLES

Bang, H. N. (2022). A Concise Appraisal of Cameroon's Hazard Risk Profile: Multi-Hazard Inventories, Causes, Consequences and Implications for Disaster Management. *GeoHazards*, *3*(1), 55–87.

Chopra, A. K., & Goel, R. K. (2001). A modal pushover analysis procedure to estimate seismic demands for buildings: theory and preliminary evaluation. *PEER 2001/03*.

(CTBUH), C. on T. B. and U. H. (2017). *CTBUH height criteria for measuring & defining tall buildings*. CTBUH.

de Plaen, R. S. M., Bastow, I. D., Chambers, E. L., Keir, D., Gallacher, R. J., & Keane, J. (2014). The development of magmatism along the Cameroon Volcanic Line: evidence from seismicity and seismic anisotropy. *Journal of Geophysical Research: Solid Earth*, *119*(5), 4233–4252.

Eser, M., Aydemir, C., & Ekiz, I. (2011). Effects of soil structure interaction on strength reduction factors. Procedia Engineering, 14, 1696–1704. https://doi.org/10.1016/j.proeng.2011.07.213

Khose, V. N., Singh, Y., & Lang, D. H. (2012). A comparative study of design base shear for RC buildings in selected seismic design codes. Earthquake Spectra, 28(3), 1047–1070. https://doi.org/10.1193/1.4000057

Koch, F. W., Wiens, D. A., Nyblade, A. A., Shore, P. J., Tibi, R., Ateba, B., Tabod, C. T., & Nnange, J. M. (2012). Upper-mantle anisotropy beneath the Cameroon Volcanic Line and Congo Craton from shear wave splitting measurements. Geophysical Journal International, 190(1), 75–86.

Noel, E. O. P., Marcelin, M. P., & Bekoa, A. (2014). Crustal structure and seismogenic zone of Cameroon: integrated seismic, geological and geophysical data. Open Journal of Earthquake Research, 3(04), 152.

Reusch, A. M., Nyblade, A. A., Wiens, D. A., Shore, P. J., Ateba, B., Tabod, C. T., & Nnange, J. M. (2010). Upper mantle structure beneath Cameroon from body wave tomography and the origin of the Cameroon Volcanic Line. Geochemistry, Geophysics, Geosystems, 11(10).

Rizk, A. S. S. (2010). Structural design of reinforced concrete tall buildings. CTBUH J, 1, 34–41.

Tokam, A.-P. K., Tabod, C. T., Nyblade, A. A., Julia, J., Wiens, D. A., & Pasyanos, M. E. (2010). Structure of the crust beneath Cameroon, West Africa, from the joint inversion of Rayleigh wave group velocities and receiver functions. Geophysical Journal International, 183(2), 1061–1076.

THESIS

DJEUKOUA NATHOU Gabrielle Laure (2018). *Comparative analysis of seismic protection systems*. (Master thesis). National Advanced School of Publics Works, Yaoundé (Cameroon).

GIEU Sébastien (2012). *Ductilité des structures en béton armé.* (Master thesis). Conservatoire National des Arts et Metiers de Paris, Paris (France).

MEGUELLATI Aboubakr (2018). *Application de la méthode d'analyse statique non-linéaire (Pushover) sur un bâtiment R+3*. (Master thesis). Université L'Abri Ben M'hidi Oum El Bouaghi, Oum El Bouaghi (Algérie).

TATCHA KANKEU Yvan Loïc (2020). *Non-linear static and linear dynamic analysis for reinforced concrete building as complementary method of analysis and design*. (Master thesis). National Advanced School of Publics Works, Yaoundé (Cameroon).

WEB SITE

https://upload.wikimedia.org/wikipedia/commons/1/16/Ingalls_building_cincinnati_2006.jpg, Accessed on May 2022.

https://www.tripadvisor.fr/Attraction_Review-g298570-d7226070-Reviews-KLCC_Park Kuala_Lumpur_Wilayah_Persekutuan.html, Accessed on May 2022.

https://st.depositphotos.com/3519321/4869/i/950/depositphotos_48698811-stock-photo-taipei-101-stands-tallest-in.jpg, Accessed on May 2022.

https://www.dubai-prestige.com/wp-content/uploads/2020/09/burj-khalifa-dubai-1.jpg, Accessed on May 2022.

http://www.uib.no/, Accessed on April 2022.

https://ici.radio-canada.ca/nouvelle/776529/seismes-tremblements-terre-10-plus-meurtriers-depuis-2010, Accessed on July 2022.

APPENDIX

Appendix A. Measuring of earthquake

A1. Intensity scales

Several intensity scales have been proposed worldwide. Some of the most common intensity scales are listed below:

- Mercalli-Cancani-Seiberg (MCS): 12-level scale used in Southern Europe.
- Modified Mercalli (MM): 12-level scale proposed in 1931 by wood and Neumann, who adapted the MCS scale to the California data set. It is used in North America and several other countries.
- Medvedev-Sponhueur-Karnik (MSK): 12-level scale developed in Central and Eastern Europe and used in several other countries.
- European Macroseismic scale (EMS): 12-level scale adopted since 1998 in Europe. It is a development of the MM scale.
- Japanese Meteorological Agency (JMA): 7-level scale used in Japan. It has been revised over the years and has recently been correlated to maximum horizontal acceleration of the ground.

A2. MAGNITUDE

Several scales exist and the most common magnitude scales are:

- Local (or Richter) magnitude (M_L): measures the maximum seismic wave amplitude A (in microns) recorded on standard Wood-Anderson seismographs located at a distance of 100 km from the earthquake epicentre. Magnitude M_L is related to A by the following relationship:

$$\boldsymbol{M_L = \log(A) - \log(A_0)} \qquad \textbf{(A.1)}$$

  where A0 is the calibration factor that depends on the distance. Earthquake with M_L greater than 5.5 causes significant damage, while an earthquake of M_L=2 is the smallest event normally felt by people.
- Body wave magnitude (m_b): measures the amplitude of P-waves with a period of about 1.0 second that is less than 10 km wavelengths. This scale is suitable for deep earthquakes which have few surface waves. Magnitude m_b is related to the amplitude A and the period T of P-waves as follows:

$$m_b = \log\left(\frac{A}{T}\right) + \sigma(\Delta) \quad \textbf{(A.2)}$$

in which σ(Δ) is a function of the epicentre distance (in degrees).

- Surface wave magnitude (M_s): is a measure of the amplitude of LR-waves with a period of 20 seconds, that is wavelength about 60 km, which are common for very distant earthquakes. This scale cannot be used to characterise deep or relatively small, regional earthquakes. This limitation is due to the characteristics of LR-waves. The relationship between amplitude A, period T, distance Δ and Ms is given by:

$$M_s = \log\left(\frac{A}{T}\right) + 1.66\log(\Delta) + 3.30 \quad \textbf{(A.3)}$$

where Δ is measured in degrees, the ground motion amplitude in microns and the period in second. Equation (1.3) is applicable for Δ >15°.

- Moment magnitude (M_W): accounts for the mechanism of shear that takes place at the earthquake sources. It is not related to any wavelength. As a result, Mw can be used to measure the whole spectrum of ground motions. Moment magnitude is defined as a function of the seismic moment M_0. This measures the extent of deformation at the earthquake source and can be evaluated as follow:

$$M_0 = \mathbf{G\,A\,\Delta u} \quad \textbf{(A.4)}$$

where G is the shear modulus of the material surrounding the fault, A is the fault rupture area and Δu is the average slip between opposite sides of the fault. The modulus G can be assumed to 32 000 MPa in the crust and 75 000 MPa in the mantle. Thus, M_w is given by:

$$M_w = 0.67\log(M_0) - 10.70 \quad \textbf{(A.5)}$$

Where M_0 is expressed in ergons. (1 joules = 10^7 ergons).

Appendix B. Tables for Methodology

- **Tables for imposed load and reduction factors**

Table B. 1. Category of use of building (Table 6.1 EN 1991-1-1)

Category	Specific Use	Example
A	Areas for domestic and residential activities	Rooms in residential buildings and houses; bedrooms and wards in hospitals; bedrooms in hotels and hostels kitchens and toilets.
B	Office areas	
C	Areas where people may congregate (with the exception of areas defined under category A, B, and D[1)])	**C1**: Areas with tables, etc. e.g. areas in schools, cafés, restaurants, dining halls, reading rooms, receptions. **C2**: Areas with fixed seats, e.g. areas in churches, theatres or cinemas, conference rooms, lecture halls, assembly halls, waiting rooms, railway waiting rooms. **C3:** Areas without obstacles for moving people, e.g. areas in museums, exhibition rooms, etc. and access areas in public and administration buildings, hotels, hospitals, railway station forecourts. **C4**: Areas with possible physical activities, e.g. dance halls, gymnastic rooms, stages. **C5**: Areas susceptible to large crowds, e.g. in buildings for public events like concert halls, sports halls including stands, terraces and access areas and railway platforms.
D	Shopping areas	**D1:** Areas in general retail shops **D2**: Areas in department stores
[1)] Attention is drawn to 6.3.1.1(2), in particular for C4 and C5. See EN 1990 when dynamic effects need to be considered. For Category E, see Table 6.3		
NOTE 1 Depending on their anticipated uses, areas likely to be categorised as C2, C3, C4 may be categorised as C5 by decision of the client and/or National annex. NOTE 2 The National annex may provide sub categories to A, B, C1 to C5, D1 and D2 NOTE 3 See 6.3.2 for storage or industrial activity		

Table B. 2. Imposed loads in buildings (Table 6.1 EN 1991-1-1)

Categories of loaded areas	q_k [kN/m²]	Q_k [kN]
Category A		
- **Floors**	1,5 to2,0	2,0 to 3,0
- **Stairs**	2,0 to4,0	2,0 to 4,0
- **Balconies**	2,5 to 4,0	2,0 to 3,0
Category B	2,0 to 3,0	1,5 to 4,5
Category C		
- C1	2,0 to 3,0	3,0 to 4,0
- C2	3,0 to 4,0	2,5 to 7,0 (4,0)
- C3	3,0 to 5,0	4,0 to 7,0
- C4	4,5 to 5,0	3,5 to 7,0
- C5	5,0 to 7,5	3,5 to 4,5
category D		
- D1	4,0 to 5,0	3,5 to 7,0 (4,0)
- D2	4,0 to 5,0	3,5 to 7,0

Table B. 3. The recommended value of factors for variable loads (Table A.1.1 of EN 1990)

Action	ψ_0	ψ_1	ψ_2
Imposed loads in buildings, category (see EN 1991-1-1)			
Category A : domestic, residential areas	0,7	0,5	0,3
Category B : office areas	0,7	0,5	0,3
Category C : congregation areas	0,7	0,7	0,6
Category D : shopping areas	0,7	0,7	0,6
Category E : storage areas	1,0	0,9	0,8
Category F : traffic area, vehicle weight ≤ 30kN	0,7	0,7	0,6
Category G : traffic area, 30kN < vehicle weight ≤ 160kN	0,7	0,5	0,3
Category H : roofs	0	0	0
Snow loads on buildings (see EN 1991-1-3)*			
Finland, Iceland, Norway, Sweden	0,70	0,50	0,20
Remainder of CEN Member States, for sites located at altitude H > 1000 m a.s.l.	0,70	0,50	0,20
Remainder of CEN Member States, for sites located at altitude H ≤ 1000 m a.s.l.	0,50	0,20	0
Wind loads on buildings (see EN 1991-1-4)	0,6	0,2	0
Temperature (non-fire) in buildings (see EN 1991-1-5)	0,6	0,5	0
NOTE The ψ values may be set by the National annex. * For countries not mentioned below, see relevant local conditions.			

- Table for wind action

Table B. 4. Illustrations of the exposure factor $c_e(z)$

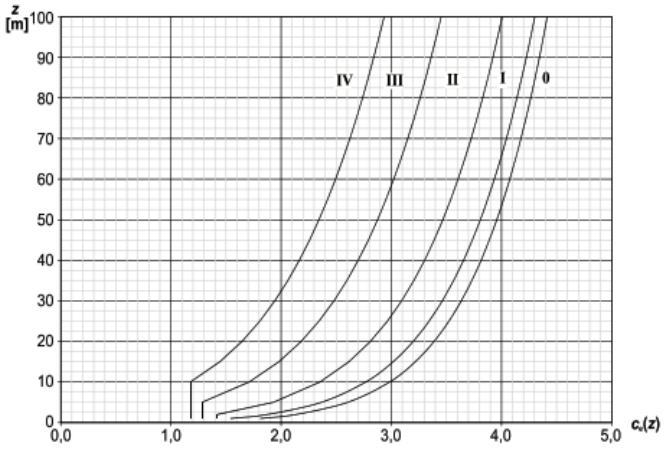

- Tables for seismic action

Table B. 5. Reference acceleration at ground level **(**Corvez & Davidovici, 2016)

Seismicity zone	a_{gR} (g)
Very low	0.4
Low	0.7
Moderate	1.1
Medium	1.6
High	3

Table B. 6 Importance coefficient (γ_1)

Building class	Importance coefficient (γ_1)
I	0.8
II	1
III	1.2
IV	1.4

Table B. 7. Soil coefficient

SOIL CLASS	S (for seismicity zone 1 to 4)	S (for seismicity zone 5)
A	1	1
B	1.35	1.2
C	1.5	1.15
D	1.6	1.35
E	1.8	1.4

Table B. 8. Values of TB, TC and TD as function of soil class

Soil class	For seismicity zone 1 to 4			For seismicity zone 5		
	T_B	T_C	T_D	T_B	T_C	T_D
A	0.03	0.2	2.5	0.15	0.4	2
B	0.05	0.25	2.5	0.15	0.5	2
C	0.06	0.4	2	0.2	0.6	2
D	0.1	0.6	1.5	0.2	0.8	2
E	0.08	0.45	1.25	0.15	0.5	2

- Tables for concrete cover and durability

Table B. 9. Minimum cover requirements with regard to bond (Table 4.2 of EN 1992-1-1)

Bond Requirement	
Arrangement of bars	Minimum cover $c_{min,b}$*
Separated	Diameter of bar
Bundled	Equivalent diameter (ϕ_n)(see 8.9.1)
*: If the nominal maximum aggregate size is greater than 32 mm, $c_{min,b}$ should be increased by 5 mm.	

Table B. 10. Values of minimum cover requirements (Table 4.4 of EN 1992-1-1)

Environmental Requirement for $c_{min,dur}$ (mm)							
Structural Class	Exposure Class according to Table 4.1						
	X0	XC1	XC2 / XC3	XC4	XD1 / XS1	XD2 / XS2	XD3 / XS3
S1	10	10	10	15	20	25	30
S2	10	10	15	20	25	30	35
S3	10	10	20	25	30	35	40
S4	10	15	25	30	35	40	45
S5	15	20	30	35	40	45	50
S6	20	25	35	40	45	50	55

Table B. 11. Exposure class related to the environmental conditions in accordance with EN 206-1 (Table 4.1 of EN 1992-1-1)

Class designation	Description of the environment	Informative examples where exposure classes may occur
1 No risk of corrosion or attack		
X0	For concrete without reinforcement or embedded metal: all exposures except where there is freeze/thaw, abrasion or chemical attack For concrete with reinforcement or embedded metal: very dry	Concrete inside buildings with very low air humidity
2 Corrosion induced by carbonation		
XC1	Dry or permanently wet	Concrete inside buildings with low air humidity Concrete permanently submerged in water
XC2	Wet, rarely dry	Concrete surfaces subject to long-term water contact Many foundations
XC3	Moderate humidity	Concrete inside buildings with moderate or high air humidity External concrete sheltered from rain
XC4	Cyclic wet and dry	Concrete surfaces subject to water contact, not within exposure class XC2
3 Corrosion induced by chlorides		
XD1	Moderate humidity	Concrete surfaces exposed to airborne chlorides
XD2	Wet, rarely dry	Swimming pools Concrete components exposed to industrial waters containing chlorides
XD3	Cyclic wet and dry	Parts of bridges exposed to spray containing chlorides Pavements Car park slabs
4 Corrosion induced by chlorides from sea water		
XS1	Exposed to airborne salt but not in direct contact with sea water	Structures near to or on the coast
XS2	Permanently submerged	Parts of marine structures
XS3	Tidal, splash and spray zones	Parts of marine structures
5. Freeze/Thaw Attack		
XF1	Moderate water saturation, without de-icing agent	Vertical concrete surfaces exposed to rain and freezing
XF2	Moderate water saturation, with de-icing agent	Vertical concrete surfaces of road structures exposed to freezing and airborne de-icing agents
XF3	High water saturation, without de-icing agents	Horizontal concrete surfaces exposed to rain and freezing
XF4	High water saturation with de-icing agents or sea water	Road and bridge decks exposed to de-icing agents Concrete surfaces exposed to direct spray containing de-icing agents and freezing Splash zone of marine structures exposed to freezing
6. Chemical attack		
XA1	Slightly aggressive chemical environment according to EN 206-1, Table 2	Natural soils and ground water
XA2	Moderately aggressive chemical environment according to EN 206-1, Table 2	Natural soils and ground water
XA3	Highly aggressive chemical environment according to EN 206-1, Table 2	Natural soils and ground water

- Tables for SLS verification

Table B. 12. K factor for deflection control

Structural System	*K*
Simply supported beam, one- or two-way spanning simply supported slab	1,0
End span of continuous beam or one-way continuous slab or two-way spanning slab continuous over one long side	1,3
Interior span of beam or one-way or two-way spanning slab	1,5
Slab supported on columns without beams (flat slab) (based on longer span)	1,2
Cantilever	0,4

Table B. 13. Recommended values of Wmax (mm)

Exposure Class	Reinforced members and prestressed members with unbonded tendons	Prestressed members with bonded tendons
	Quasi-permanent load combination	Frequent load combination
X0, XC1	0,4[1]	0,2
XC2, XC3, XC4	0,3	0,2[2]
XD1, XD2, XS1, XS2, XS3		Decompression

Note 1: For X0, XC1 exposure classes, crack width has no influence on durability and this limit is set to guarantee acceptable appearance. In the absence of appearance conditions this limit may be relaxed.
Note 2: For these exposure classes, in addition, decompression should be checked under the quasi-permanent combination of loads.

Table B. 14. Maximum bar diameters Ø* for crack control

Steel stress[2] [MPa]	Maximum bar size [mm] w_k= 0,4 mm	w_k= 0,3 mm	w_k= 0,2 mm
160	40	32	25
200	32	25	16
240	20	16	12
280	16	12	8
320	12	10	6
360	10	8	5
400	8	6	4
450	6	5	-

Table B. 15. Maximum bar spacing for crack control

Steel stress[2] [MPa]	Maximum bar spacing [mm] w_k=0,4 mm	w_k=0,3 mm	w_k=0,2 mm
160	300	300	200
200	300	250	150
240	250	200	100
280	200	150	50
320	150	100	-
360	100	50	-

- Table for soil-structure interaction modelling

Table B. 16. Value of subgrade modulus for different soil types (Forni, sd)

	Nature du sol	*C* (t/m^3)
1	terrain légèrement tourbeux et marécageux	500- 1 000
2	terrain essentiellement tourbeux et marécageux	1 000- 1 500
3	sable fin	1 000- 1 500
4	remblais d'humus, sable et gravier	1 000- 2 000
5	sol argileux détrempé	2 000- 3 000
6	sol argileux humide	4 000- 5 000
7	sol argileux sec	6 000- 8 000
8	sol argileux très sec	10 000
9	terrain compacté contenant de l'humus du sable et peu de pierres	8 000-10 000
10	même nature que ci-dessus avec beaucoup de pierres	10 000-12 000
11	gravier fin et beaucoup de sable fin	8 000-10 000
12	gravier moyen et sable fin	10 000-12 000
13	gravier moyen et sable grossier	12 000-15 000
14	gros gravier et sable grossier	15 000-20 000
15	gros gravier et peu de sable	15 000-20 000
16	gros gravier et peu de sable mais très compacté	20 000-25 000

Appendix C. Tables for Results

- **Architectural plans of the building**

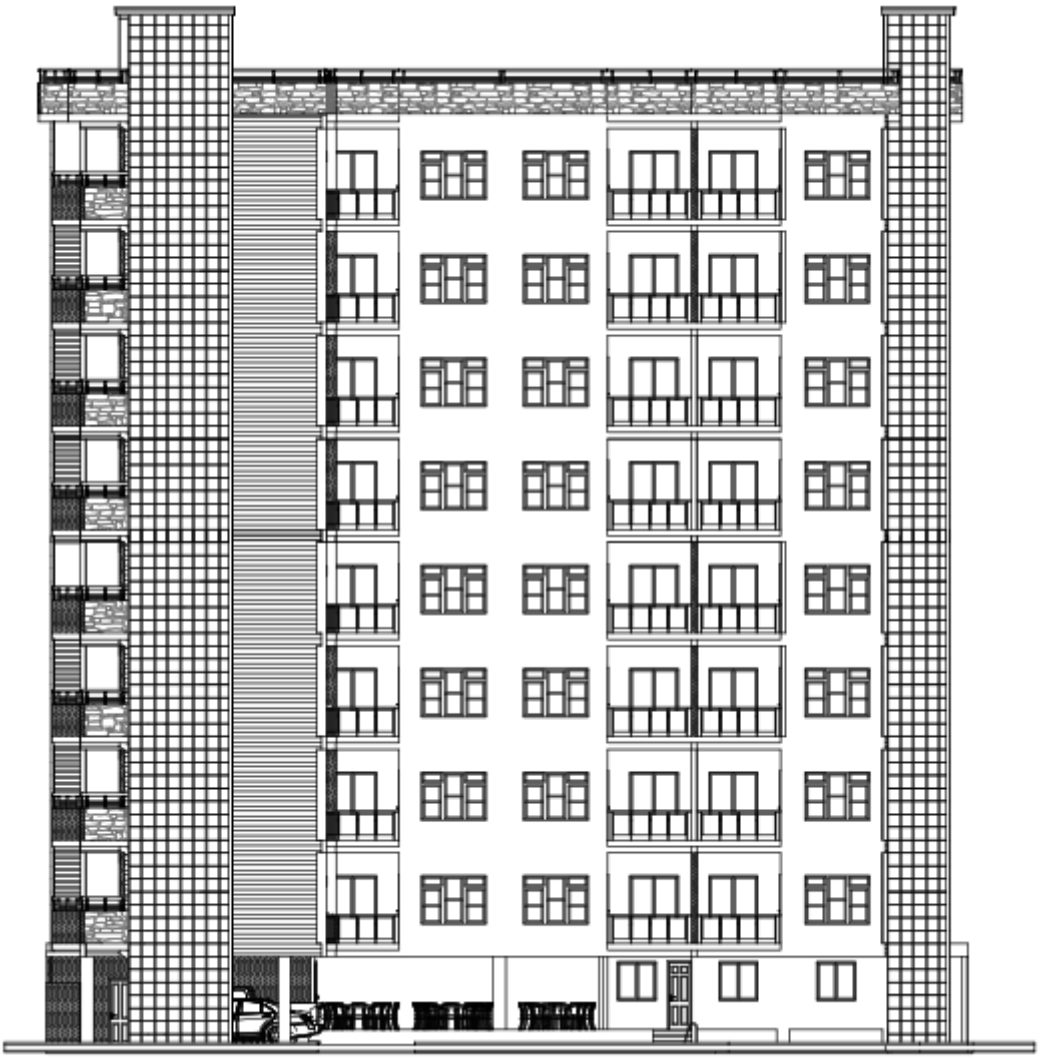

Figure C. 1. Main facade plan

- Determination of the centre of mass and the centre of rigidity

Table C. 1. Data for the determination of the centre of mass

Portion	Area (m²)	*xi (m)*	*yi (m)*	*Ai * xi*	*Ai * yi*
AB	33.81	14.09	0.6	476.38	20.29
BC	65.53	14.09	2.35	923.32	154.00
CD	110.62	14.09	5.45	1 558.64	602.88
Total	209.96			2 958.34	777.16
		x_{CM}	**y_{CM}**		
		14.1	**3.7**		

Table C. 2. Data for the determination of the centre of rigidity

Grid n°	**1**	**2**	**3**	**4**	**5**	**6**	**7**	**8**	**9**	**10**	**11**	
E (MPa)	3.E+04	3.E+04	3.E+04	3.E+04	3.E+04	3.E+04	3.E+04	3.E+04	3.E+04	3.E+04	3.E+04	
H (mm)	3.E+03	3.E+03	3.E+03	3.E+03	3.E+03	3.E+03	3.E+03	3.E+03	3.E+03	3.E+03	3.E+03	
JA,xx (mm^4)	3.1E+09	3.1E+09	3.1E+09	3.1E+09	3.1E+09	3.1E+09	3.1E+09	3.1E+09	3.1E+09	3.1E+09	3.1E+09	
JB,xx (mm^4)	3.1E+09	3.1E+09	3.1E+09	3.1E+09	3.1E+09	3.1E+09	3.1E+09	3.1E+09	3.1E+09	3.1E+09	3.1E+09	
JC,xx (mm^4)	3.1E+09	3.1E+09	3.1E+09	3.1E+09	3.1E+09	3.1E+09	3.1E+09	3.1E+09	3.1E+09	3.1E+09	3.1E+09	
JD,xx (mm^4)	3.1E+09	3.1E+09	3.1E+09	3.1E+09	3.1E+09	3.1E+09	3.1E+09	3.1E+09	3.1E+09	3.1E+09	3.1E+09	**Total**
Ky (N/m)	1.7E+05	1.7E+05	1.7E+05	1.7E+05	1.7E+05	1.7E+05	1.7E+05	1.7E+05	1.7E+05	1.7E+05	1.7E+05	**1.9.E+06**
xi (mm)	0	2.4	5.55	8.3	11.05	14.2	17.35	20.1	22.85	26	28.2	
Ky*xi (N)	**0**	**4.E+05**	**1.E+06**	**1.E+06**	**2.E+06**	**2.E+06**	**3.E+06**	**3.E+06**	**4.E+06**	**4.E+06**	**5.E+06**	**3.E+07**

Grid n°	**A**	**B**	**C**	**D**	
E (MPa)	31000	31000	31000	31000	
H (mm)	3000	3000	3000	3000	
J1,yy (mm^4)	1.E+09	1.E+09	1.E+09	1.E+09	
J2,yy (mm^4)	1.E+09	1.E+09	1.E+09	1.E+09	
J3,yy (mm^4)	1.E+09	1.E+09	1.E+09	1.E+09	
J4,yy (mm^4)	1.E+09	1.E+09	1.E+09	1.E+09	
J5,yy (mm^4)	1.E+09	1.E+09	1.E+09	1.E+09	
J6,yy (mm^4)	1.E+09	1.E+09	1.E+09	1.E+09	
J7,yy (mm^4)	1.E+09	1.E+09	1.E+09	1.E+09	
J8,yy (mm^4)	1.E+09	1.E+09	1.E+09	1.E+09	
J9,yy (mm^4)	1.E+09	1.E+09	1.E+09	1.E+09	
J10,yy (mm^4)	1.E+09	1.E+09	1.E+09	1.E+09	
J11,yy (mm^4)	1.E+09	1.E+09	1.E+09	1.E+09	**Total**
Kx (N/mm)	170500	170500	170500	170500	**682000**
yi (mm)	0	1.2	3.5	7.4	
kx*yi (N)	**0**	**204600**	**596750**	**1261700**	**2063050**

- Structural plans

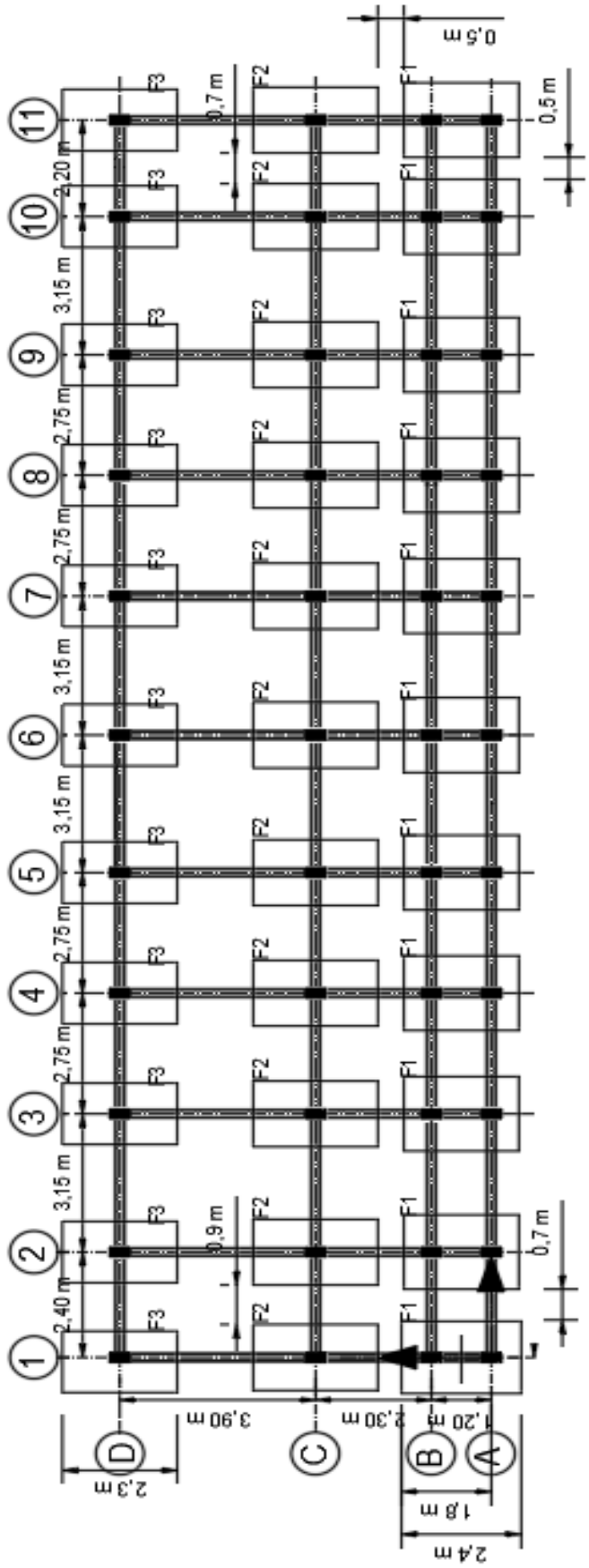

Footing	A(cm)	B(cm)	h(cm)	Qty
F1	240	165	55	11
F2	250	150	55	11
F3	230	140	55	11

Figure C. 2. Foundation plan of the building